

**Exploring the interplay between
mitochondrial metabolism and presynaptic plasticity
in early aging *Drosophila* brain**

Inaugural-Dissertation

to obtain the academic degree
Doctor rerum naturalium (Dr. rer. nat.)

submitted to the Department of Biology, Chemistry, Pharmacy
of Freie Universität Berlin

by

Lu Fei

From Hunan Province, China.

Berlin 2024

The experimental part of this thesis was conducted from October 2020 till February 2024 under the supervision of Prof. Dr. Stephan J. Sigrist at the Institute for Biology / Neurogenetics of the Freie Universität Berlin.

1st reviewer: Prof. Dr. Stephan J. Sigrist

2nd reviewer: Prof. Dr. Mathias F. Wernet

Date of defense: 9th July, 2024

Acknowledgement

I would like to firstly show my huge gratefulness to my supervisor Prof. Dr. Stephan J. Sigrist, who has constantly given lots of useful suggestions and support to my research project in the last four years. Because of him, I got the chance to learn from great scientists and master some advanced experimental skills in his lab. With his patience and excellent intellect and expertise, I also made much progress in neurogenetic knowledge and gained experience of mitochondrial metabolism in regulating presynaptic plasticity. Next, I intended to thank Prof. Dr. Ulrich Kintscher and his colleagues Anna and Giuseppe to allow me to share their working space and facilities for seahorse measurement and drosophila brain dissection in Charité Center for Cardiovascular Research (CCR). As for the study of ROS: amplex red assay and related fly stocks, I want to show my large appreciation to Prof. Dr Sean Sweeney, who sent me the required fly stocks from UK and taught me how to start the ROS measurement by sending emails. In the lab, Yongtian. Liang is the person who helped me the most with technical skills of single-brain seahorse measurement in the lab, and provided lots of useful scientific ideas on my project. His kindness and spirit of optimism always inspired me when I had some difficulties during the experiment. Special thanks would go to Marta Maglione and Atefeh Pooryasin for the collaborative work, along with Anastasia Stawrakakis, our lab managers for the trouble shooting, and ordering of experiment material needed in my project. Great thanks should go to all the other colleagues Janine Lützkendorf, Tanja Matkovic and Jennifer Woitkuhn for the support of confocal immunostaining and antibody design, especially for Krivograd, Anja and David Toppe for the help of fly flipping during my holiday and preparation of my birthday gifts, along with Oriane Turrel for sharing the duty of fly trash. Most importantly, thank my dear boyfriend Yingjie Zhao for the considerate care of my study and daily life, as well as my family members—my parents and my

cute brother, who have continuously motivated and encouraged me in the period of my difficulties. With their constant love and support, I was able to navigate the entire scientific journey and emerged as a transformed and improved individual.

Declaration of authorship

I hereby declare that I alone am responsible for the content of my doctoral dissertation and that I have only used the sources or references cited in the dissertation.

Table of Contents

1. Summary	9
2. Zusammenfassung	11
3. Introduction	13
3.1 The characteristics of aging	13
3.1.1 The underlying molecular mechanisms of aging	13
3.1.2 The anti-aging paradigms	14
3.2 Brain aging and the aging synapses	16
3.2.1 Brain aging	16
3.2.2 Age-driven synaptic alterations	17
3.3 Mitochondria—the critical aging hallmark	19
3.3.1 Mitochondrial DNA	20
3.3.2 Morphological dynamics of mitochondria	21
3.3.3 Mitochondrial calcium uptake and mitochondrial calcium entry	23
3.3.4 Mitochondrial metabolism and ATP production regulated by matrix Ca ²⁺	26
3.4 Age-driven mitochondrial dysfunction	27
3.4.1 Age-related decay of mitochondrial functionality	27
3.4.2 Main causes of mitochondrial decline: mtDNA mutation and genomic instability	29
3.4.3 “The free radical theory of ageing” and ROS signaling	30
3.4.4 ROS signaling and “mitohormesis” in promoting health and longevity	31
3.5 Mitochondria-targeted anti-ageing therapies	35
3.6 The interaction between synapses and mitochondria	37
3.6.1 The role of Mitochondria in synaptic plasticity	38
3.6.2 ROS signaling for synaptic plasticity	41
3.6.3 Mitochondrial plasticity at synapses	45
4. Materials and methods	49
4.1 Antibodies, primers and chemicals	49
4.1.1 Primary and Secondary antibodies	49
4.1.2 Primers of Oligonucleotides	50
4.1.3 Chemical agents and kit	50
4.2 Fly strains and rearing conditions	51
4.3 Longevity and Aging experiments	52
4.4 Paraquat feeding and oxidative stress resistance	53
4.5 Western blotting (WB)	53
4.6 Confocal microscopy and time-gated STED (gSTED) microscopy	55
4.6.1 Immunohistochemistry and confocal imaging, image quantification	55
4.6.2 MitoTimer staining and confocal imaging	56
4.6.3 gSTED imaging and image quantification	56
4.7 Assessment of mitochondrial functionality	57
4.7.1 Single-brain seahorse assay	57

4.7.2 Mitochondrial DNA measurement.....	61
4.7.3 ATP assay	62
4.7.4 Amplex red hydrogen peroxide assay.....	63
4.7.5 Mitochondrial ROS measurement by mitochondria-targeted redox sensor...63	
4.8 In vivo Mito-Ca ²⁺ imaging with two-photon microscopy.....	64
4.9 Statistical analysis.....	65
5. Results	66
5.1 Presynaptic plasticity (PreScale) is fine-tuned by bidirectionally genetic manipulations of mitochondrial functionality	66
5.1.1 Early-aging associated decay of mitochondrial function and ATP amounts in the Drosophila brain.....	66
5.1.2 Pan-neuronal activation of dPGC1 protects from aging-associated mitochondrial decay.....	68
5.1.3 Age protection of mitochondrial functionality delays age-induced onset of PreScale.....	71
5.1.4 Reducing ATP synthase 5A complex provokes premature PreScale	73
5.1.5 Evoking acute ROS stress can trigger premature PreScale.....	78
5.1.6 Effective antioxidant defense in neurons relaxes the need of PreScale in early brain aging.....	86
5.2 Mitochondria within MB suffice to modulate brain-wide PreScale	88
5.2.1 MB-specific overexpression of dPGC1 suppresses the brain-wide increase of PreScale.....	88
5.2.2 MB-exclusive stimulation of PGC1 does not affect brain mitochondrial function.....	89
5.2.3 MB-specific attenuation of ATP subcomponent V triggers premature PreScale	92
5.2.4 Changing mitochondrial functionality within sleep-controlling neurons, is insufficient to drive brain-wide PreScale-type plasticity.....	95
5.3 Short neuropeptide Y (sNPF) might link mitochondria status with PreScale	98
5.3.1 Robust sNPF signaling is needed for full mitochondrial activity in Drosophila brain.....	98
5.3.2 Neuronal attenuation of NPY activity impairs autophagy and propels age-dependent PreScale	101
5.3.3. Potential signaling pathways activated within the MB may link to brain-wide PreScale.....	103
5.4 PreScale might promote an energy-saving mode characterized by less mitochondrial activity and increased sNPF signaling.....	106
5.4.1 Genetically-implemented "PreScale" lowers mitochondrial abundance and respiratory function.....	106
5.4.2 The genetically-engineered PreScale promotes the expression of neuropeptide Y signaling	114
5.4.3 Mitochondrial calcium influx may contribute to the mitochondrial	

reprogramming induced by PreScale.....	115
6. Discussion.....	120
6.1 Age-induced PreScale can be tuned by genetic manipulations of mitochondrial functionality in a bi-directional manner	120
6.2 MB-secreted sNPF signaling is necessary for sustained mitochondrial capacity.....	124
6.3 Functional and morphological plasticity of mitochondria is orchestrated with PreScale	126
7. Reference.....	130
8. List of publications	142
9. Curriculum Vitae (CV).....	Error! Bookmark not defined.

1. Summary

Synapses serve as critical information hubs in inter-neuronal communication. However, preserving their optimal capacity for information processing and storage exhibits a significant challenge in ensuring successful brain aging. Our previous research demonstrated that the protein scaffolds forming presynaptic release sites are subject to dynamic plastic remodeling with aging, a process we term “PreScale”. This remodeling plays a pivotal role in managing the delicate trade-offs among survival, sleep, and memory formation and mediating brain resilience during an early, malleable stage of drosophila brain aging.

In this investigation, we disclose a reciprocal coupling between mitochondrial functional status and PreScale in the early aging brain of drosophila. The neuronal stimulation of PGC1 transcription co-activator protected the premature brain from aging-related mitochondrial dysfunction, as indicated by enhanced oxidative phosphorylation and increased ATP levels, and concurrently suppressed the aging-associated PreScale. On the contrary, neuronal attenuation of ATP synthase subcomponent V since adulthood deteriorated mitochondrial functionality during premature brain aging and simultaneously propelled PreScale. Neuron-specific fine-tuning of mitochondrial metabolism by PGC1 significantly prolonged the lifelong time of individual drosophila, mitigated ROS accumulation and bolstered the organism's overall capacity to withstand oxidative stress in later stages. whereas, the elimination of blw (ATP5A) within neurons led to outcomes diametrically opposed to PGC1. Collectively, the salutary health-promoting effects resulting from brain rejuvenation of mitochondrial dysfunction via neuronal activation of PGC1 in the early phases of brain aging opens up a novel anti-ageing paradigm for the future.

In our mechanistic exploration, ROS emerged as the molecular messenger for mitochondria in regulating the plastic change of age-dependent PreScale.

Pharmacological administration of ROS agents acutely induced PreScale within 6 hours, while neuronal overexpression of antioxidants *Cat* and *SOD2* relaxed the need to undergo age-driven PreScale. Therefore, it's tempting to speculate that, contrary to its traditional damaging identity, ROS more likely serves as a signaling carrier, modulating age-associated PreScale in early-aging fly brain.

Subsequently, in the following chapter, we progressed to confirm, comparably to autophagic impairment, MB-specific PGC1 overexpression and blw attenuation tuned in the metaplastic change of brain-wide PreScale. Furthermore, silencing ATP5A within MB neurons since adulthood led to a notable decrease in brain-wide short neuropeptide Y (sNPF) level. Given the significance of sNPF signaling in regulating PreScale, we suggest that sNPF might be the connector, linking mitochondrial functional status within MB to the spreading phenotype of PreScale throughout the entire brain.

Conversely, we proceeded to explore mitochondrial plasticity in the context of genetically-engineered PreScale. artificially-installed PreScale suffices to transform the brain metabolic state into an energy-conserving mode, as evidenced by a decrease in both brain oxidative phosphorylation and ATP levels. Thus, PreScale, potentially via modifying mitochondrial performance, seemingly acts as a precursor in regulating the brain's metabolic state. Subsequent analysis suggests that mitochondrial Ca^{2+} influx as feedback signals, might potentially modulate the adaptation of the mitochondrial state to align with the background of genetically installed PreScale.

2. Zusammenfassung

Synapsen fungieren als kritische Informationszentren in der inter-neuronalen Kommunikation. Die Erhaltung ihrer optimalen Kapazität für Informationsverarbeitung und -speicherung stellt jedoch eine bedeutende Herausforderung dar, um ein erfolgreiches Altern des Gehirns zu gewährleisten. Unsere vorangegangene Forschung hat gezeigt, dass die Proteingerüste, die präsynaptische Freisetzungstellen bilden, einem dynamischen plastischen Umbau mit dem Altern unterliegen, den wir als "PreScale" bezeichnen. In dieser Untersuchung enthüllen wir eine reziproke Kopplung zwischen dem mitochondrialen Funktionsstatus und PreScale im frühen alternden Gehirn der Fruchtfliege *Drosophila*. Die neuronale Stimulation des PGC1-Transkriptions-Koaktivators schützte das vorzeitige Gehirn vor altersbedingter mitochondrialer Dysfunktion, wie durch eine gesteigerte oxidative Phosphorylierung und erhöhte ATP-Spiegel angezeigt wurde, und unterdrückte gleichzeitig den mit dem Altern verbundenen PreScale. Im Gegensatz dazu verschlechterte die neuronale Dämpfung des ATP-Synthase-Untereinheitskomplex V seit dem Erwachsenenalter die mitochondriale Funktionalität während des vorzeitigen Gehirnalterns und trieb gleichzeitig PreScale voran. Die neuronenspezifische Feinabstimmung des mitochondrialen Stoffwechsels durch PGC1 verlängerte signifikant die lebenslange Zeit einzelner *Drosophila*, milderte die ROS-Akkumulation und stärkte die Gesamtkapazität des Organismus, oxidativen Stress in späteren Phasen zu widerstehen. Im Gegensatz dazu führte die Eliminierung von blw (ATP5A) innerhalb von Neuronen zu Ergebnissen, die diametral zu PGC1 waren. Insgesamt eröffnen die heilenden gesundheitsfördernden Effekte, die sich aus der Gehirnverjüngung bei mitochondrialer Dysfunktion durch neuronale Aktivierung von PGC1 in den frühen Phasen des Gehirnalterns ergeben, ein neuartiges Anti-Aging-Paradigma für die Zukunft.

In unserer mechanistischen Exploration tauchten ROS als molekularer Botenstoff für Mitochondrien auf, der die plastische Veränderung des altersabhängigen PreScale reguliert. Die pharmakologische Verabreichung von ROS-Agenten induzierte akut PreScale innerhalb von 6 Stunden, während die neuronale Überexpression von Antioxidantien Cat und SOD2 die Notwendigkeit des altersbedingten PreScale reduzierte. Daher liegt die Vermutung nahe, dass ROS entgegen seiner traditionellen schädlichen Identität eher als Signalträger fungiert und den altersbedingten PreScale im früh alternden Gehirn der Fliege moduliert.

Anschließend gingen wir im folgenden Kapitel dazu über, vergleichbar zur autophagischen Beeinträchtigung, die MB-spezifische PGC1-Überexpression und die Reduzierung von blw in die metaplastische Veränderung des gehirnwerten PreScale zu bestätigen. Des Weiteren führte das Abschalten von ATP5A innerhalb der MB-Neuronen seit dem Erwachsenenalter zu einem bemerkenswerten Abfall des gehirnwerten Spiegels des kurzen Neuropeptids Y (sNPF). Angesichts der Bedeutung der sNPF-Signalgebung bei der Regulation von PreScale legen wir nahe, dass sNPF als Bindeglied fungieren könnte, das den mitochondrialen Funktionsstatus innerhalb der MB mit dem sich ausbreitenden Phänotyp von PreScale im gesamten Gehirn verbindet.

Im Gegensatz dazu machten wir uns daran, die mitochondriale Plastizität im Kontext des genetisch modifizierten PreScale zu erforschen. Künstlich installierter PreScale reicht aus, um den Stoffwechselzustand des Gehirns in einen energiesparenden Modus zu transformieren, wie durch eine Abnahme der oxidativen Phosphorylierung und der ATP-Spiegel im Gehirn belegt wurde. Somit scheint PreScale, möglicherweise durch Modifizierung der mitochondrialen Leistung, als Vorläufer bei der Regulation des Stoffwechselzustands des Gehirns zu fungieren. Eine anschließende Analyse legt nahe, dass ein mitochondrialer Ca^{2+} -Einstrom als Rückkopplungssignal potenziell die Anpassung des mitochondrialen Zustands an den Hintergrund des genetisch installierten PreScale modulieren könnte.

3. Introduction

3.1 The characteristics of aging

Aging unfolds as a slow and at least at first glance inevitable biological progression, marked by the gradual deterioration of physical function and heightened vulnerability to cellular senescence (Guo *et al*, 2022). A sequence of time-dependent changes in behavior, including memory decline, sleep disorders, and mobility limitations, significantly detract from quality of life and hinder successful aging in numerous organisms. The desire to extend life expectancy and combat the aging process has been a persistent theme in human history. Furthermore, in today's world, with the global population aging, there is growing attention from scientists and medical professionals towards aging and age-related disorders.

3.1.1 The underlying molecular mechanisms of aging

In recent years, there has been a meticulous scientific examination aimed at unraveling the mystery surrounding the aging trajectory. Given the complexity of the aging mechanism, several pioneering insights into the underlying mechanisms of aging have been found, commonly referred to as aging hallmarks. A standard hallmark of aging should satisfy the following three premises: 1) they show age-dependent alterations; 2) experimental aggravation of the hallmark will facilitate the aging process; 3) the corresponding intervention to ameliorate their trend can delay the normal aging and consequently promotes the longevity extension.

Compared to the old nine aging hallmarks (López-Otín *et al*, 2013), recently the new edition of aging hallmarks (López-Otín *et al*, 2023) has expanded their point of view into twelve in total (Fig.1). These hallmarks are not absolutely independent but

interconnected with each other. Their complicated interactions obviously work together to promote the progression of aging process.

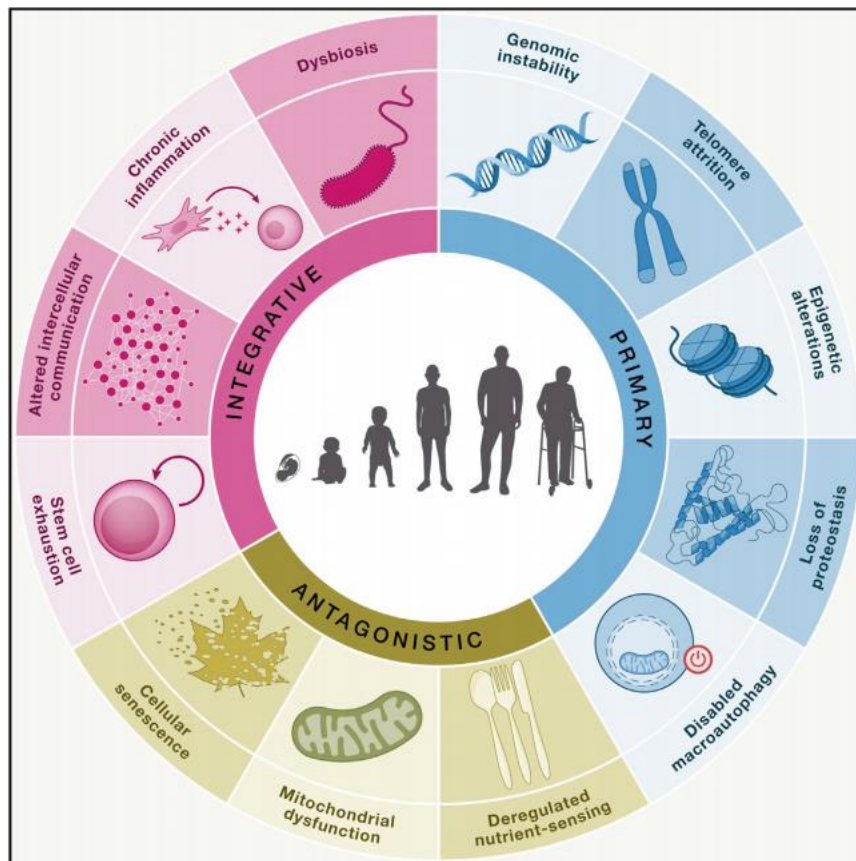


Fig.1. The hallmarks of aging. Taken from López-Otín C, et al. Cell. 2023.

3.1.2 The anti-aging paradigms

According to a report from United Nations (UN) on the aging population worldwide in 2015, the number of older people over 60 years old will become double, achieving 2.1 billion people in the next 35 years (Unies, 2015). Faced with the serious situation of population aging, it's imperative to look for novel anti-aging paradigms as solutions. Age-related alterations, such as memory decline, sleep disorders as well as age-associated disease, such as cardiovascular disease, neurodegenerative disease,

metabolic diseases and chronic respiratory diseases now have become a huge issue for people's health and fitness. The road heading for the development of new anti-aging agents and interventions has been established already a century ago (Guo *et al.*, 2022).

Here our primary focus will be on lifestyle changes and dietary supplements relevant to normal aging, rather than medications that target the pathological processes of age-related disorders (Fig.2). Supplementation, like small molecules and dietary interference such as Calorie restriction (CR) and dietary restriction (DR) have been investigated in the last three decades (Gonzalez-Freire *et al.*, 2020). A few of compounds such as rapamycin and spermidine respectively targeting the biological process of mTOR pathway and autophagy have been found to extend the lifetime and retard the age-related functional decay from yeast, drosophila to mammal models (Fontana *et al.*, 2010). These compounds and dietary manipulation are generally considered contributing to the longevity extension via improving metabolic status, especially via mitochondrial metabolic remodeling. The other anti-aging beneficial effects are conferring on the relevant aging hallmarks (Longo *et al.*, 2015). For instance, metformin, commonly used as an anti-diabetic drug was repurposed as a novel anti-aging agent due to its activation of insulin signaling. However, these aging-protective effects are not warranted in population-based clinical trials owing to the variable of ethnicity, environment, polymorphism, drug intake (first-pass elimination) and unexpected adverse effects. Personalized treatment of combining diet, exercise, and supplementary compounds might be a better way to deal with aging and age-related disorders.

3.2 Brain aging and the aging synapses

3.2.1 Brain aging

Aging, the most significant risk factor for neurodegeneration, impacts every organ in the body, with the brain being particularly susceptible. The decline of cognitive function in older adults precedes the deterioration of their essence. When considering aging, it consistently involves the gradual decline of various physical functions, and brain aging is no exception. Progressive cognitive decline, especially in memory, language, visuospatial and executive function, and recurring sleep disorders, such as REM sleep disturbance, and insomnia, are the frequent manifestations of normal brain aging which are not associated with a loss of forebrain neurons but strongly relevant to gradual and specific synaptic alterations (Morrison & Baxter, 2012).

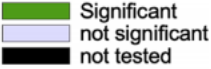
		Lifespan				
		Males		Females		
		Max	Mean	Max	Mean	
mTOR inhibitors	Rapamycin					
	Rapalogs					
Insulin pathway	Metformin					
	17- α Estradiol					
	Acarbose					
	FGF21					
NAD-SIRT6	Resveratrol					
	Simvastatin					
	STACs (SRT1720)					
	STACs (SRT2104)					
	NMN					
	Nicotinamide					
	Nicotinamide riboside					
Amino acids	NAMPT					
	Protein restriction					
	Methionine restriction					
	Tryptophan restriction					
Autophagy	Spermidine					
Senolytics	Navitoclax					
	Dasatinib + quercetin					
Rejuvenation factors	GDF11					
	GDF8					

Fig.2. Summary of the different interventions and their effect in lifespan extension in animal

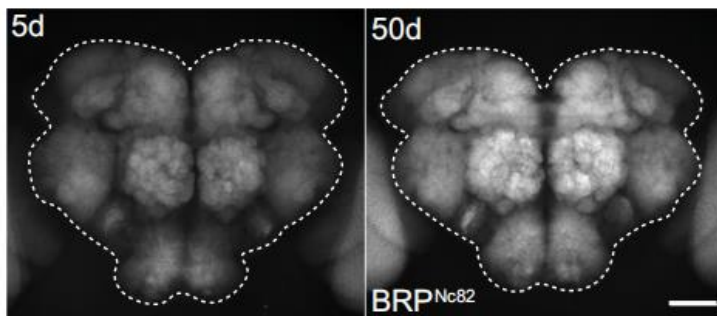
models. Taken from Gonzalez-Freire M, et al. Ageing Res Rev. 2020.

3.2.2 Age-driven synaptic alterations

In the central nervous system, synapses are the basic structure allowing for information processing between inter-neuron communications. Synapses undergo structural and functional alterations to adapt into the properties of neural circuit and brain functions. Aging provokes the change of various behaviors in the brain, especially the efficacy of learning and memory, two of the most magical capabilities of our mind. The formation, storage, and retrieval of memory cannot proceed without complicated synaptic connections. The dynamic outcome of the integrated memory process is initiated with individual synaptic connection and then broadened into more distributed changes of mounting synaptic connections of more neurons from larger neural networks which are expressed at an interactive behavior level (Kandel *et al*, 2014). Previously in *Drosophila* brain, we observed a brain-wide increase of presynaptic scaffold proteins at mid-age which was related to an age-dependent decline of forming olfactory memory in *drosophila* brain, while recently this view has extended to the whole aging trajectory (Huang *et al*, 2022). We further provided evidence that this age-associated alteration of presynaptic scaffold proteins and vesicle releasing factors, referred to as “PreScale”, increased over brain and peaked until mid-age but decreased afterwards to the baseline. Such age-driven presynaptic characteristic integrates brain resilience by steering trade-off between memory, sleep and longevity during early aging brains of *drosophila*. As a master protein in presynaptic active zone, Bruchpilot (BRP) promotes Ca²⁺-channel vesicle coupling, along with vesicle releasing (Böhme *et al*, 2016; Kittel *et al*, 2006). From our past experiment (Huang *et al.*, 2022) by imaging Calcium-dependent nuclear import of LexA

(CalexA) in specific neuron types of drosophila brain, PreScale, as a proxy of BRP, enable to reduce the Ca²⁺-dependent neuronal activity and membrane excitability in projection neuron (PN) and dorsal layer of fan-shaped body (dFB neurons).

a



b

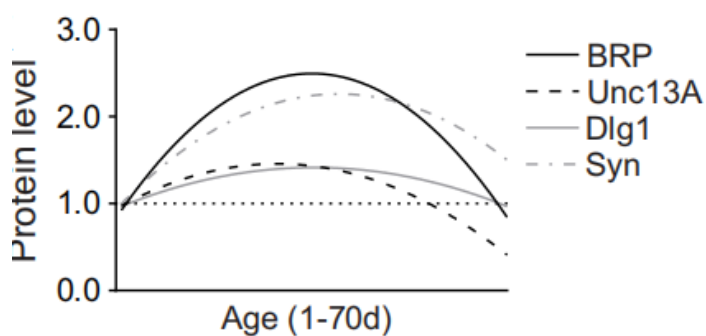


Fig.3. Age-related presynaptic alterations term as “PreScale”. Taken from Huang S, et al. PLoS Biol. 2022.

In mammals, the molecular and cellular changes observed in synapses within brain structures, particularly in the hippocampus and prefrontal cortex, during aging, can be directly associated with cognitive decline (Morrison & Baxter, 2012). The loss of hippocampal volume or with loss of neurons or synapses in the entorhinal cortex are related to pathological memory impairment in elderly humans (Rusinek *et al*, 2003) and facilitate the progression of Alzheimer’s disease (Gómez-Isla *et al*, 1996). Yet, it still remains undefined whether these synaptic adaptive responses will cause higher

susceptibility to neurodegeneration or strengthen the brain resilience against normal aging situation.

3.3 Mitochondria—the critical aging hallmark

1.3.1 Mitochondrial oxidative phosphorylation

Mitochondria, as cellular power house, are membrane-bound organelles. The outer and inner membranes with functional distinct separate mitochondria into matrix component and intermembrane space (IMS), which make it possible for the occurrence of many metabolic processes. As metabolic signaling centers, mitochondria are the main place to produce ATP via oxidative phosphorylation (OXPHOS). The tricarboxylic acid cycle (TCA) (Nunnari & Suomalainen, 2012), also known as Krebs cycles (Symposia et al, 1987) in the mitochondrial matrix, is carried out by eight enzymes to consume acetyl-CoA and water and reduce NAD⁺ to NADH. Electron carriers NADH and FADH are generated to donate electron to Electron transport chain (ETC) localized in mitochondrial inner membrane. The ETC are consisting of four complex (I -IV) which undergo conformational change through redox reaction sequence to transfer proton from matrix to IMS. Complex I , III and IV generate the proton gradient which is later released by complex V, the rotary turbine-like ATP synthase which simultaneously drives the phosphorylation of ADP to ATP (Fig.4).

Beyond ATP production, the inner electrochemical potential also plays critical role on other mitochondrial biological process. For instance, mitochondrial protein import is regulated by membrane potential, which may induce the molecular-level change of mitochondrial behavior in response to mitochondrial dysfunction. ROS as byproducts of OXPHOS, is mainly generated in mitochondria, the details of ROS generation and

its impact on mitochondrial function will be discussed in the next section **1.4.2**.

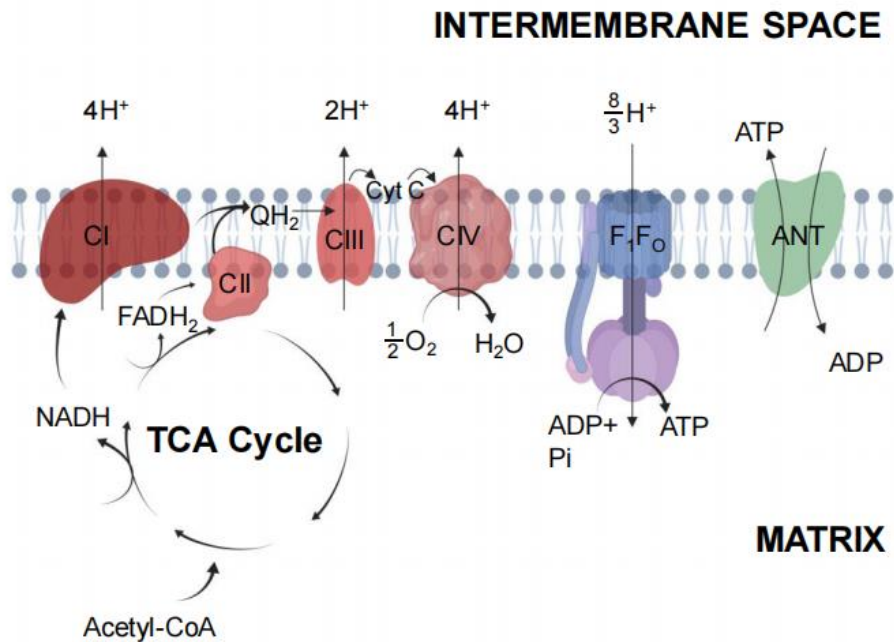


Fig.4. Mitochondrial oxidative phosphorylation. Taken from Lewis MT, et al. Int J Mol Sci. 2019.

3.3.1 Mitochondrial DNA

Mitochondrion is the only organelle with its own genome—mitochondrial DNA (mtDNA). Though only thirteen proteins are encoded by mitochondrial genome, these mitochondrial proteins are critical components during the process of OXPHOS (Anderson *et al*, 1981). Unlike nuclear genome, mtDNA lacks histone and is maternally inherited from the mother (Wallace & Chalkia, 2013). The vulnerability of mtDNA integrity can be attributed to several factors, including its high replicative index, limited efficiency of repair mechanisms, the oxidative micro-environment it resides in, and the absence of protective histones for its small DNA molecules. As a result, mtDNA is significantly influenced by age-related mutations and deletions. (López-Otín *et al.*, 2023; Sanchez-Contreras & Kennedy, 2022). Notably, ultra-sensitive sequencing

implicates that main mutations of mtDNA are more likely to derive from replication errors rather than oxidative stress (Sanchez-Contreras & Kennedy, 2022). Moreover, the strategy to avoid, attenuate, and correct the mutation of mtDNA would contribute to the healthy aging and improve age-related mitochondrial dysfunction.

3.3.2 Morphological dynamics of mitochondria

The metabolic function mitochondria perform varies across cell types and tissues. In response to the constant changing of metabolic stimuli, mitochondrial morphology is facing with dynamical change which is modeled by alternative events of fusion and fission in two mitochondrial membranes (Wai & Langer, 2016). Continual fusion and fission are very critical to maintain mitochondrial integrity and homeostasis. Fusion alleviates metabolic or environmental stress through complementing functional mitochondria with partially damaged ones. The diffusion and sharing components between organelles yield maximum potential of oxidative capacity (Youle & van der Bliek, 2012), while mitochondrial fission is required to generate new organelles and promote the removal of damaged mitochondria which also contributes to the quality control (Fig.5). The molecular machinery of mitochondrial fusion in the outer and inner membrane is mostly modulated by dynamin-like GTPases. Mitofusins, including mitofusin1 and mitofusin2 (Mfn1 and Mfn2) mediate outer membrane (OM) fusion. For example, removal of either Mfn1 or Mfn2 or ablation of GTPase activity would inhibit mitochondrial fusion, leading to a fragmented mitochondrial network of cultured cells (Mishra & Chan, 2014). Optic atrophy1 (OPA1) is another dynamin-like GTPase on the inner membrane (IM) with multiple forms in mammalian cells and tissues. Alternative splicing of OPA1 can give rise to long form (L-OPA1) and short form (S-OPA1). Based on the observation, OPA1 regulates fusion of inner membrane (IM). Knock-down of OPA1 prevents fusion but contributes to fragmentation and L-OPA1 not S-

OPA1 is more likely to be fusion competent(Ishihara *et al*, 2006). The molecular machinery of mitochondrial fission is respectively dependent on Dynamin-related protein 1 (DRP1) for OM fission and S-OPA1 and mitochondrial protein,18kDa (MTP18) for IM fission. Once DRP1 senses the specific cellular signal and is translocated from cytosol to mitochondrial OM, a conformational change of DRP1 would result in a contractile force to trigger outer membrane scission(Mears *et al*, 2011).

Mitochondrial morphology is dynamically adaptive to metabolic change. Higher oxidative respiration and increased ATP level is usually associated with greater fusion, while abrogation of fusion is often related to impaired ATP production and ROS generation. For example, fasting is reported to cause mitochondrial elongation in skeletal muscles (Jheng *et al*, 2012) while a high-fat diet led to mitochondrial fission and reduced Mfn2 levels in a rat model (Schneeberger *et al*, 2013). Metabolic input regulates mitochondrial morphological dynamics by mediating both of fusion and fission molecular machinery.

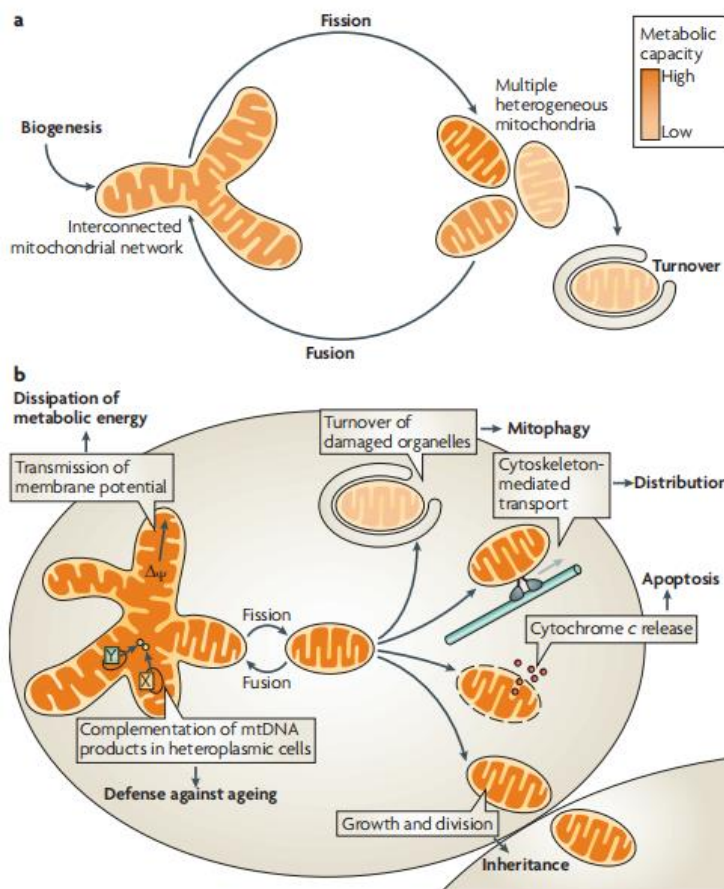


Fig.5. Biological functions of mitochondrial dynamics.

Taken from Westermann B. Nat Rev Mol Cell Biol. 2010

3.3.3 Mitochondrial calcium uptake and mitochondrial calcium entry

Ca^{2+} accumulation in energized mitochondria has been identified half a century ago. In 1961 several studies started to find Ca^{2+} segregation in mitochondria, and a few of them directly measured Ca^{2+} uptake in isolated mitochondria (Deluca & Engstrom, 1961; Lehninger *et al*, 1963; Vasington & Murphy, 1962). On the basis of the Nernst equation, potential gradient resulting from the proton transport of the electron transport chain also becomes a large driving force to pull the Ca^{2+} ion into mitochondria. Now mitochondrial calcium probe carried with Ca^{2+} -sensitive photo protein aequorin (Rizzuto *et al*, 1992) or GFP-based protein construct (Miyawaki *et al*, 1999; Nagai *et al*, 2001) enables to directly assist to measure Ca^{2+} influx into mitochondrial matrix.

Import of Ca^{2+} ion into the matrix through inner mitochondrial membrane (IMM) should rely on an electrogenic channel, called mitochondrial calcium uniporter (MCU) on the IMM. Indeed, the rise and peak of mitochondrial calcium concentration follows with the change of cytosolic Ca^{2+} (Szabadkai *et al*, 2003). One demonstration is that mitochondrial Ca^{2+} uptake occurs in high Ca^{2+} region where Ca^{2+} release from some channels elicits a very strong elevation of cytosolic Ca^{2+} including inositol-1,4,5-trisphosphate-sensitive channels (IP3 receptor) and ryanodine-sensitive channels (RyR) on the endoplasmic reticulum (ER) (Rizzuto *et al*, 1998; Szalai *et al*, 2000) (Fig.6). The ER is the major intracellular pool for Ca^{2+} storage (Somlyo, 1984). The close proximity between mitochondria and ER Ca^{2+} releasing channels transiently enable a prompt Ca^{2+} accumulation in the mitochondria.

Ca^{2+} accumulation into the matrix has to pass through two membranes: IMM and OMM, so components for mitochondrial Ca^{2+} import should be divided into Ca^{2+} channels of IM and OM depending on their locations. Voltage-gated anion channel (VDAC) on the OMM is the gatekeeper for the uptake of cytosolic Ca^{2+} into the OMM, and forms the first bottleneck of rapid mitochondrial Ca^{2+} uptake into the matrix. It was said that VDAC1 established a protein-protein interaction with IP₃R on the ER to transfer the low amplitude Ca^{2+} signal in apoptosis (De Stefani *et al*, 2012).

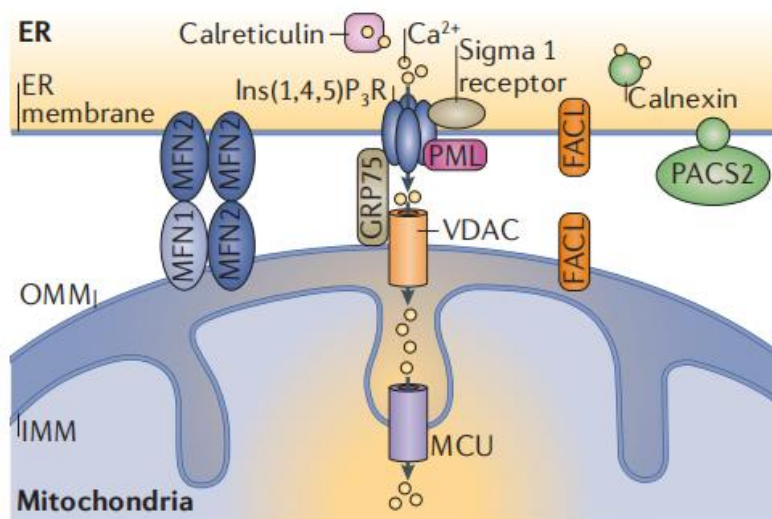


Fig.6. The build-up of ER-mitochondria junction. Taken from Rizzuto R, et al. Nat Rev Mol Cell Biol. 2012.

MCU is the mitochondrial inner calcium channel and characterized as low conductance and highly selective Ca^{2+} channel (Kirichok *et al*, 2004). It binds Ca^{2+} with very high affinity potentiating high Ca^{2+} selectivity in spite of low level of external Ca^{2+} . In terms of the precise regulation of pleiotropic action to Ca^{2+} in mitochondria, MCU is not the only mitochondrial calcium entry (MCE) on the IMM (Fig.7). The mammalian mitochondrial uniporter complex consists of the inner membrane-spanning subunits MCU as the main pore-forming protein, its paralog MCUB, and a small component—essential MCU regulator (EMRE), together with the regulatory subunit mitochondrial calcium uptake1-3 (MICU1-3) (Kamer & Mootha, 2015; Tufi *et al*, 2019b). The Co-existence of MCU and EMRE is critical and sufficient to sustain the uniporter activity in yeast. These experiments indicate that these components are highly conserved across eukaryotes (Bick *et al*, 2012). In MCU knock-out (KO) mice, cardiac mitochondria were incapable of rapidly taking up calcium. The loss of EMRE in drosophila blocks the fast calcium uptake but doesn't cause lethality during development and MICU3 mutant flies is viable with mild neurological dysfunction, while

abrogation of MCU leads to short-lived flies (Tufi *et al.*, 2019b). Genetic interaction analysis found they were functionally independent from each other and not irreplaceable.

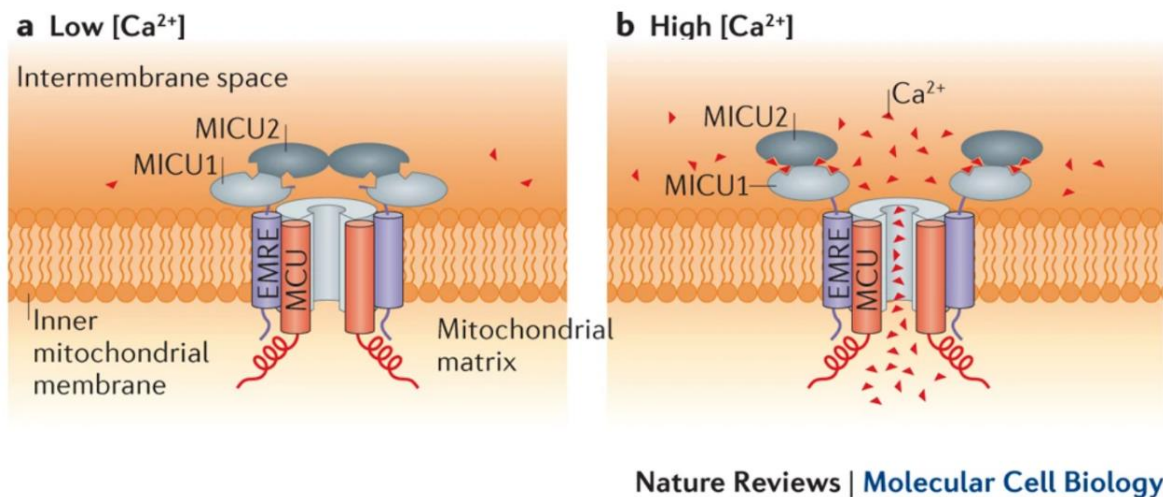


Fig.7. The Ca²⁺-mediated regulation of mitochondrial uniporter complex. Taken from Kamer KJ, et al. Nat Rev Mol Cell Biol. 2015.

3.3.4 Mitochondrial metabolism and ATP production regulated by matrix Ca²⁺

Mitochondrial Ca²⁺ in the matrix poses a crucial regulation of mitochondrial metabolism and ATP production (Boyman *et al.*, 2020b). Mounting evidences have supported the management of mitochondrial Ca²⁺ signaling on mitochondrial metabolism. For instance, defecting mitochondrial calcium uptake was proved to decrease mitochondrial ATP synthesis and compromise oxidative respiration in both drosophila (Tufi *et al.*, 2019b) and mice (Pan *et al.*, 2013) models. Moreover, some studies revealed that the activity of partially purified pyruvate dehydrogenases and

other matrix-localized dehydrogenases in the Krebs cycle were found to be Ca^{2+} -sensitive (Denton *et al*, 1972; McCormack & Denton, 1979), other evidences support matrix Ca^{2+} capably induces cyclic AMP (cAMP) signal and this intramitochondrial cAMP signals are engaged in mitochondrial ATP production (Di Benedetto *et al*, 2013). Collectively, matrix Ca^{2+} sufficiently and efficiently tunes in mitochondrial metabolism through Ca^{2+} -dependent signaling pathways.

3.4 Age-driven mitochondrial dysfunction

3.4.1 Age-related decay of mitochondrial functionality

Mitochondrial decline is long appreciated as one of the hallmarks of aging, suggesting that organism aging and age-related disorders are tightly associated with imbalance in energy supply and demand (Amorim *et al*, 2022). Similarly, we previously observed a drastic decay of mitochondrial respiration with aging by comparing oxygen consumption rate (OCR) in *Drosophila* brains at the age of 3d, 15d and 30d (Liang *et al*, 2021). Based on “the free radical theory”, the progressive oxidative damage was once suggested as a specific driver of aging. However, no clear evidence showed that the clearance of ROS by overexpressing antioxidant would give benefits on longevity of the organism. Besides, the increase of ROS production would not definitely kill the animals and shorten the lifespan (Van Raamsdonk & Hekimi, 2012). Hence, the role of ROS on the aging has been reconsidered. The robustness of mitochondria and metabolic regulation are essential to the maintenance of overall fitness. Age-related mitochondrial dysfunction may be the main reasons for a few age-induced metabolic disease across various organs and tissues, especially with high energy need in human body listed as Fig.8.

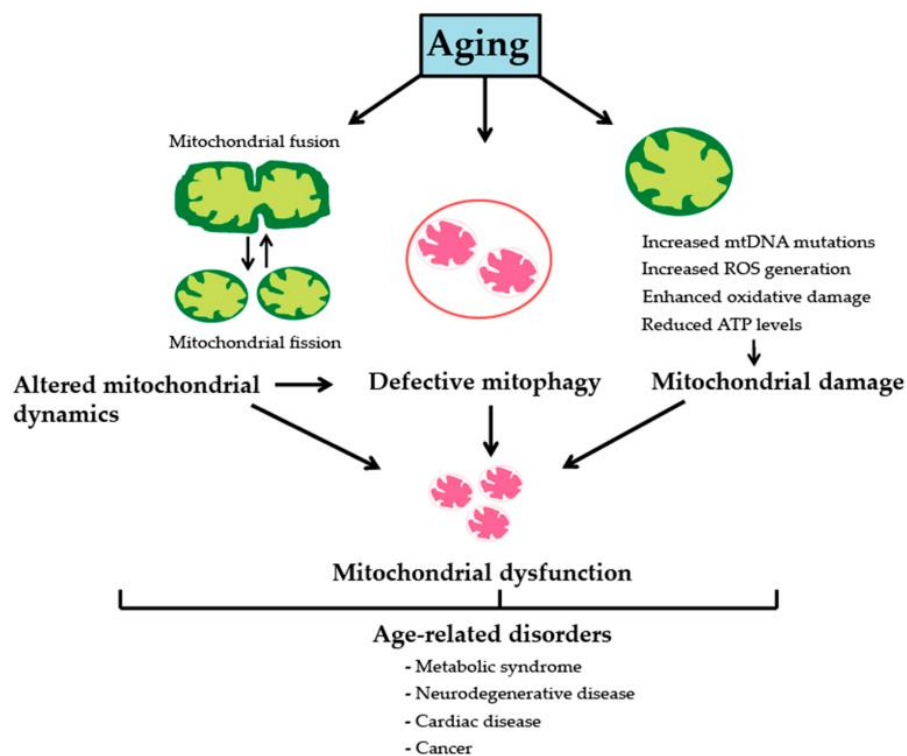


Fig.8. Mitochondrial decline in aging and age-related disorders. Progressive mitochondrial dysfunction is mostly attributed to mtDNA mutation, genomic instability in the nucleus and accumulated oxidative stress from increased ROS production, which might further lead to more oxidative damage, a decline of OXPHOS respiration rate and a reduction of ATP generation. Mitochondrial dynamics is also altered with ageing. Imbalance of fusion and fission would impair mitophagy and lead to untimely removal of damaged mitochondria. Taken from Srivastava S. *Genes* (Basel). 2017.

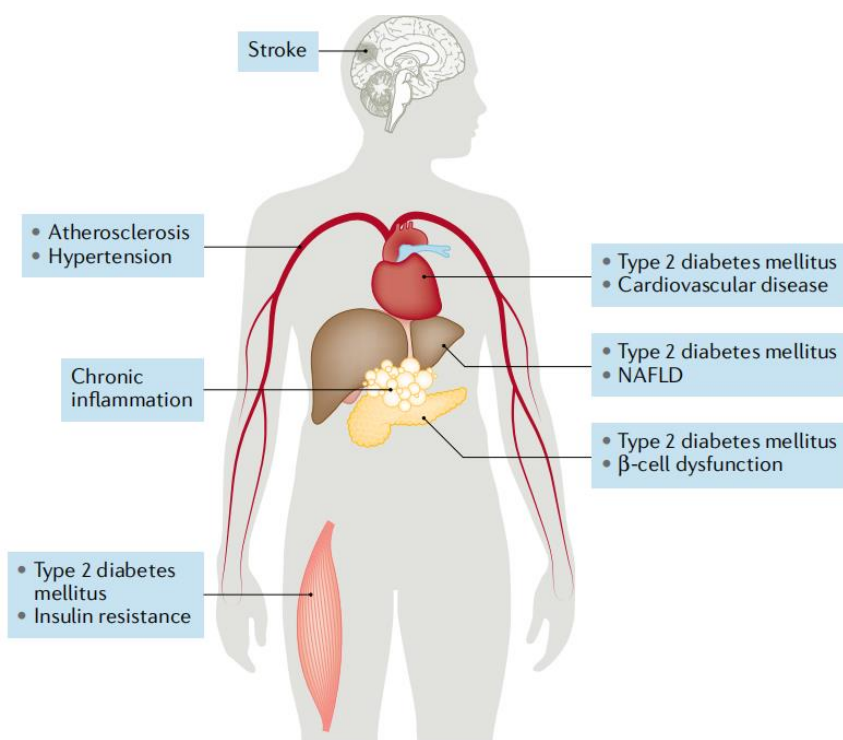


Fig.9. Mitochondrial decay in age-related metabolic disorders. Taken from Amorim JA, et al. Nat Rev Endocrinol. 2022

3.4.2 Main causes of mitochondrial decline: mtDNA mutation and genomic instability

Maternally inherited mtDNA and parental nuclear DNA determine the fitness and energetic capacity of the organism. MtDNA due to its special structure without protective histones, is very sensitive and vulnerable to the age-caused environment variations, so the number of mtDNA mutation increases when the individual gets older (Cortopassi & Arnheim, 1990). Progressive mtDNA mutation and deletions recapitulate the biomarkers of premature aging, such as shortened longevity, hearing loss in mtDNA mutator mouse (Niu et al, 2007). Apart from that, though mtDNA only encodes thirteen mitochondrial proteins, the resultant decline of mutation and deletions of mtDNA causes oxidative damage and loss of energy capacity, and ultimately cell death.

Genomic instability in the nucleus, as another aging hallmark, can also affect the mitochondrial physiology during ageing. Notably, nuclear DNA damage response (DDR) can be triggered with endogenous and exogenous threat. On top of that, a variety of DNA repair mechanism evolved to ensure the correction of nuclear genome. The DNA repair process is also energy-demanding, and long-term and constant DNA disruption would result in mitochondrial deficits and metabolic imbalance.

3.4.3 “The free radical theory of ageing” and ROS signaling

The accumulation of mitochondrial oxidative stress, as the basis of “free radical theory of ageing” has long been recognized as the contributor of aging-related decline, but recently became very controversial concerning its role on ageing (Amorim *et al.*, 2022). The oxidative stress theory of aging (Liguori *et al.*, 2018) reminds us that age-related functional alterations are associated with the accumulation of ROS, and this accumulation now is meant to signal for maintaining organism homeostasis (Shadel & Horvath, 2015). ROS is formed when only one electron is transferred by a redox donor to oxygen, and the main types of ROS which we intend to stress here is superoxide and hydrogen peroxide (H_2O_2). As we mentioned earlier, ROS is the by-product of OXPHOS, and complex I and III are deemed as the major locations where mitochondrial ROS are generated (Murphy, 2009). Superoxide (O_2^-) is produced in both sides of IMM, which means, O_2^- is present in both mitochondrial matrix and intermembrane space (IMS). Superoxide dismutase enzymes, including SOD1 and SOD2 enable to convert anionic free-radical superoxide (O_2^-) into H_2O_2 , which is then allowed to diffuse across mitochondrial OM and into the cytoplasm. And yet, whether H_2O_2 experience free diffuse or diffuse through special channels still needs to be well elucidated. O_2^- unlike H_2O_2 , is a negatively charged molecule and cannot diffuse freely, so O_2^- behaves distinctly different from hydrogen superoxide.

Redox-dependent modifications such as oxidation, glutathiolation and S-nitrosation in modified proteins may bring about cellular redox-switch regulatory mechanism (Finkel, 2012; Go *et al*, 2015). Apart from directly signaling in cytoplasm, superoxide and H₂O₂ capably oxidize some mitochondrial proteins as second messengers released into the cell plasm (Fig.10).

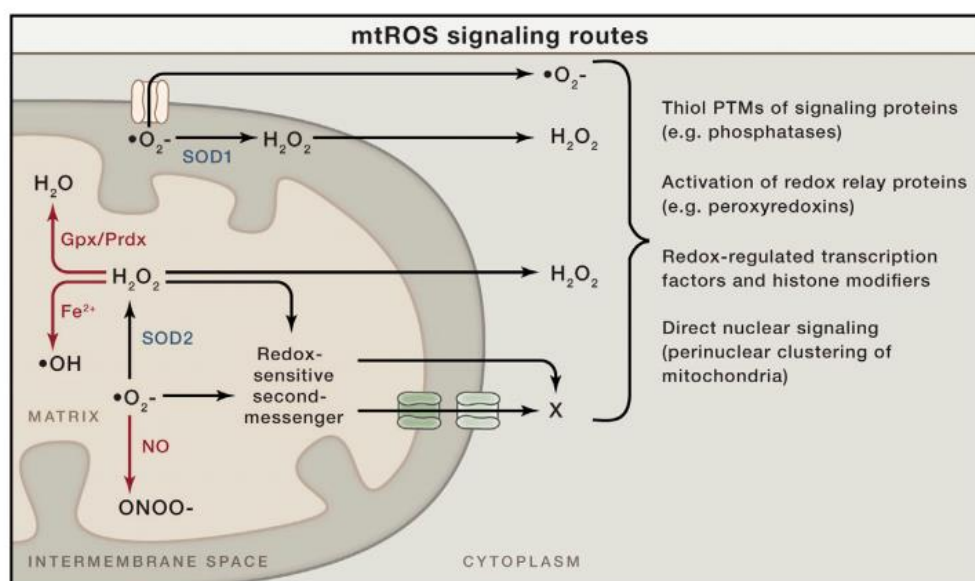


Fig.10. mitochondrial ROS signaling routes. Taken from Shadel GS, et al. Cell. 2015.

3.4.4 ROS signaling and “mitohormesis” in promoting health and longevity

Extensive studies now support the active role of mitochondrial ROS signaling on adaptive response and organism physiology (Hamanaka & Chandel, 2010; Ristow & Zarse, 2010; Yun & Finkel, 2014). Mitochondrial production of ROS is critical for sustaining the oxidative homeostasis and propagation of several signaling pathway. In *C. elegans*, increased mitochondrial ROS generation and signaling pathway were reported to extend the longevity. These investigations challenged “the free radical

theory” and raised up that ROS predisposed to serve as “pro-longevity” signals rather than a damaging, “pro-aging” signal. This traditional idea started to change since restriction of glucose was found extend the lifespan and promote mitochondrial respiration in worm aging (Schulz *et al*, 2007). The concept of “mitohormesis” has increasingly gained attention of many scholars focusing on anti-aging paradigm. Mitohormesis is a process in which a relatively low concentration of ROS produced in the mitochondria serves as a signaling molecule and initiates a cascade of signaling events in promoting health and lifespan.

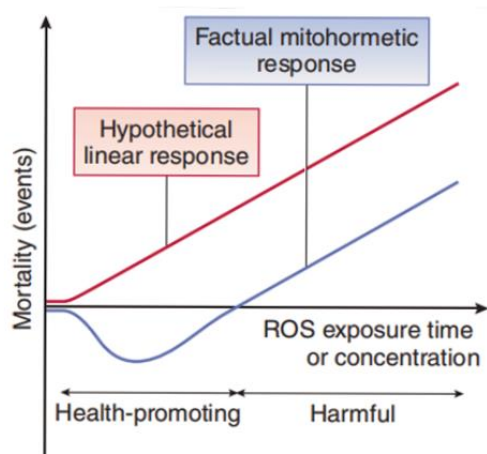


Fig.11. The links between mitohormesis and the amount of ROS. Taken from Ristow M. Nat Med. 2014

Mitochondrial hormesis engages a nonlinear response to the amount of mtROS upon endogenous stress (Ristow, 2014) (Fig.11). When ROS level is relatively low, it comes to a beneficial health-promoting zone; whereas, when ROS concentration and exposure time keep rising, the harmful effects and mortality would arise and increase. Excessive load of ROS has long considered as the main cause of oxidative stress, so

antioxidants which oppose the effects of ROS correspondingly become a popular dietary supplement in people's daily life. Nonetheless, placebo-controlled intervention studies did not prove the profitable impact of antioxidant supplement. Evidences were gained in a few meta-analyses with large population-based intervention trials. The first meta-analysis including 24 high quality studies with 324653 population revealed that neither vitamin E nor vitamin A precursor- β Carotene did harm or benefit in preventing cardiovascular disease(CVD) or cancer (Fortmann *et al*, 2013). A similar outcome was also reported by another meta-analysis conducted to evaluate the benefit of dietary supplementation (multivitamin, vitamin B, E or with vitamin A) on cognitive or physical function in persons with mild cognitive impairment (MCI) (Lin *et al*, 2013). Moreover, a disappointing randomized clinical trial (RCT) involving around 6000 people at the age of 65 taking multivitamin found no difference in cognitive performance after over 12 years follow-up (Grodstein *et al*, 2013). Vitamin A, C and D and β Carotene are the supplementary intake of antioxidants. However, intaking fruits and vegetables are indispensable for people's daily life. The advantages of intaking fruits and vegetables may happen to contain these antioxidants but not really derived from ROS quenching effects of these antioxidants.

It should be mentioned that, physical exercise, especially endurance training was about to produce more ROS. long-term increase of physical activity is well known to prevent metabolic syndrome, CVD and dementia, and prolong human lifetime (Warburton *et al*, 2006). Recently, plenty of molecular evidence have proven that ROS enables initiating a molecular stress response in promoting health and longevity (Fig.12).

Proper limitation of energy intake, also known as calorie restriction (CR) has long been recognized as an anti-aging paradigm. The longevity-extending effect of CR is attributed to activate mitochondrial respiration in yeast (Lin *et al*, 2002) and promote the formation of additional ROS in *C.elegans* (Schulz *et al.*, 2007), and antioxidant feeding abolished this extension effect in worms, which further confirmed the initial

signaling role of ROS. Apart from CR, mild mitochondrial dysfunction and deficit insulin signaling prolonged the lifetime of worms (Yang & Hekimi, 2010) and drosophila (Owusu-Ansah *et al*, 2013) which have suggested to connect with transient increase of ROS.

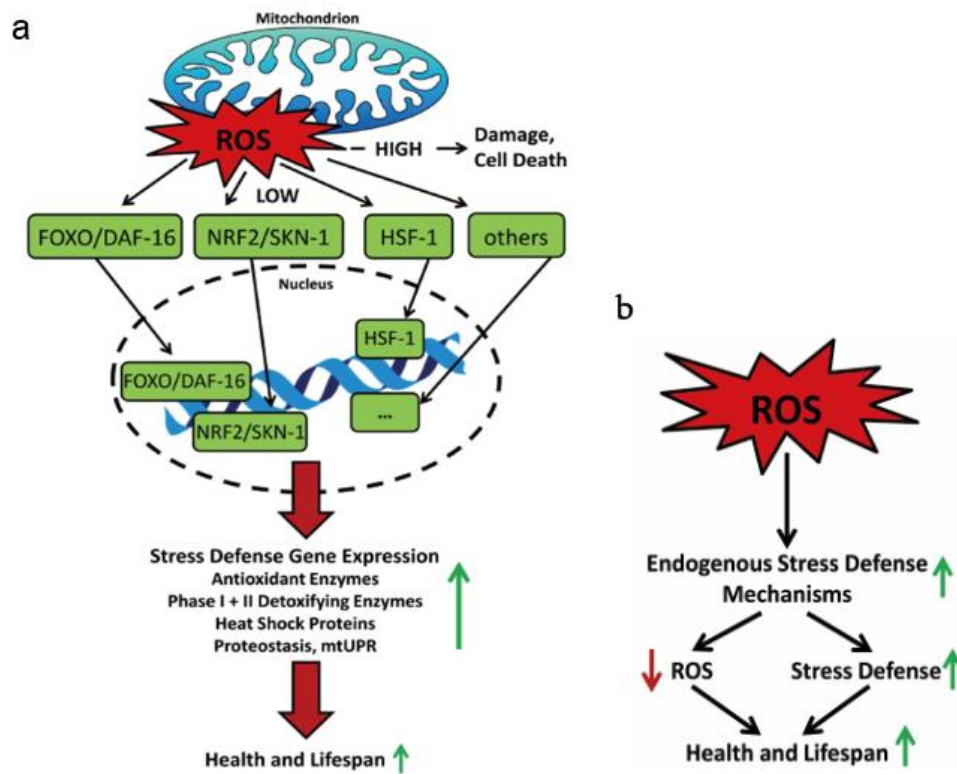


Fig.12. A molecular basis of how ROS stimulates transcription changes to promote health and lifespan. Taken from Ristow M, Schmeisser K. Dose Response. 2014

Though a very high amount of ROS leads to cell death, increased mitochondrial ROS serving as signaling molecules, activates retrograde response and causes transcriptional changes in the nucleus when faced with external pressure. The perceived downstream effectors of transient elevated ROS have included the transcription factor hypoxia-inducible factor-1 (HIF1), nuclear factor-like 2 (NRF2) and forkhead box O proteins (FoxOs), the mitochondrial unfolded protein response

(UPRmt) which to certain extent have been proved in some experiments in vivo and in vitro (Sena & Chandel, 2012; Yun & Finkel, 2014). On the basis of “mitohormesis”, upon stress increased mitochondrial ROS production are more likely to activate “mitochondrial retrograde response” and link with transcription change in the nucleus to reversely strengthen mitochondrial activity and stress resistance, which might serve as the mechanistic basis of lifespan-extending effects of health-promoting interventions, such as physical exercise and CR. Nonetheless, in-depth investigations should be warranted to further elucidate the latent regulatory mechanism.

3.5 Mitochondria-targeted anti-ageing therapies

In addition to intervention of lifestyle, such as exercise, CR and fasting, pharmacological treatment targeting mitochondria has increasingly been appreciated in anti-aging paradigms. According to their different regulatory mechanism, several categories have been made to explain their respective functions and benefit in age-induced mitochondrial dysfunction.

Among them, one type is small molecules like polyphenols. Resveratrol is one of commonly known polyphenols, and its health-promoting and lifespan-extending benefit has been validated in various animal models, such as yeast, worms, drosophila and mice models (Baur *et al*, 2006). Multiple studies demonstrated resveratrol improves mitochondrial physiology (Davinelli *et al*, 2020; Price *et al*, 2012). Resveratrol-treated mice have been observed to boost mitochondrial biogenesis and functionality, increase the level of nicotinamide adenine dinucleotide (NAD⁺) in a NAD-dependent deacetylase sirtuin-1 (SIRT1)-dependent manner (Price *et al*, 2012). Notably, another small molecule, called metformin, a widely-used anti-diabetes drug potentiates mitochondrial energy production through activating AMP-activated protein kinase (AMPK). Besides, mTOR inhibition by rapamycin has showed great beneficial efficacy on health and longevity in multiple models (Garay, 2021). Also, rapamycin

exhibits protective properties on diet-induced obesity: improving insulin resistance and enhancing mitochondrial biogenesis (Deepa *et al*, 2013).

Drug type	Drug name	Most advanced stage
Small molecule	Resveratrol	Clinical
	SRT1720	Preclinical
	SRT2104	Clinical
	Punicalagin	Preclinical
	Epicatechin	Clinical
	Oleuropein	Preclinical
	Metformin	Clinical
	Imeglimin	Clinical
	TPP-thiazole	Preclinical
	Rapamycin	Clinical
	Leucine	Clinical
NAD ⁺ -boosting molecules	Nicotinamide mononucleotide	Clinical
	Nicotinamide riboside	Clinical
	Nicotinamide	Preclinical
Mitochondrial uncouplers	DNP methyl ether	Preclinical
	Controlled release mitochondrial protonophore	Preclinical
	Niclosamide ethanolamine	Preclinical
	1,3-bis(dichlorophenyl)urea	Preclinical
	CZ5	Preclinical
	OPC-163493	Preclinical
	BAM15 and derivatives	Preclinical
	Compound 6j	Preclinical
HU6	Clinical	
Mitochondrially-targeted antioxidants	Mitochondrially-targeted coenzyme Q	Clinical
	Mitochondrially-targeted vitamin E	Preclinical
	Elamipretide	Clinical

Table1. Modifying therapies targeting mitochondria in age-related metabolic disorders.

Taken from Amorim JA, et al. Nat Rev Endocrinol. 2022.

The second mitochondria-targeted intervention extensively tested is NAD⁺-boosting molecules. NAD⁺ level significantly dropped with aging, and supplementation used to

boost NAD⁺ level in the organism has been recognized as a way to alleviate aging-related metabolic disorders (Rajman *et al*, 2018). Supplementation of NAD⁺ precursor nicotinamide mononucleotide (NMN) and nicotinamide riboside both enable to facilitate mitochondrial function and improve glucose homeostasis in mice with obesity (Cantó *et al*, 2012). Moreover, small molecules, like mitochondrial uncoupler is to reduce mitochondrial coupling efficiency, and consequently activate nutrient oxidation to synthesize ATP. The mitochondrial uncoupler 2,4-dinitrophenol (DNP) has manifested the potential therapeutic benefit in obesity and other metabolic disease (TAINTER *et al*, 1933). Mice treated with low-doses DNP increased mitochondrial respiration activity, reduced oxidative stress and body weight and enhanced the lifetime (Caldeira da Silva *et al*, 2008). Lastly, aging is associated with the accumulation of oxidative stress, so mitochondria-targeted antioxidants have been explored as a protective strategy of age-driven diseases. Mitochondria-targeted coenzyme Q (mitoCo Q) now has been widely applied in clinical therapy due to its benefit of neuroprotection (Zhou *et al*, 2018) and amelioration of oxidative stress (James *et al*, 2007) in preclinical studies. More detailed categories of mitochondria-targeted molecules and its preclinical or clinical status are listed in **Table1** (Amorim *et al.*, 2022).

3.6 The interaction between synapses and mitochondria

The brain only occupies less than 2% mass of the whole body, but it has to utilize over 20% of the total energy consumption. Most of the energy expenses derive from active neuronal activity, during which the occurrence of action potential has to reverse the potential gradients across the cytoplasm membrane and synaptic vesicle are releasing and recycled at the synaptic terminal (Rossi & Pekkurnaz, 2019). Large amounts of mitochondria tightly pack at the synapses and constantly provide the ATP

supply and buffer Ca^{2+} due to its mobility and energy provision during synaptic information processing (Ly & Verstreken, 2006). Mitochondrial activities are regulating synaptic activity. Reversely, in response to the changing energy and metabolic state at the synapses, mitochondria are also undergoing functional and morphological alterations, called “mitochondrial plasticity” (Rossi & Pekkurnaz, 2019). Herein a summary about recent findings will be made to discuss on the mutual interconnection between mitochondria and synapses.

3.6.1 The role of Mitochondria in synaptic plasticity

The glycolysis provides very limited (only 10%) energy capacity of neurons, so mitochondrial oxidative respiration delivers the main energy support to fuel synaptic processes. ATP produced by mitochondria is essential to many events at the synapses. For instance, the maintenance of many ion channels and pumps activities are dependent on ATP. Specifically, neuronal mitochondria have a significant role in keeping the homeostasis of cellular calcium. In addition to directly buffering calcium, mitochondria also support the necessary energy supply for the activity of Ca^{2+} -ATPase and indirectly preserve Na^+ gradient which strongly impacts the $\text{Na}^+/\text{Ca}^{2+}$ exchanger activity (Duarte *et al*, 1991). Besides, calcium-triggered vesicle fusion with presynaptic membrane and neurotransmitter releasing and recycling are both highly ATP consuming processes (Rangaraju *et al*, 2019). Especially, local generation of ATP from mitochondria promotes endo- and exocytosis, and facilitates vesicle refilling and neurotransmitter re-uptake at presynaptic terminal (Pekkurnaz & Wang, 2022). Energy generation and consumption at the synapses are shown in Fig.13.

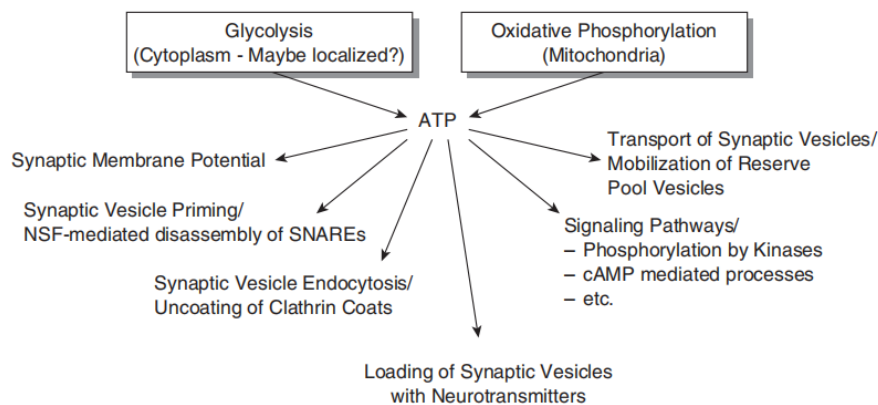


Fig.13. ATP generation and consumption at the synapses. Taken from Ly CV, Verstreken P. Neuroscientist. 2006.

Mitochondria are known to buffer calcium at synapses. Mitochondrial calcium has significant physiological properties of regulating synaptic transmission (Fig.14). Mitochondrial calcium buffering operates even at neuronal resting state. Primarily, calcium buffered by mitochondria influences large evoked calcium responses in most of cell types. It was observed in mouse taste cells that mitochondria still contribute to buffer Ca^{2+} which leaks from ER calcium releasing pool even when neurons are at rest (Hacker & Medler, 2008), whereas block of mature zebrafish hair cell inhibits presynaptic calcium influx and affects synaptic integrity (Wong *et al*, 2019). Moreover, spontaneous mitochondrial calcium upload would alter cellular $NAD^+/NADH$ ratio, which further decreases synaptic size (Wong *et al.*, 2019).

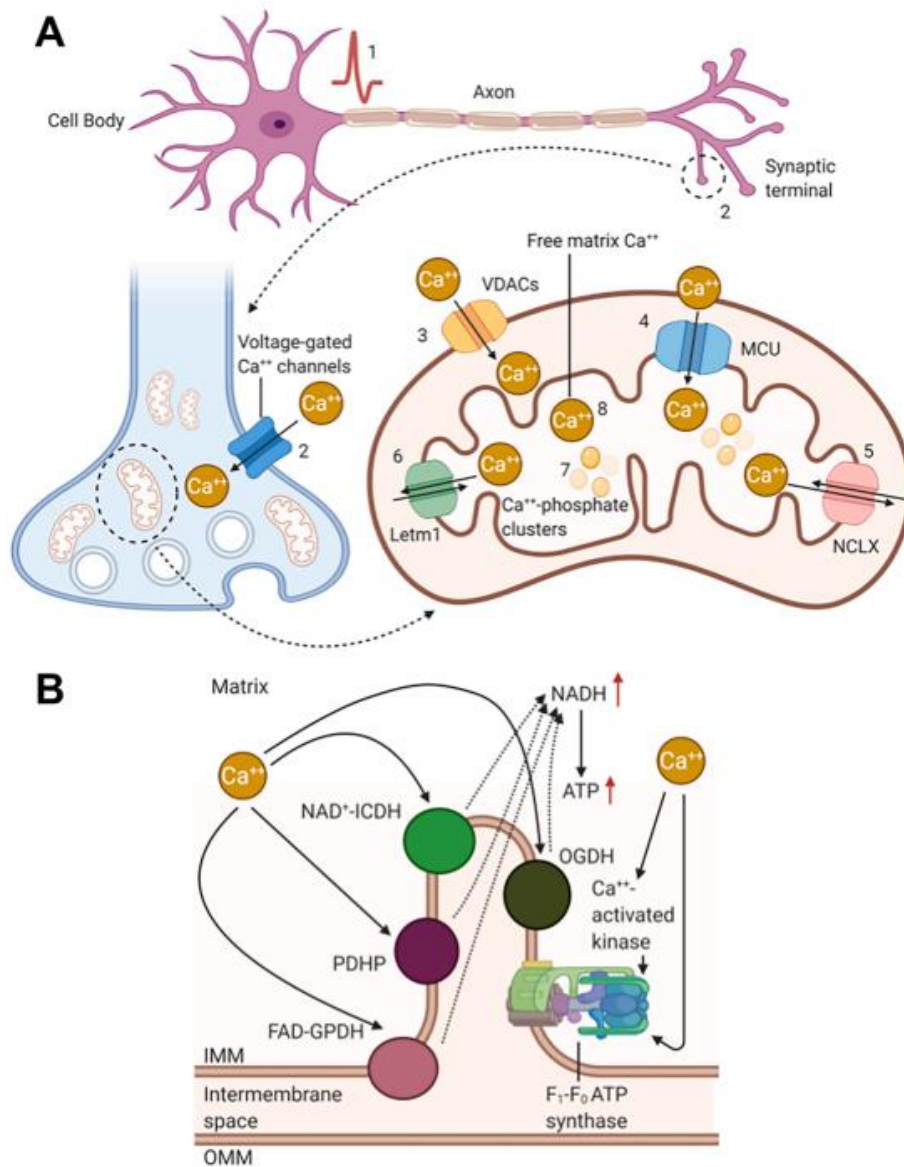


Fig.14. Mechanisms of mitochondrial Ca^{2+} influx and activity-dependent increase in ATP production at synapse. Taken from Datta S, et al. Mitochondrion. 2021.

Action potential generated in the axons opens calcium channel on the presynaptic membranes, Ca^{2+} consequently rapidly flows into the presynaptic bouton, and results in the fusion of synaptic vesicle with presynaptic membrane. Increased Ca^{2+} presynaptic influx also contributes to the increase of mitochondrial Ca^{2+} influx. As we mentioned before, mitochondrial Ca^{2+} uptake regulates mitochondrial metabolism and

ATP production. Thus, elevated mitochondrial Ca^{2+} intake facilitates activity-driven ATP synthesis to satisfy the energy requirement during synaptic transmission (Rangaraju *et al*, 2014). Ca^{2+} in the matrix enables to affect ATP generation through the activation of several mitochondrial dehydrogenase enzymes, such as glycerol phosphate dehydrogenase, pyruvate dehydrogenase phosphatase, NAD^+ isocitrate dehydrogenase, and 2-oxoglutarate dehydrogenase (Denton *et al*, 1978), and mitochondrial ATP synthase (Territo *et al*, 2000). The specific mechanism of Ca^{2+} -dependent ATP production in mitochondria is illustrated in Fig. **14B**. Another important role of mitochondrial Ca^{2+} influx is during high frequency stimulation, mitochondria uptake extra cytosolic Ca^{2+} and gradually release over time (Tang & Zucker, 1997). Mitochondrial Ca^{2+} release was reported to enhance vesicular release probability but not altering global presynaptic $[\text{Ca}^{2+}]$ during short-term facilitation (Yang *et al*, 2021). It was hypothesized that mitochondrial ATP production can help with sustaining synaptic transmission during weaker stimulation while activity-driven ATP facilitation is also involved during a stronger higher frequency stimulation. The contribution of glycolysis versus oxidative phosphorylation for presynaptic function is not well defined. Nevertheless, OXPHOS enables to fuel higher energy demanding process like vesicle endocytic recovery (Sobieski *et al*, 2017). Taken together, mitochondrial calcium influx and ATP production indeed play a critical role for the successful and sustained transmission in response to high frequency stimulation.

3.6.2 ROS signaling for synaptic plasticity

Concerning the relations between mitochondria and synapses, the essential role of ROS for synaptic plasticity has to be separately sketched out.

Neuronal plasticity is important to the development of neural networks and underlies learning and memory process. Synaptic plasticity is characterized by its capability to adjust its strength, structure and connectivity responding to experienced activity.

Synaptic strength can either be facilitated or ameliorated relying on distinct context and the nature of the coming stimulation.

Intrinsic and pharmacologically forced synaptic inactivity induces mitochondrial ROS generation (Sidlauskaite *et al*, 2018), In addition, the activation of NMDA receptor can trigger ROS generation within mitochondria (Bindokas *et al*, 1996; Dugan *et al*, 1995). Synapse pruning during development was reviewed to be a beneficial process to select and eliminate the weak inputs, thus refining neuronal connections during development given the limited availability of unique cues (Neniskyte & Gross, 2017; Riccomagno & Kolodkin, 2015). Neuronal activity ties mitochondrial ROS production to synaptic pruning. At the neuromuscular junction (NMJ) with its structural simplicity, size and accessibility, mitochondrial ROS was observed to behave as synaptic activity sentinels and regulates the phenotypical consequences of synaptic inactivity. Increased mitochondrial ROS production was proposed to prune inactive synapses by activating intrinsic apoptosis (Cobley, 2018; Sidlauskaite *et al*, 2018). In addition, under pathological condition, oxidative stress can regulate synaptic terminal overgrowth. In a drosophila model of lysosomal storage disease (LSD) (Milton *et al*, 2011), increased autophagy results in elevated ROS level and increased oxidative stress enables the activation of JNK/AP-1 signaling pathway, which potentiates synaptic terminal overgrowth and regulates synaptic strength.

Moreover, the role of ROS for synaptic transmission has been demonstrated by several models and regions of neuron (Fig.15).

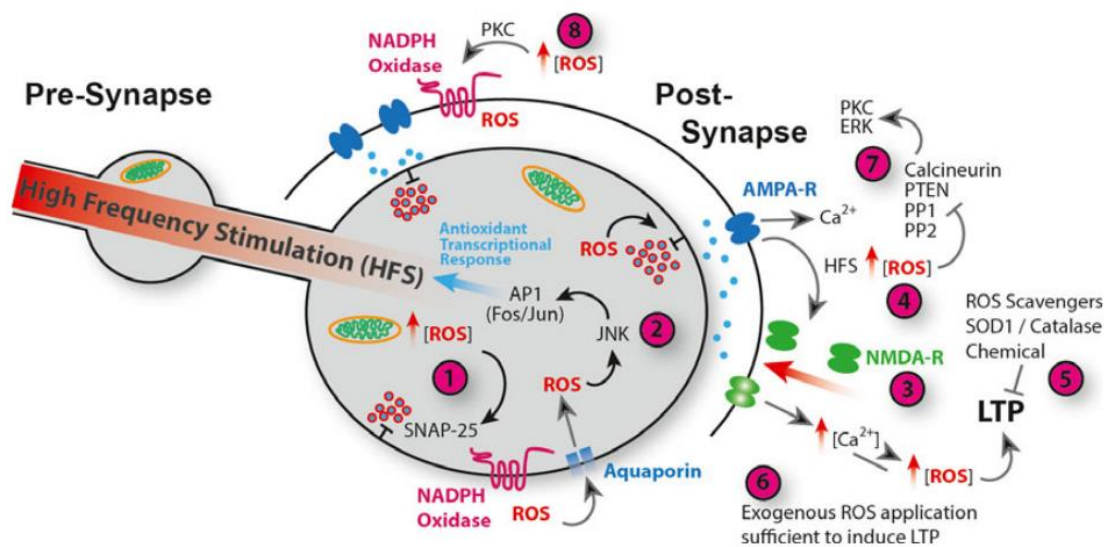


Fig.15. ROS regulation of synaptic plasticity. (1). ROS at pre-synapses generated by mitochondria or NADPH oxidase inhibits releasing probabilities by direct oxidation of fusion protein—SNAP-25; (2) Activation of JNK and AP-1 signaling pathway induced by increased ROS level promotes the transcriptional expression of antioxidant encoding genes and mediates adaptive response in neurons to oxidative stress; (3) The HFS for inducing LTP also leads to opening of postsynaptic NMDA receptor and increased extracellular Ca^{2+} ; (4) HFS results in ROS elevation, and transforms to a oxidative environment at the synaptic terminal; (5) HFS-induced LTP needs ROS regulation; (6) ROS exposure is sufficient to induce a long lasting potentiation.(7) ROS regulates synaptic plasticity pathway through inhibition of redox-sensitive effector proteins PP1, PP2, PTEN and Calcineurin leading to enhanced kinase signalling containing ERK and PKC; (8) ROS-stimulated PKC enables the activation of NADPH oxidase and further escalate ROS generation. Taken from Oswald MCW, et al. FEBS Lett. 2018

Dysregulation of ROS by interfering with the expression of antioxidant, such as SOD1 or Catalase blocks the long-term potentiation (LTP) in hippocampal slices (Gahtan *et al*, 1998; Klann *et al*, 1998). Stimulation of JNK and AP-1 induced by elevated ROS level was found to promote transcriptional expression of antioxidant

encoding genes *Srxn-1* (Baxter & Hardingham, 2016; Ugbo *et al*, 2020), and the effector protein of AP-1 mediates synaptic long-term plasticity (Sanyal *et al*, 2002). The high-frequency stimulation (HFS) for inducing LTP also leads to opening of postsynaptic NMDA receptor and increased extracellular Ca^{2+} . Application of ROS by exposure to xanthine/xanthine oxidase(x/xo) is sufficient to induce a long-lasting potentiation and LTP via activation of protein kinase C(PKC) (Klann *et al.*, 1998; Knapp & Klann, 2002a). Source targets of ROS and the interplay between ROS regulatory pathway and Ca^{2+} signaling would be involved in synaptic plasticity. ROS regulates redox modification effector proteins involved in several signaling pathway. Redox sensitive protein phosphatases (PP), such as PP1, calcineurin (Namgaladze *et al*, 2002), the phosphatase and tensin homolog deleted on chromosome 10 (PTEN) (Wu *et al*, 2013) are under the control of ROS. Neuronal ROS behaves as a second messenger to tune in neuronal plasticity and structural plasticity via partly modulation of PTEN-PI3K signaling leading to activated kinase signaling containing ERK and PKC (Oswald *et al*, 2018). Meanwhile, direct regulation of synaptic protein by redox modification also seems accessible. At frog NMJ, extracellular recordings (Giniatullin & Giniatullin, 2003) indicated prolonged presynaptic calcium influx with the application of high H_2O_2 , which means ROS inhibited the evoked quantal release. Further experiments have implicated the inhibitory regulation of vesicle releasing might derive from the direct oxidation of pre-synaptic ROS sensor—synaptosomal-Associated Protein, 25kDa(SNAP25), one of the essential fusion proteins (Giniatullin *et al*, 2006). Collectively, ROS enables adjustment of synaptic strength or potentiates direct modification of the composition of synaptic protein complexes.

3.6.3 Mitochondrial plasticity at synapses

“Mitochondrial plasticity” at synaptic sites, refers to the dynamic network of mitochondria has to experience functional and structural adaptations in response to synaptic metabolic need. Mitochondria have the capacity to go through functional, morphological and metabolic distinctions across various cell types, largely depending on their mobility and dynamic change of fusion-fission rates (Benador *et al*, 2019) (Fig.15). Mitochondria usually move along the cytoskeletal tracks. In neurons and fibroblasts, mitochondria transport along microtubules or the actin cytoskeleton from the cell body to the typically very distant synaptic terminal. Relative to other cell types, the density of neuronal mitochondria is much higher. Given that neuron is highly polarized cell with extraordinary energy requirements, mitochondria with their wide distribution at both pre- and post- synapses and mobility, are appropriate candidates to fulfill the energy need.

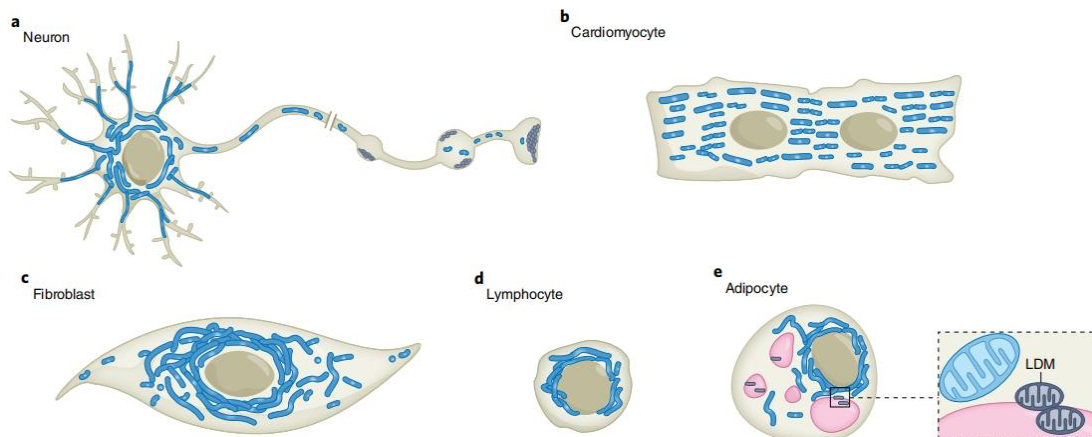


Fig.16. Distinct mitochondrial network in different cell types. Mitochondrial morphology is tailored to fit into the metabolic need of various cells (Pekkurnaz & Wang, 2022). Taken from Pekkurnaz G, et al. Nat Metab. 2022.

Synaptic activity mediates mitochondrial motility (trafficking and positioning) and energy metabolism at axons and dendrites. The precise positioning and localization of mitochondria is essential to sustain energy homeostasis and synaptic function. For instance, deletion of the critical fusion protein dynamin-related protein 1 (Drp1) in mice dopaminergic neurons (DAN) disrupted mitochondrial movement in axons and rapidly eliminated nigrostriatal DAN (Berthet *et al*, 2014). Similarly, mitofusin2 (Mfn2) mutation in mouse dorsal root ganglion (DRG) cultures suppressed mitochondrial transport and led to axon degeneration (Misko *et al*, 2012). Nascent neurons largely depend on glycolysis for ATP provision, while during neuronal differentiation, neuronal metabolism has gradually shifted to oxidative phosphorylation concomitant with up-regulation of mitochondrial biogenesis (Agostini *et al*, 2016). Selective capture and immobilization of mitochondria is indispensable for the maintenance and growth of axonal branches (Courchet *et al*, 2013). As neurons get mature, the vast majority of mitochondria settle down at the axons which may not be rapidly altered by stimulation of synaptic plasticity (Smit-Rigter *et al*, 2016), such as theta burst stimulation-mediated long-term LTP (Smith *et al*, 2016). Despite mitochondria are not present at every single synapse, the existence of mitochondria at presynaptic terminals augments quantal releasing probability (Smith *et al.*, 2016) and promote synaptic stability (Lees *et al*, 2019). The long-distance transport of mitochondria to synapses relies on microtubule and local actin cytoskeleton (Fig.17). Still, in presynaptic bouton, activity induced energy deficits activates the AMP-activated protein kinase (AMPK)-p21-activated kinase (PAK) energy signaling pathway and triggers the phosphorylation of motor protein myosin VI which drives mitochondrial recruitment. Mitochondria can later be docked on either microtubule or local actin cytoskeleton via syntaphilin (Li *et al*, 2020). Synaptic activity facilitates ATP production including glycolysis and oxidative respiration which is likely induced by Ca²⁺ influx (Rossi & Pekkurnaz, 2019). Glycolysis is the first metabolic pathway to convert glucose into pyruvate and generate two ATP molecules, while oxidative respiration consumes oxygen and yields almost 36 ATP

molecules via TCA cycle. The variation of ATP production makes glycolysis more flexibility for rapid energy supply while oxidative phosphorylation offers more stable and efficient energy provision. In order to meet the activity-driven energy demands during synaptic transmission, there exist several metabolic adaptations at presynaptic boutons. First of all, the mobilization of the glucose transporter (GLUT4) to transport glucose into axonal presynaptic membrane allows a more efficient energy supply required for active synaptic activity (Ashrafi *et al*, 2017). Besides, under condition of intense energy need, Glycolytic enzymes can redistribute and colocalize to form the glycolytic metabolon locally adjacent to synapses (Jang *et al*, 2016).

Mitochondrial architecture is another indication of altered mitochondrial function. Morphological dynamics via constant fusion and fission, cristae structure and formation of mitochondrial nanotunnels all contribute to synaptic function (Fig.16b). Ablation of Mitochondrial fission factor (MFF) was observed to cause elongated presynaptic mitochondria and decrease presynaptic release during neurotransmission (Lewis *et al*, 2018). On the other hand, mitochondria are reshaped by instant synaptic energy requirement. Ultrastructure features of presynaptic mitochondria are coupled with synaptic strength. GABAergic inputs contain respectively regular spiking and fast spiking interneuron. Fast spiking interneuron shows relatively high synaptic activity and presents higher cristae density of mitochondria compared to slow-firing interneurons (Cserép *et al*, 2018). Taken together, mitochondrial heterogeneity orchestrates diverse metabolic regulatory response to the spatial-temporal metabolic burden of the neuron.

Mitochondrial decay and synaptic alterations are both appreciated as significant contributors to the aging process in the human brain. While mitochondria are highly prevalent in presynaptic boutons and located proximally to synaptic release sites, potential crosstalk between the early aging of these subsystems remains enigmatic. *Drosophila melanogaster*, characterized by a numerical simpler genome conducive to numerous advanced transgenic operations and a relatively short lifespan facilitating

the monitoring of physical changes throughout the aging trajectory, serves as a valuable animal model for investigating aging and neurodegenerative diseases. Here, we set out to build up genetic *Drosophila* models to analyze the interconnections between mitochondrial status and the synaptic changes associated with early brain aging.

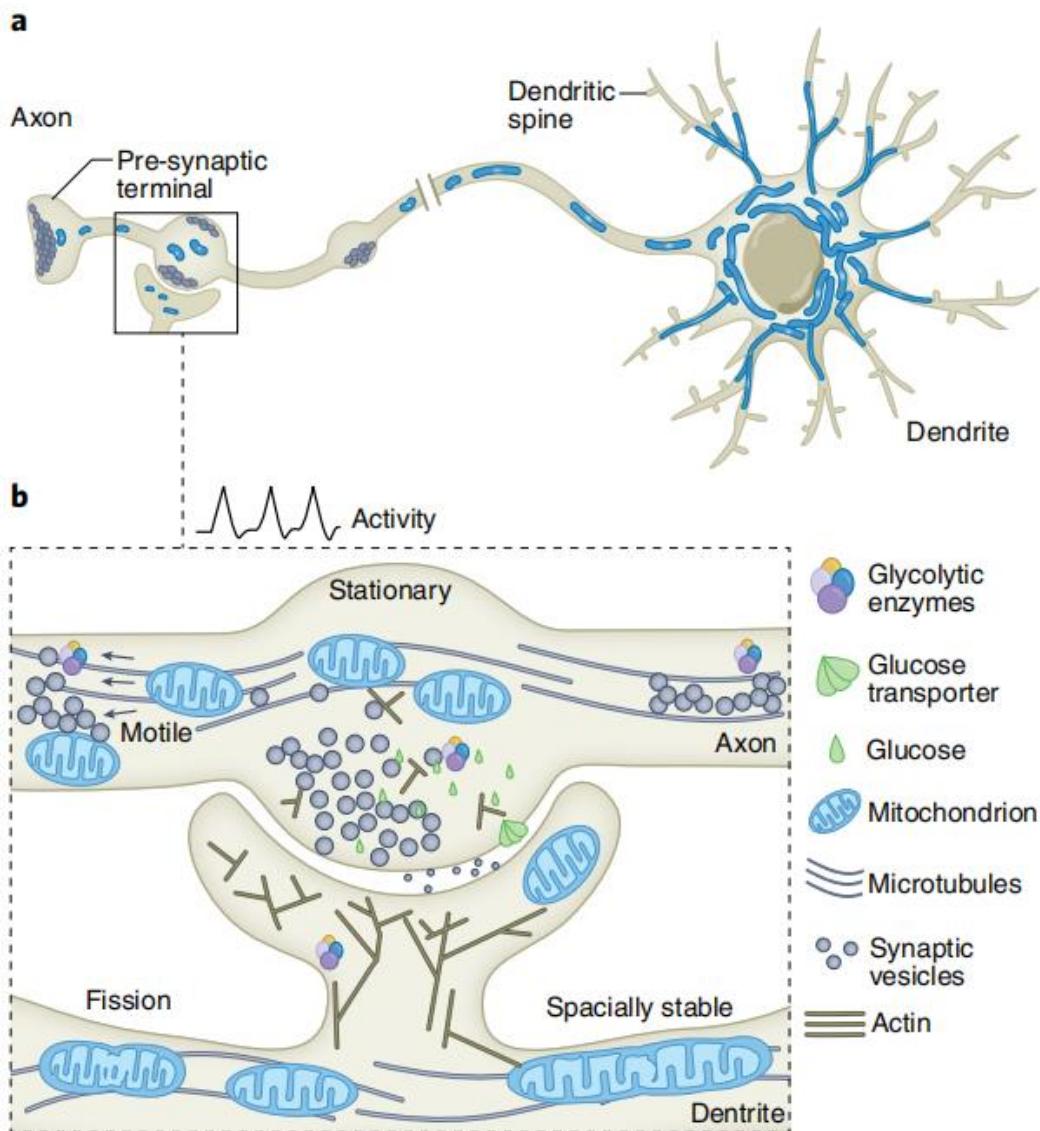


Fig.17. Mitochondrial morphology and positioning in synapses. Taken from Pekkurnaz G, Wang X. *Nat Metab.* 2022.

4. Materials and methods

4.1 Antibodies, primers and chemicals

4.1.1 Primary and Secondary antibodies

The primary and secondary antibodies used in this project are respectively listed in Table3 and Table4.

Table2. the primary antibodies used in this project

Antibody	Species	Dilution	Source
Anti-BRP ^{NC82}	Mouse	IHC 1:50	Developmental Studies Hybridoma Bank
Anti-BRP ^{D2}	rabbit	WB 1:20,000	Sigrist's lab
Anti-Drep2	rabbit	IHC 1:500	Sigrist's lab
Anti-Drep2	Guinea pig	IHC 1:500	Sigrist's lab
Anti-ATP5A	Mouse	IHC 1:500 gSTED 1:200	abcam
Anti-COXIV	rabbit	IHC 1:500 gSTED 1:100	abcam
Anti-sNPF	rabbit	IHC 1:1000	Jan Veenstra
Anti-Ref(2)P	rabbit	IHC 1:5000	Gabor Juhasz
Anti-Dlg	rabbit	WB 1:50,000	Ulrich Thomas
Anti-Tubulin	mouse	WB 1:10,000	Sigma
Anti-GFP	Chicken	IHC 1:1500	abcam

Table3. the secondary antibodies used in this project

Fluorophore	Species	Dilution	Source
Alexa Fluor488	Goat anti mouse	1:400	invitrogen
Alexa Fluor488	Goat anti chicken	1:400	invitrogen
Cy3	Goat anti mouse	1:400	invitrogen
Cy5	Goat anti rabbit	1:400	invitrogen
STAR RED	Goat anti mouse	1:200	invitrogen

Alexa 594	Goat anti rabbit	1:200	invitrogen
HRP conjugated	Goat anti rabbit	1:5000	Jackson ImmunoResearch
HRP conjugated	Goat anti mouse	1:5000	Jackson ImmunoResearch

4.1.2 Primers of Oligonucleotides

Oligonucleotides listed in Table5 were used for the real-time qPCR experiment to amplify mitochondria-encoded genes and nucleus-encoded genes.

Table4. Primers used in this project

Primer	Sequence (5'→3')	Targeted gene
COI_fwd	GAATTAGGACATCCTGGAGC	<i>cytochrome oxidase subunit I (COI)</i>
COI_rev	GCACTAATCAATTTCCAAATCC	<i>cytochrome oxidase subunit I (COI)</i>
GAPDH_fwd	GACGAAATCAAGGCTAAGGTCG	<i>glyceraldehyde 3-phosphate dehydrogenase (GAPDH)</i>
GAPDH_rev	AATGGGTGTCGCTGAAGAAGTC	<i>glyceraldehyde 3-phosphate dehydrogenase (GAPDH)</i>

4.1.3 Chemical agents and kit

The chemical compounds and kit utilized for DNA extraction, H₂O₂ and ATP measurement, protein quantification, and tests for mitochondrial respiration are listed in Table6.

Table5. chemical compounds and kit used in this project

Chemical agents	Source	Identifier
Hydrogen peroxide (H ₂ O ₂)	Roth, GmbH	Cat# 9681.3
N-ethyl maleimide (NEM)	Sigma	Cat# 04259-5g
Paraquat (PQ)	Sigma	Cat# 856177-1g
Sucrose	Carl Roth GmbH	Cat# 4621.2
Normal goat serum (NGS)	Sigma	Cat# S2007
Vectashield	Vectorlabs	Cat# H-1000
NucleoSpin Tissue DNA extraction kit	Macherey-Nagel GmbH & Co. KG, Germany	Cat# 740952

Amplex red H ₂ O ₂ kit	ThermoFisher Scientific	Cat# A22188
CellTiter-Glo™ Luminescent Cell Viability Assay Kit	Promega	Cat# G7571
Seahorse mitochondrial biosciences mito stress kit	Seahorse Biosciences, Agilent	Cat# 102418-000
Pierce BCA Protein Assay Kit	ThermoFisher Scientific	Cat# 23227

4.2 Fly strains and rearing conditions

Flies were all raised under standard laboratory conditions and their feeding are based on modified Bloomington recipe adapted from <https://bdsc.indiana.edu/information/recipes/bloomfood.html> .

under 12/12h light/dark cycles with 65% humidity at 25°C. For UAS/Gal4 system, flies were kept at 29°C incubator to maximize the effect of RNA interference transgenes. Besides, due to the application of temperature-sensitive *gal80ts*, flies with *tubulin-gal80ts* transgene were firstly kept at 18 °C to inhibit the effect of Gal4 and F1 offspring were transferred to 29°C since the first day of eclosion. All of flies used in the experiment were the F1 progeny. The crosses of parents were flipped into new vials every two or three days, and the old vials would only be kept for around 14 days in case the F2 generation hatch out.

w¹¹¹⁸ was used as wildtype (*wt*) control. All fly strains were backcrossed into *w¹¹¹⁸* background for at least six generations to avoid interference of uncertain genetic background. A *brp* P [acman] construct (Huang et al., 2022) was integrated into the 5' UTR of CG11357 (Matkovic *et al*, 2013) to add more *brp* gene copy number from *wt* (2xBRP) to 4xBRP. We crossed 4xBRP flies with isogenized *wt* to get 3xBRP flies.

Table6. Transgenic fly stocks used in this project.

Fly stock	Source	Identifier
<i>w¹¹¹⁸</i>	Sigrist lab	
<i>elav-gal4</i>	Sigrist lab	
<i>elav-gal4; tubulin-gal80ts</i>	Sigrist lab	
<i>Ok107-gal4</i>	Sigrist lab	

<i>tubulin-gal80ts;;Ok107-gal4</i>	Sigrist lab	
<i>Gh146-gal4</i>	Sigrist lab	
<i>R23E10-Gal4</i>	BDSC	#49032
<i>R58H05-Gal4</i>	BDSC	#39198
<i>UAS-dPGC1</i>	David W Walker's lab	
<i>UAS-blw RNAi</i>	VDRC	#34664
<i>UAS-blw RNAi</i>	VDRC	#34663
<i>UAS-Catalase</i>	Sean T Sweeney's lab	
<i>UAS-SOD2</i>	Sean T Sweeney's lab	
<i>UAS-SOD1</i>	Sean T Sweeney's lab	
<i>UAS-DUOX</i>	Sean T Sweeney's lab	
<i>UAS-IP3R RNAi</i>	BDSC	#25937
<i>UAS-RyR RNAi</i>	BDSC	#29445
<i>UAS-MCU RNAi</i>	BDSC	#42580
<i>brp P[acman]</i>	Sigrist lab	
<i>UAS-snpfr RNAi</i>	Peter Soba's lab	
<i>sNPF^{cc00448}</i>	Peter Soba's lab	
<i>UAS-foxo RNAi</i>	VDRC	#107086
<i>UAS-foxo RNAi</i>	VDRC	#106097
<i>UAS-mnb RNAi</i>	VDRC	# 28628
<i>UAS-mnb RNAi</i>	VDRC	#107066
<i>UAS-rutabaga RNAi</i>	VDRC	#5569
<i>UAS-rutabaga RNAi</i>	VDRC	#101769
<i>UAS-dunce RNAi</i>	Lisa Scheunemann's lab	
<i>UAS-4mtGcamp3</i>	Ronald L Davis's lab	
<i>UAS-mitoTimer</i>	BDSC	#57323
<i>IF/CyO</i>	Sigrist lab	

BDSC, Bloomington Drosophila Stock Center; VDRC, Vienna Drosophila Stock Center.

4.3 Longevity and Aging experiments

Flies used in longevity experiment were collected on the day of their eclosion. Firstly, we would let female and male mate for 24 hours before separating them into single vial by gender, then 20 flies with the same gender were selected into each vial and

flipped every other day or through the weekend. 70-100 flies were collected in each group for one biological replicate. Longevity experiments were conducted for at least three replicates and more than 200 flies were included in single gender of each genotype. Aging experiment was conducted similar as the longevity assay. We still collected flies since the first day of eclosion but female and male flies were mixed in one vial. In case limited space would stress flies out, around 25-30 flies were kept in per vial, and transferred into new vials every 2-3 days until the anticipated age came.

4.4 Paraquat feeding and oxidative stress resistance

Paraquat long used as herbicide for farmers, generates superoxide anion radical and hydrogen peroxide through redox-sensitive reactions and increases oxidative stress in a cell, tissue and organ. We fed flies with paraquat (PQ) to artificially and chronically inflict more oxidative burden on flies and their siblings. First of all, we intended to evaluate oxidative resistance of flies at certain age, so aging experiments were conducted following what we described before. One day before the anticipated age, females and males were separated into different vials with 20 flies per vial overnight, then transferred into a small vial with three-layer filter paper soaked with 500ml 5% sucrose-5mM paraquat solution the next day. Control flies were kept in the same type of small vials with three-fold filter paper soaked with 500ml 5% sucrose solution to avoid thirst and starvation situation. Flies were flipped into new vials with fresh solution every other day and simultaneously we recorded the occurrence of death until all flies were dead. Log-rank analysis performed by GraphPad Prism was used to analyze comparison of survival rate.

4.5 Western blotting (WB)

In order to address the regulatory mechanism of ROS signaling on synapses, we

performed WB experiments to monitor the state of pre- and post-synaptic proteins under H₂O₂ treatment. Thus, we firstly had to dilute H₂O₂ (Roth, GmbH, Hydrogen peroxide 30%) with 5% sucrose to get a concentration gradient of H₂O₂ ranging from 2% to 20%. Similar as PQ treatment, 15 flies were then transferred into a small vial with three-layer filter paper soaked with 500ml 5% sucrose- H₂O₂ solution and would live a certain time interval from 6 hours to 48 hours on *w¹¹¹⁸* flies at certain age, *w¹¹¹⁸* flies at the same age fed with 5% sucrose solution for the same time interval were kept as controls.

WB was performed as previously described (Liang *et al.*, 2021). 6-8 female fly brains were dissected in hemolymph-like saline solution (HL3) and homogenized in lysis buffer for 1 hour at 4°C on a rotator in cold room, followed by 5 min full-speed centrifugation. Before immunoblotting, samples were heated with sample buffer at 95 °C for 5 min. The sample volume equal to one to two brains was loaded on commercial gradient gels (4-20%) used (BioRad #4561096) and immunoblotted, protein transfer involves the transfer of proteins separated in a gel by electrophoresis to a solid support matrix. The blotted gel was placed in direct contact with nitrocellulose membrane (Amersham, Potran), and then the gel-membrane pair merged with transferring buffer was sandwiched between two electrodes. Membrane transferring took one and half an hour. After transferring, ponceau S membrane staining was applied to visualize protein transfer to the membrane. Next, membrane was blocked with 5% milk for 1 hour. After the incubation of the primary and secondary antibodies, lastly, membrane was incubated with ECL solution (Thermo Scientific #32132) for 10 min and developed in the dark room with Kodak/GE films. The developed films were scanned by an EPSON V330 scanner in 16-bit grayscale tiff format. Tubulin was used as the loading control to normalize protein intensities by ImageJ software.

4.6 Confocal microscopy and time-gated STED (gSTED) microscopy

4.6.1 Immunohistochemistry and confocal imaging, image quantification

Immunohistochemistry was performed as mentioned previously^(Huang *et al.*, 2022). Female fly brains were dissected in hemolymph-like saline (HL3) or Ringer's solutions and kept on ice. Once the dissection was done, fly brains were immediately transferred into 4% paraformaldehyde (PFA) solution and placed on a shaker for 40 minutes in room temperature (RT). After fixation, brains were washed by 0.7% PBS-T (PBS with 0.7% Triton X-100) one time, then blocked in 10% 0.7% PBST solution with 10% normal goat serum (NGS) for at least 2 h at RT. After blocking, brains were incubated in primary antibodies diluted with 0.7% PBST and 5% NGS for at least 48 hours in cold room (at 4°C). Afterwards, 0.7% PBST was used again to wash brain samples for 5-6 times on a shaker each for 15 minutes. Then brains were incubated in secondary antibodies diluted with 0.7% PBST and 5% NGS for 24 hours in darkness. Secondary antibodies with fluorophores should avoid to be directly exposed under the light. Followed by 5-6 times washing again, brains were mounted with 6.5-7ul vectashield and stored in darkness in cold room overnight.

Images were acquired by a Leica TCS SP8 confocal microscope (Leica Microsystems). 1024 × 1024 images were scanned at 400 Hz using 4x line, acquisition settings to avoid saturation were set constantly for all groups of each immunostaining. ImageJ (Fiji) software was utilized to analyze acquired images. Confocal stacks were merged into a single z-plane by using the average projection function, the region of central brain (ROI) in average projected image for one brain was manually chosen using free-hand function in ImageJ. The fluorescence intensity of ROI was measured and normalized to the area of the central brain in Control group.

4.6.2 MitoTimer staining and confocal imaging

MitoTimer is a fluorescent probe targeted to the mitochondrial matrix and exhibits fluorescence shifts from Green to Red. “Green” refers to fresh, newly generated mitochondria, once mitochondria get mature, or oxidized, MitoTimer would irreversibly turn into “red”. Hence, Green to red ratio is usually used to evaluate the turnover and healthy state of mitochondria. The immunostaining for MitoTimer is close to conventional confocal staining, but the whole procedures are even simplified since MitoTimer per se is a fluorescent protein. Primary and secondary antibody is unnecessary during MitoTimer immunostaining. Female fly brains were dissected in HL3 and kept on ice, and then immediately fixed with 4% PFA solution for 40 mins at room temperature. After washed with PBS for 3 times, brains were directly mounted with Vectashield and stored at 4°C overnight. Images were acquired by a Leica TCS SP8 confocal microscope. Both excited by 488nm laser, emission capture for the green (new) fluorescence is collected in the 497–531 nm range, while red (old) fluorescence emission is collected in the 583–695 nm range. The image quantification for center brain follows the rules in confocal scan, and green to red fluorescent ratio is used for the data evaluation.

4.6.3 gSTED imaging and image quantification

The basic procedures of gSTED staining are the same as the conventional confocal staining. However, due to the requirement of higher resolution of gSTED, primary antibodies should always be given at a higher concentration in order to get well-defined images. Additionally, brains were mounted in ProLong Gold Antifade Mountant (Thermo Fischer Scientific, P36934) with high-precision 1.5H coverslips (Carl Roth). The mounted slides should be firstly left at room temperature for 24 hours then kept at 4 °C (cold room) for storage. the gSTED scan should be completed within 4-5 days

after the staining in case of the decline of fluorescent signal.

Time gated STED (gSTED) microscopy was performed using an Abberior Instruments Expert Line STED setup equipped with an inverted IX83 microscope (Olympus, Japan), two pulsed STED lasers for depletion at 775 nm (0.98 ns pulse duration, up to 80 MHz repetition rate) and at 595 nm (0.52 ns pulse duration, 40 MHz repetition rate) and pulsed excitation lasers (at 488 nm, 561 nm and 640 nm). Multi-channel 2D confocal and gSTED images were acquired with a 100× oil-immersion objective lens (UPLSAPO100XO, Olympus, NA = 1.4), with a pixel dwell time of 2 μs, with 10x and 30x line accumulation, respectively, at 16-bit sampling and a field of view of 10 μm x 10 μm. Lateral pixel size was set to 20 nm. The dyes STAR RED and Alexa Fluor 594 were depleted at 775 nm. Time gating was set at 750 ps with a width of 8 ns. Fluorescence signals were detected sequentially by line by avalanche photodiode detectors at appropriate spectral regions. These procedures were operated by the software Inspector (version 16.3.15507, Abberior Instruments, Germany).

Raw gSTED images were processed for Richardson-Lucy deconvolution with default settings using the Inspector software (version 16.3.15507, Abberior Instruments, Germany). The point spread function was automatically computed with a 2D Lorentzian function having a full-width half-maximum of 40 nm, based on measurements with 40 nm Crimson beads. The quantification of mitochondrial morphologic parameters followed the past experiments^(Ring et al., 2022). For gSTED imaging, two different biological replicates were conducted and results were pooled for data analysis.

4.7 Assessment of mitochondrial functionality

4.7.1 Single-brain seahorse assay

Single-brain seahorse assay was modified on the basis of our previous measurement

(Liang *et al.*, 2021) of mitochondrial respiration using seahorse XFe96 analyzer. Adult fly brains were anesthetized on ice and then dissected in assay medium made by supplemented Schneider's medium (ThermoFisher #21720024) containing 1 mM sodium pyruvate to boost mitochondrial oxidative respiration, as depicted priorly (Homem *et al.*, 2014; Liang *et al.*, 2021). The sensor cartridge (Seahorse XF Calibrant Solution 500 mL #100840-000) per well should be hydrated with 200ul calibrant solution overnight or for at least 6 hours prior to the assay at 25 °C. The loading of compounds (Oligomycin: complex V inhibitor; FCCP: proton gradient uncoupler; Antimycin A & Rotenone: complex I, III inhibitor) with modified concentration and calibration of the cartridge sensor were performed on the same day of the assay. Considering the existence of blood-brain barrier (BBB) and the penetration of chemical compounds, we evaluated their efficacy on the dissected single brain with modified concentration and identified the following optimal concentration for single brain assay listed as below (**Table7**).

Table7. chemical compounds used in seahorse mito stress test kit and optimized drug concentration

Chemical compounds (following the injection sequence)	Optimized concentration before injection	Drug targets
oligomycin	100uM	ATP synthase inhibitor
FCCP	25uM	Mitochondrial uncoupler: disrupting IMM proton gradient and increasing oxygen consumption
Rotenone/antimycin A	50uM each	Inhibitor of complex I (rotenone) and III (antimycin A)

Note: the compound injection will result in 10X dilution of individual compound concentration.

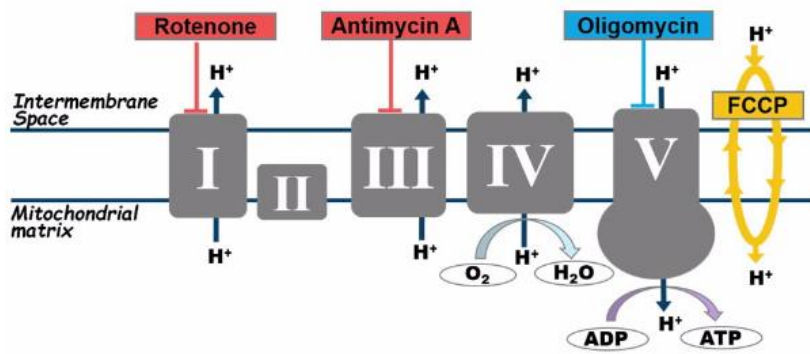


Fig.18. Respective mitochondrial targets of chemical compounds. Taken from Seahorse bioscience, Agilent Technologies.

Followed the protocol of single brain seahorse assay described earlier (Neville *et al*, 2018a; Neville *et al*, 2018b). Firstly, 50ul assay medium containing single dissected brain was transferred to an Agilent 96-well cell plate (Agilent, 102416-100). If the brain was floating in the assay medium, a probe was applied to sink the single brain into the bottom of the well and locate the brain in the center of the three raised spheres to ensure the accurate measurement of oxygen consumption and pH change. One micro-restrainer with plastic ring side facing towards was pushed to the bottom by the same probe to avoid the movement of individual fly brain. The manufacturing process of micro-restrainer was described in the past experiment (Mackert *et al*, 2022). Extra 130ul assay medium was added to the well to get the final 180ul solution in each well. Oxygen consumption rate (OCR) was measured by the XFe96 analyzer at 25 ± 2 °C which is considered as the most suitable temperature for oxidative respiration of the drosophila cell culture. After the OCR measurement, assay medium was carefully removed and single brain in each well was left inside for the determination of protein concentration. Individual brain at the bottom of the well was firstly digested by RIPA lysis buffer (ThermoFisher#89900) for 15-20 mins at room temperature until the whole brain structure gets transparent. With Pierce™ BCA Protein Assay kit, the precise protein concentration of each well was obtained based on the standard curve

generated by using pre-diluted BSA standards. OCR was normalized by protein levels afterwards.

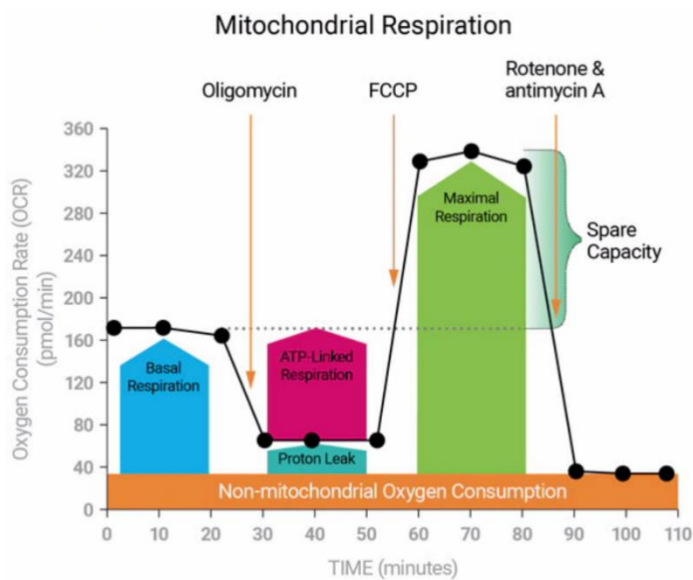


Fig.19. The profile of seahorse XF cell mito stress test: the dynamic OCR shift with the injection of different chemical compounds and the calculation of the key parameters, such as basal respiration, maximal respiration and ATP production. Taken from Seahorse bioscience, Agilent Technologies.

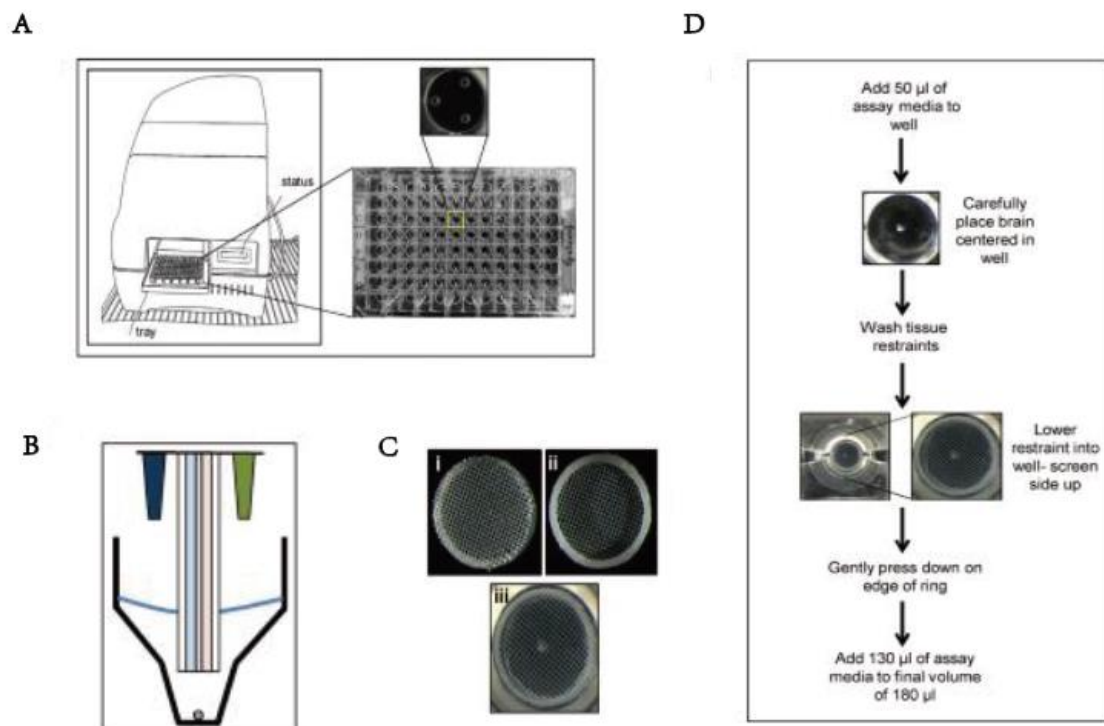


Fig.20. Operation of micro-tissue restrainer for single-brain mito stress test using the seahorse XFe96 analyzer. A) models of the XFe96 metabolic analyzer and cell plate. B) the model of the XFe96 probes (blue: oxygen consumption detection, pink: extracellular acidification detection) with injection ports (dark blue and green), and tissue being measured (grey circle). C). Images of tissue restraint. D). Procedure for analyzing *Drosophila* brain with the seahorse XFe96 analyzer using the tissue restraint. Taken from Neville KE, et al. *J Neurosci Methods*. 2018.

4.7.2 Mitochondrial DNA measurement

Female fly brains were anesthetized on ice and dissected in hemolymph-like saline (HL3). The dissected 10 fly brains were immediately frozen with liquid nitrogen. Proceeded on the basis of the previous protocol^(Liang *et al.*, 2021), the total DNA from 10 adult female brains per genotype were extracted according to the instructions of the

NucleoSpin Tissue kit (Macherey-nagel GmbH). MtDNA content was quantified by taking ratio between a mitochondrial-encoded cytochrome oxidase subunit I (COI) and nuclear-encoded glyceraldehyde 3-phosphate dehydrogenase (GAPDH) (mtDNA/nDNA) using quantitative real time PCR (qPCR) System CFX OPUS 96. Primer sequences were reported in the materials (Rera *et al*, 2011). Three biological replicates were pooled together for statistics.

4.7.3 ATP assay

Luminescent Cell Viability Assay was utilized to evaluate ATP level in fly heads. 15 female flies for each genotype were decapitated and fly heads were homogenized in 100 μ L Glo lysis buffer (Promega #E2661) quickly subjected to rapid freezing in liquid nitrogen later, based on previous assays (Pogson *et al*, 2014; Tufi *et al*, 2019a). Homogenates were diluted 1/20 with the Glo lysis buffer and mixed with the luminescent solution (CellTiter-Glo Luminescent Cell Viability Assay/Cell TiterGlo 2.0 Assay, Promega). After the incubation of 60 mins at room temperature, luminescence was measured with a plate reader (M200 P infinite Pro). The average luminescent signal from technical triplicates was normalized to protein levels, which were quantified using the Pierce™ BCA Protein Assay kit (Thermo Fisher #23227). Data from 2-4 independent experiments were pooled for data analysis.



Fig.21. The luciferase reaction for ATP detection. In the co-occurring presence of Mg²⁺, ATP and molecular oxygen, luciferase enables the catalysis of mono-oxygenation of luciferin. Taken

from www.promega.com/protocols/, Promega corporation.

4.7.4 Amplex red hydrogen peroxide assay

Amplex Red hydrogen peroxide Assay as depicted formerly (Ugbode *et al.*, 2020) for H₂O₂ measurement was performed to quantify the level of H₂O₂ in *Drosophila* heads. 5µl Amplex Red reagent(50uM) (Amplex Red hydrogen Peroxide/Peroxidase Assay kit, Thermo Fisher, #22188) and 10ul HRP (10u/ml) were added in every 1ml of HL₃ medium. Both female and male fly heads were measured in the experiments. 5 fly heads were added quickly in 200ul volume of reagent and then pulverized with a homogenizer. After homogenization, samples were vortexed and quickly centrifuged, then incubated at 25°C for 90min under darkness. Afterwards, the samples were vortexed again and 80µl aliquoted into a 96 well plate wells, the absorbance was measured using a microplate reader (M200 P infinite Pro) equipped for excitation in the range of 530-560nm, the absorbance rate was corrected with protein levels, quantified by Pierce™ BCA Protein Assay kit (Thermo Fisher #23227). The Amplex Red reagent alone was used to subtract the background and two-three duplicates of independent biological experiments were pooled for statistics.

4.7.5 Mitochondrial ROS measurement by mitochondria-targeted redox sensor

A genetical-encoded mitochondria-targeted probe was introduced to detect the age-dependent alterations of mitochondrial H₂O₂. UAS-mito-RoGFP2-Orp1 is coupling the redox-sensitive green fluorescent protein 2(ro-GFP2) with the yeast H₂O₂ sensor protein—oxidant receptor peroxidase-1(Orp1) in the mitochondrial matrix(Albrecht *et al.*, 2011; Barata & Dick, 2013). Pan-neuronal driver *elav-gal4* was crossed with the redox sensor UAS-mito-RoGFP2-Orp1 and kept in 25°C. Only the first generation(F1) offsprings of 5d-, 30d-, 50day age were used for the mtROS

assessment. Female flies were anesthetized on ice and quickly dissected in cold HL3 solution containing 20mM N-ethyl maleimide (NEM) to prevent rapid oxidation(Albrecht *et al.*, 2011). After the dissection, the brains were transferred into fresh NEM and incubated for 15 mins. Once washed with 1xPBS, brains were fixed with 4% PFA for 30 mins at room temperature on a shaker. After incubation, brains were washed 3-4 times every 10 minutes with 1xPBS and then mounted with vectashield and stored at 4°C overnight. The confocal imaging was carried out the day after the mounting. 20mM dithiothreitol and 2mM diamide were added during brain preparation to identify the dynamic range of biosensor in drosophila brain. The brain samples are sequentially excited by the 405 and 488 nm laser lines. For the excitation, the emitted fluorescence wavelength is obtained between 500 and 530 nm. The ratio of the 405/488 nm fluorescence intensities presents the redox state of roGFP2-Orp1.

4.8 In vivo Mito-Ca²⁺ imaging with two-photon microscopy

5d-old female flies were used for live imaging performed by two-photon microscope (Leica) equipped with a 20x water-immersion objective (NA = 1, Leica) as earlier depicted(Pooryasin *et al.*, 2021). **mitoGCaMP3** was excited at 920 nm.

A custom-built device was used as odor delivery system to supply odors with a constant flow rate of 1 ml/s to the fly's antennae for 2 s. Onset and duration of the odor stimulus were controlled using a custom-written LABVIEW program. 3-octanol (OCT) (diluted 1:100 in paraffin oil) was used in live imaging. Image processing and analysis were performed using Fiji software (1.52P). For correcting the potential slight movements in the x-y direction, recorded images were aligned using TurboReg plugin. Afterwards, regions of interest (ROIs) were manually defined in the calyx from two focal planes. The maximum three responsive micro-glomerular structures were selected as ROIs per animal. For signal quantification, the average pixel intensity of

ten frames before stimulus onset was determined as F_0 . ΔF is the difference between fluorescence and F_0 , and resulting values were divided by F_0 and displayed as percent. Time to peak was measured from 10% to 90% of the maximum amplitude ($\text{Max } \Delta F/F_0$). False color-coded images were produced accordingly by subtracting the average of three frames before stimulus onset from the average of three frames after stimulus onset and dividing the resulting image by the average of the before stimulus. For display, images are median filtered with a pixel range of five.

4.9 Statistical analysis.

The statistical analyses were carried out by using GraphPad Prism software. Student t-tests were employed to assess differences between two groups when the data met normal distribution, as determined by the Shapiro–Wilk test. For comparisons among multiple groups, one-way ANOVA with Bonferroni correction was applied. In the case of non-normal data analysis for gSTED, the nonparametric Kruskal–Wallis test was utilized. A significance threshold of $p < 0.05$ was adopted, and the strength of significance was indicated by the number of asterisks: (* $p < 0.05$, ** $p < 0.01$, *** $p < 0.001$, **** $p < 0.0001$).

5. Results

5.1 Presynaptic plasticity (PreScale) is fine-tuned by bidirectionally genetic manipulations of mitochondrial functionality

5.1.1 Early-aging associated decay of mitochondrial function and ATP amounts in the *Drosophila* brain

Mitochondrial dysfunction is iterated as a crucial hallmark of aging, characterized by reduced ATP production, destabilized ETC organization and increased generation of ROS (López-Otín *et al.*, 2023). In the past Seahorse experiment, we identified a drastic decline in mitochondrial oxidative respiration in ageing *Drosophila* brains (Liang *et al.*, 2021). However, we didn't observe a significant change in ATP production following oligomycin administration. The CellTiter-Glo Luminescent Cell Viability Assay, as described earlier, offers the great opportunity to detect total ATP content in the whole brain (Pogson *et al.*, 2014; Tufi *et al.*, 2019a). With the aim of specifically assessing age-related ATP alterations in *Drosophila* brains, we decided to employ this ATP assay to compare ATP level in fly brains at 5 days, 15 days, and 30 days of age. Notably, a significant reduction of ATP content was observed in aging fly brains relative to young animals, shown in Fig. **22a**. Thus, aging is obviously associated with a significant decline in ATP levels in *Drosophila* brains. In order to comprehensively understand mitochondrial alterations throughout ageing trajectory in fly brains, we further measured mitochondrial turnover by expressing mitoTimer in these neurons (Gottlieb & Stotland, 2015). The green signal of mitoTimer refers to biosynthetically younger mitochondria, irreversibly turning into red when mitochondria get mature or face age-promoting conditions such as intense ROS stress. The green to red ratio of mitoTimer fluorescence allows for the quantification of relative changes in mitochondrial turnover. The 15d-old fly brains displayed a pronounced reduction in the green to red

fluorescence ratio compared to their younger siblings, as illustrated in Fig.22c, which further solidifies the evidence for mitochondrial decay during the ageing process. Moreover, the oxidative stress theory of ageing(Liguori *et al.*, 2018) underscores that the accumulation of reactive oxygen species (ROS). ROS, as byproducts of mitochondrial oxidative respiration, is intricately linked to age-related functional decline. Consequently, we opted to quantify the ROS levels in fly brains at 5 days, 15 days, and 30 days of age to investigate the potential influence of ageing on ROS levels. The amplex red assay was adopted to monitor hydrogen peroxide (H₂O₂) level, as explained previously(Ugbode *et al.*, 2020). Remarkably, a notable accumulation of ROS was detected in fly heads with the progression of age (Fig.22b).

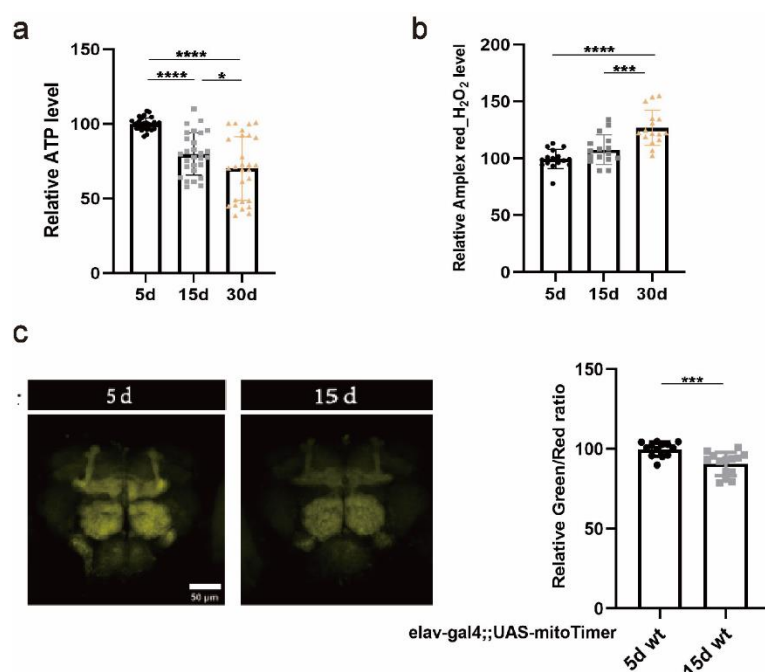


Fig.22. Early-aging associated decay of mitochondrial function and ATP amounts in *Drosophila* brain. (a). Relative ATP content in 5d,15d,30d fly heads. (b) Relative hydrogen peroxide(H₂O₂) levels (Amplex red absorbance rate normalized to protein content) in 5d, 15d and 30d fly heads; (c) Representative confocal images immunostained for UAS-mitoTimer in 5d and 15d fly brains, scale bar:50µm; Quantification of mitoTimer Green/Red ratio in 15d wt and 5d wt fly

brains.

5.1.2 Pan-neuronal activation of dPGC1 protects from aging-associated mitochondrial decay

Transcription co-activator Peroxisome proliferator-activated receptor gamma coactivator 1 (PGC1), recognized as the drosophila PGC1 homolog(dPGC1), is believed to enhance mitochondrial biogenesis by co-activating nuclear transcription factors and essential for the proper expression of numerous genes encoding mitochondrial proteins (Tiefenbock et al, 2010). Moreover, it has been proved(Rera et al., 2011) up-regulation of dPGC1 in the digestive tract enables to boost mitochondrial activity and delay the onset of early-aging related changes in the intestine, and simultaneously extends the lifetime of drosophila.

In order to address the mitochondrial phenotypic consequences of neuron-specific dPGC1 overexpression, we utilized the UAS/Gal4 system by combining UAS-dPGC1 transcript with pan-neuronal driver *e/av-gal4*. Besides, we performed six generations of backcrossing to isogenize dPGC1 into *w¹¹¹⁸* background. The overexpressing effect of the dPGC1 transcript in flies was confirmed by quantitative PCR (Rera et al., 2011). 15d of fly age, the premature period of aging, was perceived as our priority to investigate early-aging phenotype. Oxidative respiration, proxied by oxygen consumption rate (OCR), is the main mode of energy production within mitochondria (Brand et al, 2013). The robustness of the electron transport chain (ETC) complexes serves for efficient oxygen consumption and ATP generation. To determine whether UAS-dPGC1 boosted mitochondrial respiration in drosophila brains, we evaluated basal OCR using a single-brain seahorse assay (Dietz et al, 2019; Neville et al., 2018a; Neville et al., 2018b) in fly brains of *e/av/dPGC1* and the driver control. Relative to control flies, *e/av/dPGC1* flies exhibited a significantly elevated level of mitochondrial basal respiration in the brain (Fig.23a-b). Hence, pan-

neuronal overexpression of *Drosophila* PGC1 evidently enables the preservation of mitochondrial respiration from the natural decline typically associated with advancing age (Liang et al., 2021). On top of that, we also assessed ATP amount in *Drosophila* brains of neuronal overexpression of dPGC1 by ATP assay. Consistent with basal respiration rate, *elav/dPGC1* fly brains showed an apparently higher ATP level compared to the corresponding control siblings (Fig.23c). Building upon our understanding that aging compromises mitochondrial turnover in older fly brains, we proceeded to investigate whether neuronal overexpression of PGC1 could effectively mitigate this decline in mitochondrial turnover. MitoTimer staining indicated neuronal activation of PGC1 resulted in more newly-generated mitochondria (Fig.23d-e) and delayed the deterioration of mitochondrial turnover associated with ageing. Besides, ageing is severely inflicted to instability of mitochondrial genome (Fontana & Gahlon, 2020; López-Otín et al., 2013), and the quantification of mitochondrial DNA amount (mtDNA) using quantitative real-time PCR(qPCR) was considered as the precise method to assess mitochondrial mass (Tessema et al, 2023). Therefore, we examined mitochondrial DNA amount as additional readout of PGC1 effects on fly brains. MtDNA/nuclear DNA (nDNA) ratio revealed distinctly increased amounts of mitochondrial DNA normalized to amounts of nuclear DNA (nDNA) in 10d *elav/dPGC1* flies (Fig.23f), and presented a higher tendency in 15d *elav/dPGC1* flies relative to control flies at the same age. Building on our previous study(Ring *et al.*, 2022), we extended our investigation into the mitochondrial morphology upon upregulating dPGC1. Our focus still remained on mushroom body neurons, with particular attention to the calyx region in the olfactory system, where projection neurons (PN) synapse on the dendrites of Kenyon cells(Aso *et al*, 2014). Staining against classical mitochondrial marker-ATP5A by gSTED microscopy(Ring *et al.*, 2022), we demonstrated that neuronal-specific overexpression of dPGC1 led to more tubular and branched structure of mitochondria based on the analyzed deconvolved images (Fig.23g). Though there was a slight increase in the number of mitochondria,

it did not reach statistical significance, suggesting a potential “fusion phenotype” of synaptic mitochondria in the calyx region.

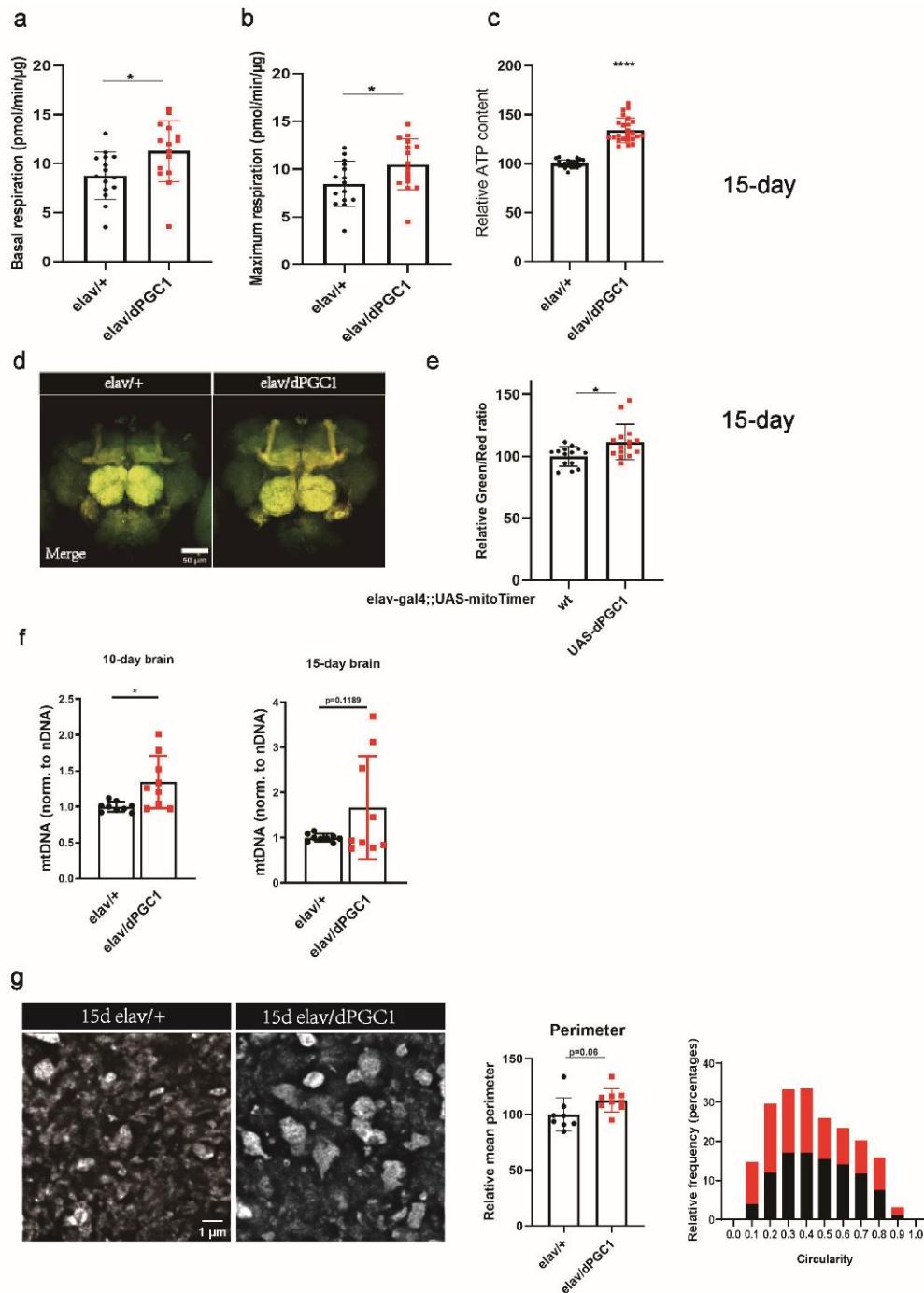


Fig.23. Neuron-specific activation of dPGC1 protects from aging-associated mitochondrial decay. (a-b). single-brain seahorse mito stress test. (a) Basal and (c) maximum oxidative respiration rate (OCR). OCR was measured with single brain of 15-day *elav/dPGC1* and *elav/+*

animals at $25^{\circ}\text{C}\pm 2^{\circ}\text{C}$ following oligomycin, FCCP, and antimycin A and rotenone treatment using the Seahorse XFe96 Analyzer. The OCR measurement was normalized to protein content. Data are pooled from two independent experiments (n = 15 fly brains); (c). Relative ATP content in 15d *elav/dPGC1* and 15d *elav/+* fly heads (n=30-45 independent heads; *p < 0.05; unpaired t test); (d). Representative confocal images immunostained for UAS-mitoTimer in 15d *elav/+* and *elav/dPGC1* fly brains, scale bar:50 μm ; (e) Quantification of mitoTimer Green/Red ratio in 15d *elav/+* and 15d *elav/dPGC1* fly brains (n = 13-15 independent brains; *p < 0.05; unpaired t test); (f). qPCR of mitochondrial DNA copy number normalized to nuclear DNA in 10d and 15d *elav/dPGC1* compared to corresponding driver control in drosophila brains. Data are pooled from three independent biological replicates (n=30 animals in total) *p < 0.05, two-tailed paired Student's t test). (g) Representative gSTED deconvolved (decon) images of mitochondrial morphology immunostained with ATP5A in calyx of drosophila brains in 15d *elav/+* and *elav/dPGC1*, scale bar: 1 μm ; Quantification of mitochondrial morphology: perimeter, and frequency distribution of circularity normalized to corresponding driver control of ATP5A-stained mitochondria. Dot plots show all data points along with the mean (bar) \pm SD (n=9-11 independent animal brains) *P < 0.05. Unpaired, two-tailed t-test.

5.1.3 Age protection of mitochondrial functionality delays age-induced onset of PreScale

Aging is the driving force of brain-wide increase of presynaptic active zone proteins (Gupta *et al.*, 2016). More precisely, our former study demonstrated that a brain-wide increase of presynaptic master protein Bruchpilot (BRP) and BRP-related releasing factor was associated with mid-age brain ageing ("PreScale") (Huang *et al.*, 2022). The presynaptic protein BRP, known as the master protein of the active zone scaffold in pre-synapses, facilitates efficient synaptic vesicle releasing and patterns presynaptic plasticity (Kittel *et al.*, 2006; Matkovic *et al.*, 2013; Wagh *et al.*,

2006). To investigate the presynaptic consequences of age-protected mitochondrial status, we performed immunofluorescence staining with BRP^{nc82} antibody. Surprisingly, neuronal PGC1 overexpression was noted to markedly reduce brain BRP fluorescence intensity in early aging(15d) fly brains when compared to its control counterparts (Fig.24a). In an effort to Figure out the long-term influence of pan-neuronal PGC1 upregulation during the ageing process, we monitored the lifetime of *elav/dPGC1* and corresponding controls. According to the survival curve, *elav/dPGC1* significantly extended the lifespan of male flies, while slight change of longevity was detected in females (Fig.24b and 24c). Rejuvenation of mitochondrial functionality by PGC1 reminded us of the anti-aging agent-spermidine. Spermidine rearing (Gupta *et al.*, 2016) not only restored mitochondrial dysfunction at advancing age, but also prevented age-related BRP increase in drosophila brains. Neuronal upregulation of PGC1 ingeniously mimicked the spermidine-mediated protection from ageing and might guide the discovery of another healthy ageing paradigm in the upcoming aging research.

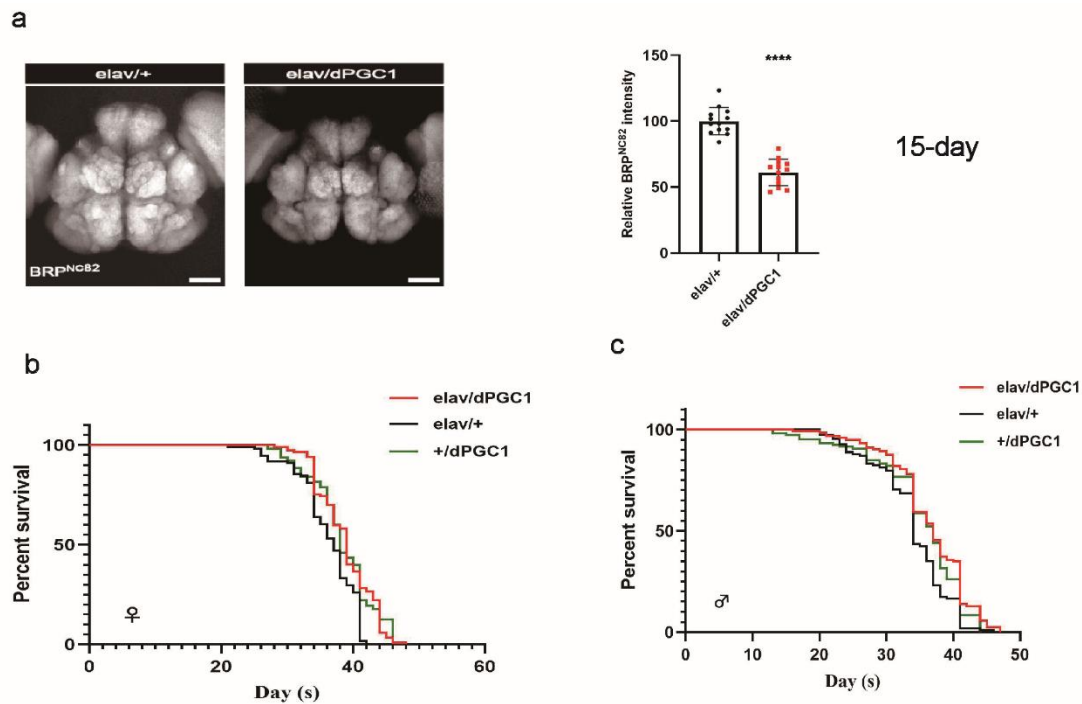


Fig.24. Age protection of mitochondrial functionality delays age-induced onset of PreScale plasticity. Adult brain, 15d. (a). *elav/+* and *elav/dPGC1*, immunostained for BRP^{nc82}, scale bar:50um; Quantification of BRP^{nc82} intensity within the central brain region normalized to control (n = 13-14 independent brains; ***p < 0.001; unpaired t test); (b-c). lifespan analysis for *elav/dPGC1* and corresponding control flies, (b) females and (c) males, n>200 for both genotypes, 3 replicates. ****p < 0.0001; Log-rank (Mantel-Cox) test.

5.1.4 Reducing ATP synthase 5A complex provokes premature PreScale

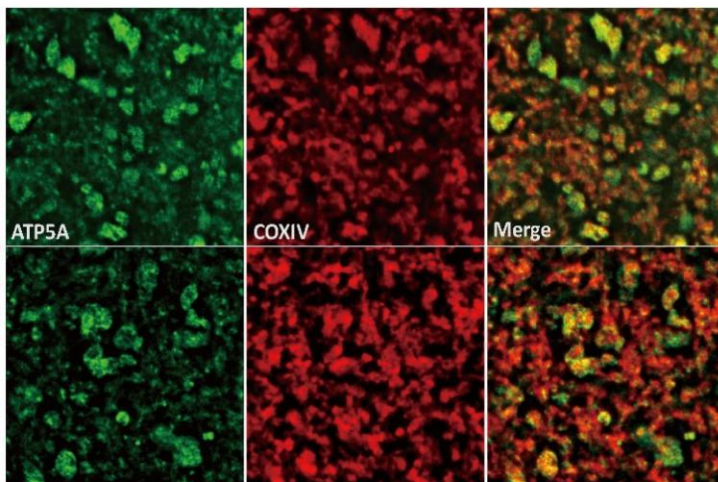
Based on our analysis of the ATP assay, ATP amount in drosophila brain is drastically suffered from ageing. In addition, our previous proteomics (Liang *et al.*, 2021) disclosed spermidine-rearing enhances the abundance of mitochondrial proteins, especially ATP synthase complex and protects against age-induced memory impairment (Gupta *et al.*, 2016). Both of the findings point out that, energy supplier—ATP molecule might potentially serve as the modulators of age-related alterations.

Hence, we shifted our focus to the ATP synthase complex.

Bellwether (*blw*), known as ATP5A, encodes ATP synthase complex V subunit α , knock-down of *blw* in drosophila caused lethality (Garcia *et al*, 2017) and *blw* homozygous mutant resulted in impaired ATP production and ROS accumulation in the larva fat body (Di Cara *et al*, 2013). To address the role of *blw* in age-related mitochondrial alterations, we endeavored to genetically manipulate the expression of *blw* in the drosophila brain and assess its impact on mitochondrial functionality. Thus, we established neuronal attenuation of *blw* by combining pan-neuronal driver *elav* with RNA interference transgenic construct *blw-RNAi^{GD11030}*. Expectedly, pan-neuronal deficiency of *blw* resulted in lethality and flies only can reach the pupae stage but did not eclose, we speculated that removing energy supply from the whole brain probably hampers the physical growth of the drosophila. To circumvent this lethality problem, we took advantages of TARGET system (McGuire *et al*, 2003), the temperature-sensitive Gal80 (Gal80ts) proteins can repress the function of Gal4 system at the permissive temperature 18°C, but has inability to bind Gal4 at the restrictive temperature of over 29°C. We started with *tubulin-gal80ts* combined together with *elav-gal4* to block the RNAi effect on *blw* before eclosion so that flies can grow up without developmental delay, and then switched on *RNAi* after eclosion by transferring the newly hatched adult flies to 29°C. The immunostaining with *blw*(ATP5A) antibody (Ju *et al*, 2012) revealed, neuronal deficiency of *blw* since adulthood induced a clear reduction of *blw* protein level in 15d-old *elav;tubulin-gal80ts/blw RNAi* flies relative to the corresponding driver control shown in Fig. **26a**. Mitochondrial basal respiration and ATP level were measured respectively by single-brain seahorse assay and ATP Assay. Noticeably, defective mitochondrial basal respiration and decreased ATP level were observed in neuronal *blw* ablation fly brains when compared to controls (Fig. **26b-c**). It is evident that, neuronal silencing of ATP synthase subcomponent since adulthood further exacerbated age-related mitochondrial dysfunction in drosophila brains. Subsequently, we continued to

analyze the mitochondrial morphological difference between blw knock-down (KD) and control flies by gSTED. As genetic knockdown of blw artificially reduces the expression of ATP synthase 5A, we turned to another mitochondrial marker-COXIV and analyzed mitochondrial morphology in the calyx. Crucially, COXIV and blw (ATP5A) were confirmed to tightly co-localized in both synaptic terminal of calyx and Kenyon cell bodies by gSTED staining (Fig.25a-b). In the calyx of 15d blw RNAi fly brains, we witnessed increased quantity of mitochondria appearing with smaller size and more rounded shape (Fig.26d). This morphological change resembles the reported fragmented and swollen phenotype of mitochondria in an Alzheimer's disease (AD) model (Wang & Davis, 2021).

a



b

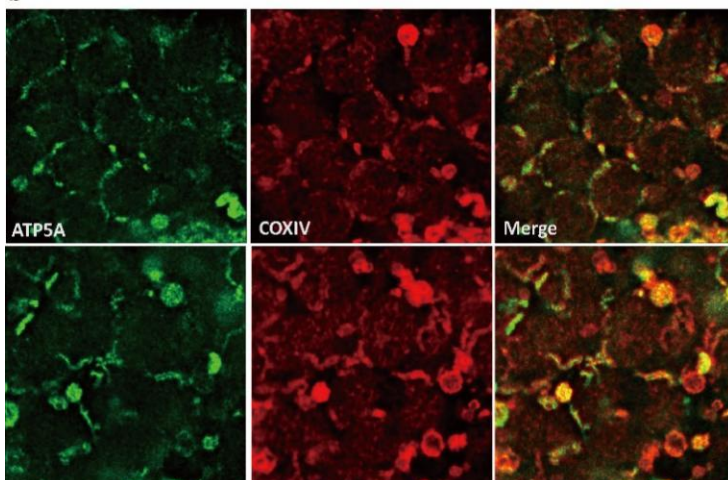


Fig.25. ATP5A and CoxIV are co-localized in calyx and Kenyon cell body of the drosophila

central brain. (a) Representative gSTED deconvolved (decon) images of mitochondrial morphology immunostained with ATP5A and CoxIV in calyx of drosophila brains in wildtype, scale bar: 1 μ m; (b) Representative gSTED deconvolved (decon) images of mitochondrial morphology immunostained with ATP5A and CoxIV in kenyon cell body of drosophila brains in wildtype, scale bar: 1 μ m;

Silencing ATP synthase 5A in neurons exacerbated mitochondrial decline, providing an opportunity to investigate presynaptic changes under impaired mitochondrial conditions at early aging stage. Therefore, we conducted brain immunostaining with BRP^{nc82} antibody in 15d *elav;tubulin-gal80ts/blw RNAi* and control fly brains. Conspicuously, pan-neuronal attenuation of *blw* in adult flies resulted in a notable elevation of BRP intensity brain-wide compared to the corresponding control siblings (Fig.26e). Additional exacerbation of age-induced mitochondrial dysfunction steered PreScale towards even higher limit. Furthermore, with the aim of exploring the long-term effect of neuronal ATP ablation in fly brains, we monitored the longevity of flies with pan-neuronal *blw* attenuation and its specific driver controls. Indeed, neuronal ablation of *blw* noticeably reduced the lifespan of drosophila. Survival curve of female and male flies both exhibited a significant statistic difference between two groups (Fig.26f-g).

Taken together, genetically-provoked changes of mitochondrial functionality at early aging stage can obviously tune the normally age-associated PreScale in a bi-directional manner.

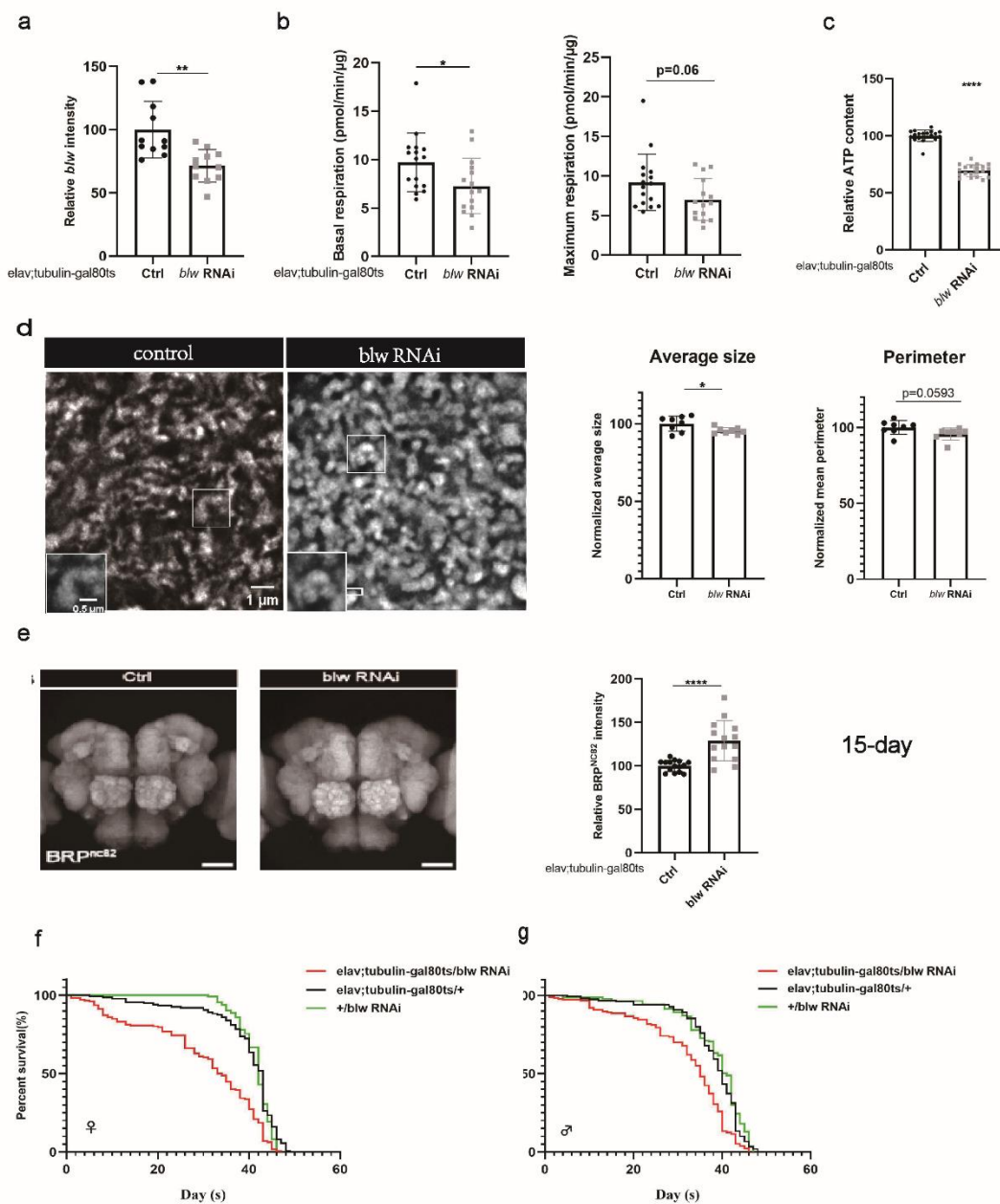


Fig.26. Reducing ATP synthase 5A complex provokes premature PreScale. Adult brain, 15d. (a). Quantification of ATP5A (*blw*) intensity within the central brain region normalized to control ($n = 13-14$ independent brains; $***p < 0.001$; unpaired t test). (b). single-brain seahorse mito stress test. Basal and maximum OCR in fly brains of *elav;tubulin-gal80ts/blw* RNAi compared to corresponding control. Data are pooled from two independent experiments ($n = 15-16$ fly brains), $***p < 0.001$, $**p < 0.01$, $*p < 0.05$, ns, no significance, unpaired, two-tailed t-test. (c). Relative ATP

content in the whole brain of *elav;tubulin-gal80ts/blw* RNAi normalized to the corresponding control at the same age. (d) Representative gSTED deconvolved (decon) images of mitochondrial morphology immunostained with ATP5A in calyx of *Drosophila* brains in 15d *blw* RNAi and corresponding control, scale bar: 1 μ m; Quantification of mitochondrial morphology: average size and perimeter normalized to corresponding driver control of ATP5A-stained mitochondria. Scale bar: 1 μ m; Dot plots show all data points along with the mean (bar) \pm SD (n=9-11 independent animal brains) *P < 0.05. Unpaired, two-tailed t-test. (e). *elav;tubulin-gal80ts/+*, and *elav;tubulin-gal80ts/blw* RNAi, immunostained for BRP^{nc82}, scale bar: 50 μ m; Quantification of BRP^{nc82} intensity within the central brain region normalized to control (n = 13-14 independent brains; ***p < 0.001; unpaired t test); (f-g). lifespan analysis for *elav;tubulin-gal80ts/blw* RNAi and corresponding control flies, (f) females and (g) males, n>200 for both genotypes, 3 replicates. ****p < 0.0001; Log-rank (Mantel-Cox) test.

5.1.5 Evoking acute ROS stress can trigger premature PreScale

We next intended to elucidate the underlying mechanism of age-related presynaptic alterations mediated by mitochondrial functional status. As previously described, changes in mitochondrial respiration and ATP levels triggered alterations in age-associated PreScale. On the basis of the chemiosmotic theory (Mitchell, 1961), mitochondrial oxidative phosphorylation depends on ETC complexes to transfer protons, consume oxygen and synthesize ATP. Genetic inhibition of *blw* impairs the normal activity of H⁺-ATP synthase and disrupted the proton transfer into matrix (Formentini *et al*, 2012), leading to a significant increase in ROS generation within mitochondria (Brand *et al*, 2004). Contrarily, activation of *Drosophila* PGC1 homologue was reported to reduce ROS level in aged fly intestines (Rera *et al.*, 2011) and aged mice skeletal muscles (Ascenzi *et al*, 2019). Moreover, the oxidative stress theory of ageing (Liguori *et al.*, 2018) suggests that age-related functional decline is associated

with the accumulation of ROS, and mitochondrial ROS (mitoROS) has been increasingly appreciated for the signaling role in organism homeostasis (Shadel & Horvath, 2015). Apart from directly signaling in cytoplasm, superoxide and H₂O₂ capably oxidize some mitochondrial proteins as second messengers released into the cell plasm. Notably, a considerable accumulation of ROS was detected in aging fly brains (Fig. **22b**). Consequently, we assumed that ROS might play a critical role in the regulation of PreScale. Thus, we set out to evaluate ROS level in fly brains of neuronal *PGC1* overexpression and *blw* ablation together with their related controls. Moreover, we subjected these transgenic flies to increased oxidative stress by adding paraquat (PQ) and afterward monitored their susceptibility to ROS. In accordance with the current findings, pan-neuronal stimulation of *PGC1* markedly attenuated the level of ROS (Fig. **27a**) and evidently enhanced the physical strength of flies to tolerate oxidative stress in male flies (Fig. **27c**). Whereas, inhibiting *blw* (ATP5A) rendered flies more vulnerable to oxidative stress, as evidenced by increased ROS production in their brains (Fig. **27b**) and compromised endurance against oxidative stress in both sexes according to survival curve with PQ feeding (Fig. **27d**).

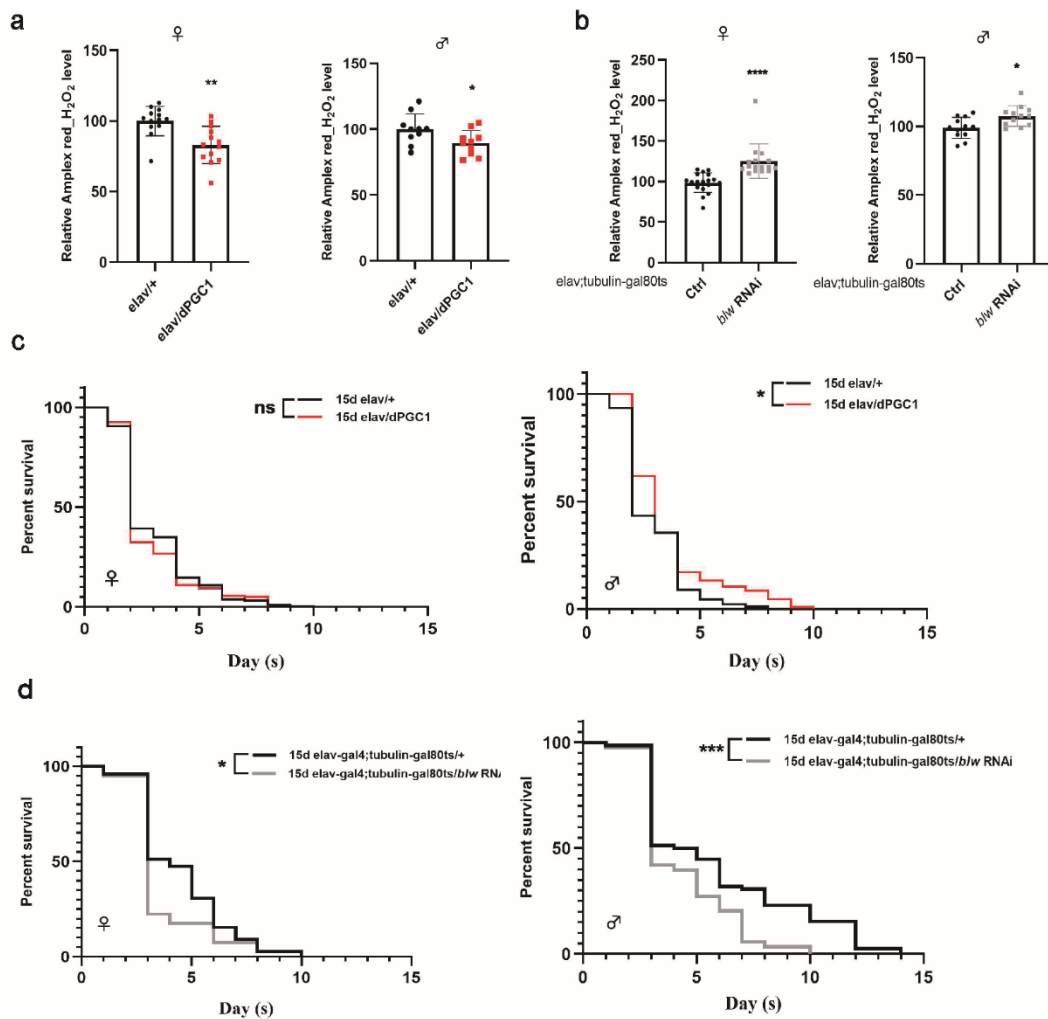


Fig.27. ROS level in fly brains and resilience against oxidative stress. (a) Relative hydrogen peroxide(H₂O₂) levels in *elav*/dPGC1 and *elav*/+ females and males fly brains (n=10-12 independent animal brains, **p < 0.01, *P < 0.05, Unpaired, two-tailed t-test); (b) Relative hydrogen peroxide(H₂O₂) levels in *elav*;tubulin-gal80ts/blw RNAi and control females and males fly brains (n=10-12 independent animal brains, **p < 0.01, *P < 0.05, Unpaired, two-tailed t-test); (c) Survival rate against 5mM paraquat in *elav*/dPGC1 and *elav*/+ females and males (n>200 animals per genotype, *p < 0.05, ns, no significance, Log-rank (Mantel-Cox) test); (d) Survival rate against 5mM paraquat in *elav*;tubulin-gal80ts/blw RNAi and control females and males (n>200 animals per genotype, *p < 0.05, ns, no significance, Log-rank (Mantel-Cox) test).

As noted, we confirmed an age-induced increase in ROS levels, and identified a bidirectional shift in ROS levels with opposing genetic manipulations of mitochondrial functionality (through neuronal PGC1 overexpression and *blw* ablation). Thus, ROS signaling might per se play a role in age-driven PreScale. Hence, in an effort to dissect the connection between ROS level and PreScale at early aging stage, we first performed pharmacological interventions.

Our intention was to understand whether acute administration of ROS-inducing agents could trigger PreScale. Considering superoxide and H₂O₂ as the two primary types of ROS, we opted to externally expose young wild-type flies to H₂O₂ as a means of ROS assault. Understanding that the immediate effects of drugs are often dictated by dosage (drug concentration) and the timing of administration (Holford, 2017), we conducted a screening Western blot to track the changes in the protein level of BRP and the homolog of the mammalian scaffold protein PSD95, Discs large (Dlg) (Gilestro *et al*, 2009; Jeong *et al*, 2019). Varying concentrations (2%, 10%, 20% H₂O₂) and successive time intervals (6h, 14h, 24h) of H₂O₂ treatment were established to determine the minimal dose and timing. According to the western blots, we found, the lowest H₂O₂ concentration of 2% within 6 hours was sufficient to visualize the effect of BRP upscaling, while 20% H₂O₂ was obviously a strong toxin and led to the early fatal event of animals. Therefore, we determined that 2% H₂O₂ is an appropriate concentration and 6 hours as the minimum effective duration for H₂O₂ exposure (Fig. **28a-c**). To corroborate these findings from western blots, we also performed brain immunostaining using BRP^{NC82} antibody. A significant increase in BRP levels was found after 6-hour administration of 2% H₂O₂ (Fig. **28d**). Moreover, by comparing individual western blot conducted at various time points, we noticed an intriguing pattern: the BRP level exhibited a reverse U-shaped pattern. The elevation of BRP and Dlg levels commenced at 6 hours, peaked around 12-14 hours, and subsequently dropped to baseline levels by 24 hours (Fig. **28a-c**). In order to further substantiate this

observation, we performed a quantitative western blot analysis with BRP and Dlg antibody, following the specific time points (6h-14h-24h-48h) as well as 2% concentration of H₂O₂ administration compared to unfed siblings. As expected, the quantitative analysis corroborated the observed trend. The decline observed at 24 hours continued through to 48 hours of treatment, with BRP and Dlg levels falling further below the initial baseline (Fig.28e). Nonlinear fitting via quadratic regression concurrently indicated that BRP and Dlg level peaked at approximately 12-h (Fig.28f). Taken together, acute introduction of H₂O₂ is capable of initiating PreScale within 6 hours. Inducing acute ROS stress can initiate premature PreScale.

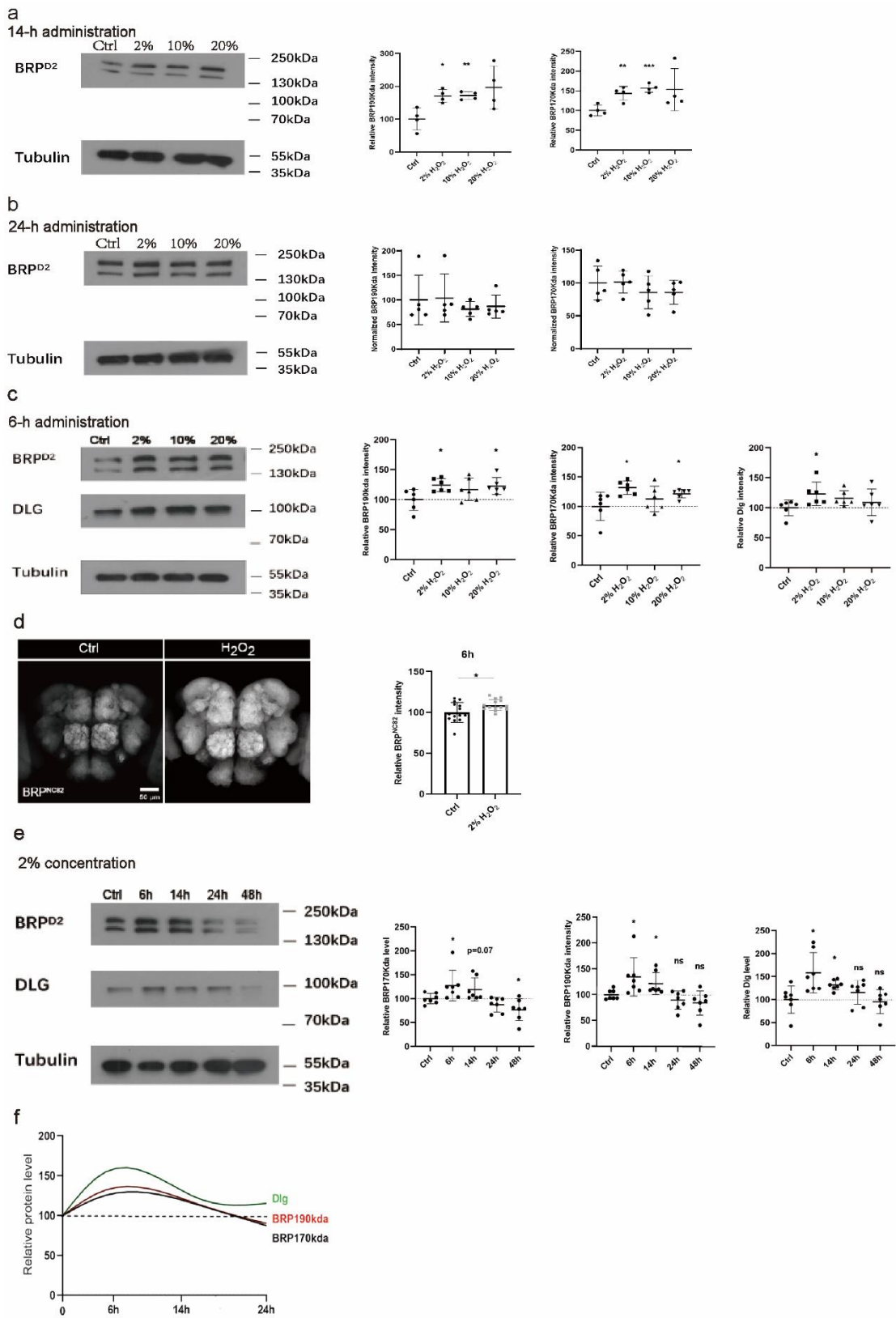


Fig.28. Evoking acute ROS stress can trigger premature PreScale. Adult brain, 5d.(a-c) Representative western blots in (a) 14hr, (b) 24hr, (c) 6hr administration of 2%,10%,20% H₂O₂; Quantification of relative level of BRP190Kda, BRP170Kda and Dlg; (One-way ANOVA with Bonferroni multiple comparisons test, adjusted*p < 0.05, **p < 0.01, n = 4-5 biological replicates) (d).Representative confocal images immunostained for BRP^{nc82} after 6hr administration of H₂O₂, quantification of BRP^{nc82} intensity within the central brain region normalized to control (n = 13-14 independent brains; ***p < 0.001; unpaired t test) in 5d-old flies; (e) Representative western blots in 6h-14h-24h-48h induction of 2% H₂O₂; Quantification of relative level of BRP190Kda, BRP170Kda, and Dlg; (adjusted*p < 0.05, **p < 0.01, n = 6–8 biological replicates. One-way ANOVA with Bonferroni multiple comparisons test); (f)Nonlinear line fitting quadratic regression of the protein levels of BRP and Dlg.

Despite the distinct mechanisms of ROS generation, we also found a similar pattern of BRP changes with PQ feeding (Fig.29a-b). However, to our surprise, young and aged animals manifested distinctive variations of ROS sensitivity when exposed to PQ. Based on analyzed staining results, after 14h PQ treatment, BRP level remained unchanged in 5d-old fly brains, but obviously increased in the brains of 30-day-old animals compared to their unfed siblings at respective ages (Fig.29a). Accordingly, when confronted with identical ROS challenges, young animals demonstrated greater presynaptic resilience and remained stable, whereas their older counterparts required the upregulation of PreScale to adapt into external stress. We additionally also measured mitochondria ROS in an age-related fashion by employing mitochondria-targeted genetically encoded ROS sensor—UAS-mito-roGFP2-orp1 in 5d, 30d, 50d fly brains and we detected an age-dependent increase of mitochondrial ROS level (Fig.29c).

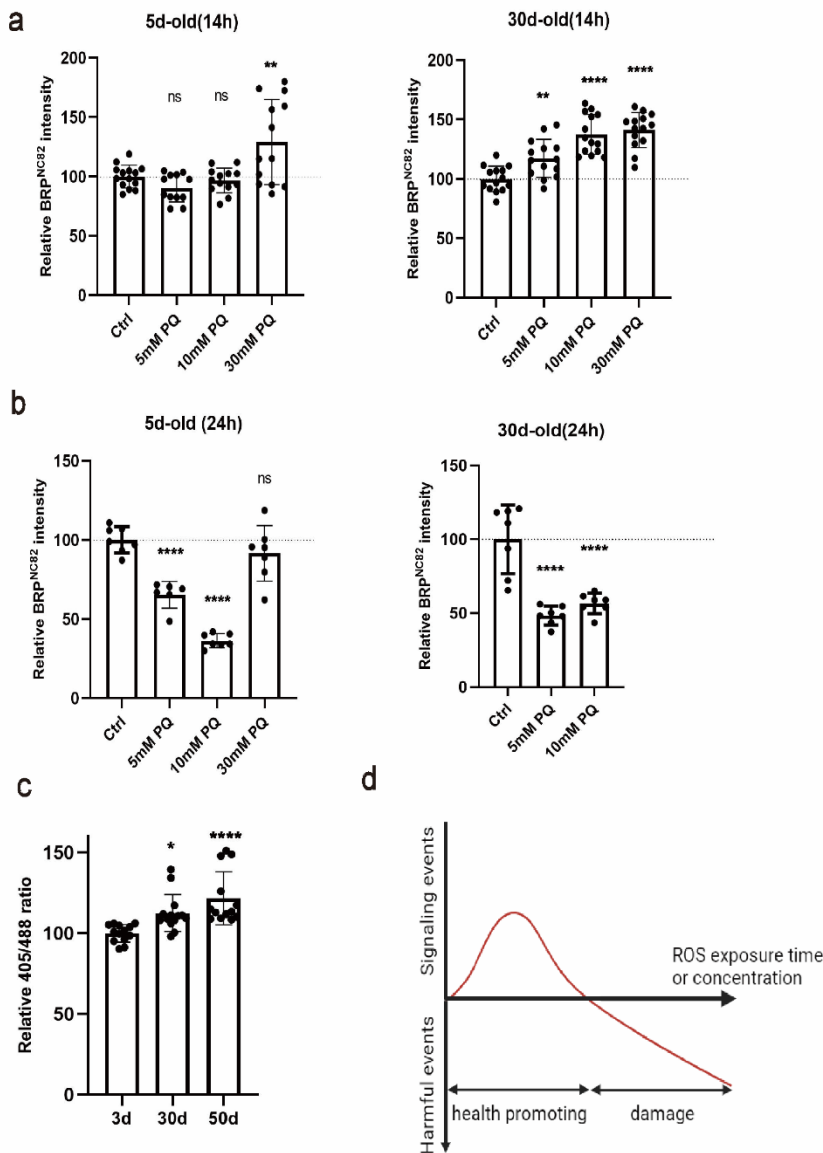


Fig.29. Evoking acute ROS stress can trigger premature PreScale. (a) Quantification of BRP^{nc82} intensity within the central brain region after 14hr administration of 5mM,10mM and 30mM PQ normalized to blank control (5% sucrose) respectively in 5d-old and 30d-old fly brains. (b) Quantification of BRP^{nc82} intensity within the central brain region after 24hr administration of 5mM,10mM and 30mM PQ normalized to blank control (5% sucrose) respectively in 5d-old and 30d-old fly brains. (c). Quantifications of relative 405/488 ratio measured by neuronal mitochondrial ROS biosensor (*elav/mito-roGFP2-orp1*) in fly brain of 5d,30d,50d wildtype; (d) Nonlinear response to ROS exposure.

Based on the genetic manipulation and external pharmacological intervention of ROS-inducing agents, we got inspired, ROS signaling serves more likely as a signaling molecule than a simple damaging agent during the regulatory process of premature PreScale, as presented in Fig.29d.

5.1.6 Effective antioxidant defense in neurons relaxes the need of PreScale in early brain aging

To further validate the results from pharmacological treatments, we turned back to the genetic operations by artificially quenching ROS in fly brains. Our unpublished proteomic data comparing the head extracts with or without MB-specific Atg5 attenuation in early-ageing (10d-old) flies revealed, in the context of impaired autophagic status within the mushroom body (MB), antioxidant proteins, including Catalase (Cat) and Glutathione S-transferase E1 (GstE1), were significantly upregulated compared to control siblings. This might indicate some antioxidant proteins Cat and GstE1 gets activated after autophagy impairment in fly brain. As we described previously (Bhukel *et al*, 2019), neuronal and MB-specific attenuation of autophagy provoked PreScale. The aforementioned evidences might also suggest a potential connection between age-related PreScale and antioxidant defense mechanism.

Cat and Superoxide Dismutase2 (SOD2) are both acting as ROS scavengers: *Cat* catalyzes H_2O_2 into H_2O and oxygen, while SOD2 binds to the superoxide byproducts and converts them into H_2O_2 and diatomic oxygen. UAS/Gal4 system was employed to activate neuronal expression of *Cat* and *SOD2*. *UAS-Cat* and *UAS-SOD2* homozygous fly line was separately crossed with pan-neuronal driver line *elav*. Overexpression of catalase (Missirlis *et al*, 2001) in *UAS-Cat* transcripts was proved by RNA in situ hybridization, and 3-fold increase of SOD2 activity was also confirmed

before (Missirlis *et al*, 2003) in *UAS-SOD2* transgene. Immuno-histological examination displayed a clear reduction of BRP fluorescence intensity in fly brains of *Cat* and *SOD2* overexpression compared to the age-matched control counterparts (Fig.30a-b). Accordingly, mitigating ROS levels in premature fly brain through enhancing antioxidant function has the capacity to suppress the age-associated increase of PreScale. The presence of an effective antioxidant defensive mechanism in neurons relaxes the necessity for PreScale at the initial stage of brain aging, suggesting the crucial role of robust antioxidant activities in slowing down or modifying the early processes of brain aging, via reducing the need for additional protective measures or interventions like PreScale.

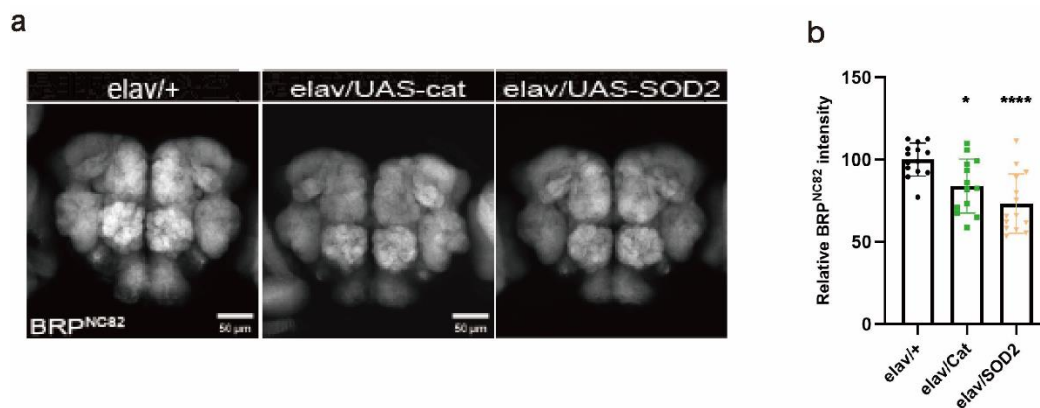


Fig.30. Effective antioxidant defense in neurons relaxes the need of PreScale in early brain aging. Adult brain, 15d. Immunostained for BRP^{nc82} in (a) *elav/+*, *elav/UAS-catalase*, and *elav/UAS-SOD2*; scale bar:50um; (b) Quantification of BRP^{nc82} intensity within the central brain region normalized to control (n = 13-14 independent brains; adjusted *p < 0.05, **p < 0.01, n = 13-14 independent animal brains. One-way ANOVA with Bonferroni multiple comparisons test).

5.2 Mitochondria within MB suffice to modulate brain-wide PreScale

5.2.1 MB-specific overexpression of dPGC1 suppresses the brain-wide increase of PreScale

We formerly elicited impairment of autophagy within the MB—the learning center in *Drosophila* brain sufficed to trigger BRP upscaling brain-wide (Bhukel *et al.*, 2019). The autophagic status of MB neurons hierarchically control over presynaptic ultrastructure throughout the brain (Bhukel *et al.*, 2019). As indicated by the findings from neuronal manipulation of mitochondrial functionality, we speculate, whether mitochondrial status within MB neurons could also potentially induce a brain-wide spreading of this presynaptic phenotype. Thus, we set out to activate dPGC1 exclusively within the MB by combining *UAS-dPGC1* transgene with the MB driver line *OK107-Gal4(OK107)*. Subsequently, we performed the immune-histological examinations with BRP antibody to view the presynaptic consequences of the MB stimulating effect of PGC1 in 15d fly brains. Strikingly, a significant reduction in BRP intensity was observed uniformly across all regions of the brain in 15d-old *OK107/dPGC1* flies, rather than just confined to the MB region relative to the control flies at the same age (Fig. **31a**). To determine the significant impact of specific MB activation of dPGC1, we monitored the lifespans of MB-specific stimulation of PGC1 as well as the corresponding driver controls. However, stimulation of dPGC1 exclusively within the MB did not exhibit the same life-promoting effects as observed after pan-neuronal overexpression. Only a minimal difference was noted between *OK107/dPGC1* flies and their corresponding driver controls (Fig. **31b-c**).

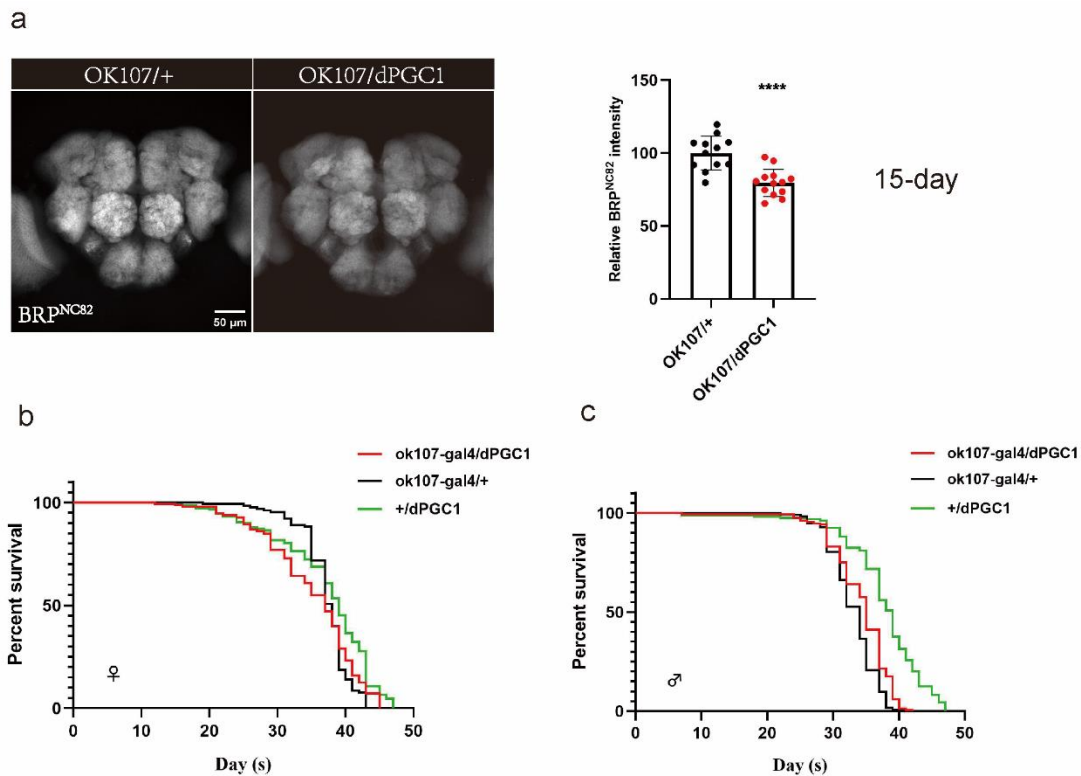


Fig.31. MB-specific overexpression of dPGC1 suppresses the brain-wide increase of PreScale. Adult brain, 15d-old. (a). Representative confocal images immunostained for BRP^{nc82} intensity in *OK107/+* and *OK107/dPGC1* fly brain, quantification of BRP^{nc82} intensity within the central brain region normalized to control (n = 13-14 independent brains; ***p < 0.001; unpaired t test); (b-c). lifespan analysis for *OK107/dPGC1* and corresponding control flies, (b) females and (c) males, n>200 for both genotypes, 3 replicates. ****p < 0.0001; Log-rank (Mantel-Cox) test.

5.2.2 MB-exclusive stimulation of PGC1 does not affect brain mitochondrial function

Accumulating evidence has confirmed the dominant position of the MB in coordinating energy metabolism and memory formation (Plaçais *et al*, 2017; Sgammeglia & Sprecher, 2022). Specifically, in *Drosophila* ageing brain, MB seemingly executes a high-

level integration of metabolic and energetic status to determine the memory formation (Bhukel *et al.*, 2019; Plaçais *et al.*, 2017; Tsao *et al.*, 2018). Obviously, in our investigation, enhancing mitochondrial biogenesis (PGC1 overexpression) in the MB is capable of preventing the increase of age-dependent PreScale across the entire brain. We continued to seek an explanation for this intriguing phenomenon and asked whether MB neurons suffices to hierarchically govern mitochondrial metabolism over the other regions of aging brain. Therefore, we decided to assess mitochondrial functionality in the premature brain after MB-specific stimulation of PGC1. Single-brain seahorse Mito Stress test and ATP assay were carried out to measure mitochondrial oxidative respiration and whole ATP amount in fly brains. However, neither oxygen consumption nor ATP content showed a significant change in the fly brains of 15d *OK107/dPGC1* relative to the control animals (Fig. **32a-b**).

Taken together, although PGC1 stimulation in MB effectively protects from PreScale in early brain aging, exclusive upregulation of dPGC1 within the MB does not noticeably affect mitochondrial respiration in the entire brain.

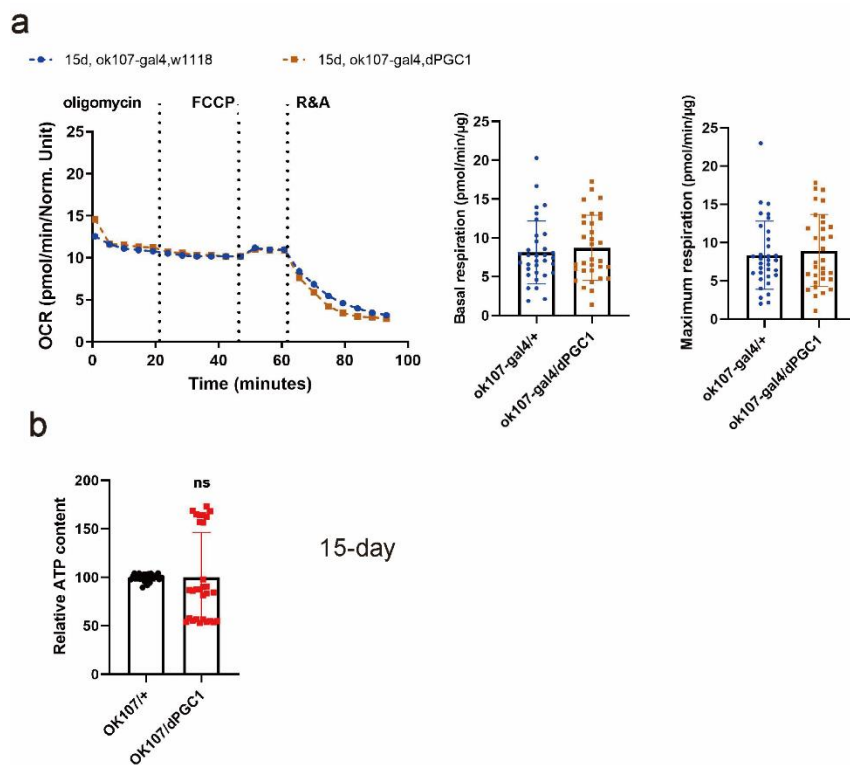


Fig.32. MB-exclusive stimulation of PGC1 does not affect brain mitochondrial function. Adult brain. 15d.(a). Single-brain seahorse Mito Stress test. Basal and maximum OCR in fly brains of *OK107/dPGC1* compared to corresponding control. Data are pooled from two independent experiments ($n = 28-30$ fly brains), $***p < 0.001$, $**p < 0.01$, $*p < 0.05$, ns, no significance, unpaired, two-tailed t-test. OCR was measured with the single brain of 15-day old *OK107/dPGC1* and *OK107/+* animals at $25^{\circ}\text{C} \pm 2^{\circ}\text{C}$ following oligomycin, FCCP, and antimycin A and rotenone treatment using the Seahorse XFe96 Analyzer. The OCR measurement was normalized to protein content. Data are pooled from two independent experiments ($n = 15-16$ fly brains); (b). Relative ATP content in 15d *OK107/dPGC1* and 15d *OK107/+* fly heads ($n=30-45$ independent heads; $*p < 0.05$; unpaired t test).

5.2.3 MB-specific attenuation of ATP subcomponent γ triggers premature PreScale

From the findings above, we have proved both PGC1 activation and *blw* knock-down in pan-neuronal cases capably tune in age-driven PreScale. Moreover, changes of mitochondrial status specifically in the MB did apparently regulate presynaptic plasticity in other parts of premature brain in a non-cell autonomous fashion. Together, we proposed to explore whether MB-specific impairment of ATP synthase subunit succeeds in controlling BRP plasticity over the entire regions of premature brain. *UAS-blw RNAi^{GD11030}* transgene was combined with MB driver *OK107*. We noticed a recurring issue where the flies with *OK107/blw* RNAi transgenic modification experienced the similar developmental delay, suggesting an essential role of energy provision in MB neurons for maintaining overall fitness. As a result, the TARGET system was employed to silence *blw* in the MB and prevent the emergence of developmental deficits in the transgenic flies. As formerly depicted, *tubulin-gal80ts* can inhibit the activity of *OK107* at 18 °C but loses its functionality at 29 °C. Thus, we raised the parental flies in a low-temperature environment (at 18 °C) and subsequently transferred the newly-hatched F1 progeny to 29 °C. With the purpose of uncovering the latent effect of MB-specific inhibition of ATP synthase subcomponent on age-related change in the presynaptic scaffold, we performed brain immunostaining using BRP^{nc82} antibody. The quantification of brain images revealed a noticeable increase in BRP intensity in *blw* knockdown fly brains relative to their controls (Fig. **33a**). As we observed in neuronal inhibition of *blw*, mere MB attenuation of ATP synthesis subunit 5A since the adulthood did induce premature PreScale. Survival Curve further showed an apparently shortened lifetime in both female and male flies with MB-specific *blw* deficiency compared to the age-matched control animals (Fig. **33b**).

To address the possible mechanism underlying the reduced lifelong time associated with MB-exclusive *blw* attenuation, we proceeded with measuring mitochondrial

respiration and ATP level in fly brains. Visibly, a substantial decline in both basal and maximum OCR was found in 15d fly brains with MB-specific *b/w* attenuation when compared to its control flies (Fig.33c). A prolonged deficiency in energy supply, resulting from reduced mitochondrial oxidative respiration, could potentially explain the reduced lifespan observed in flies with MB-specific KD of *blw*. However, ATP assays revealed no significant differences between the genetic ablation of *blw* and its controls (Fig.33d). Accordingly, ATP molecule per se did not exhibit a similar trend to decrease across the whole brain, indicating that ATP molecule should not be considered as the signaling carrier within the MB to orchestra brain-wide presynaptic activity.

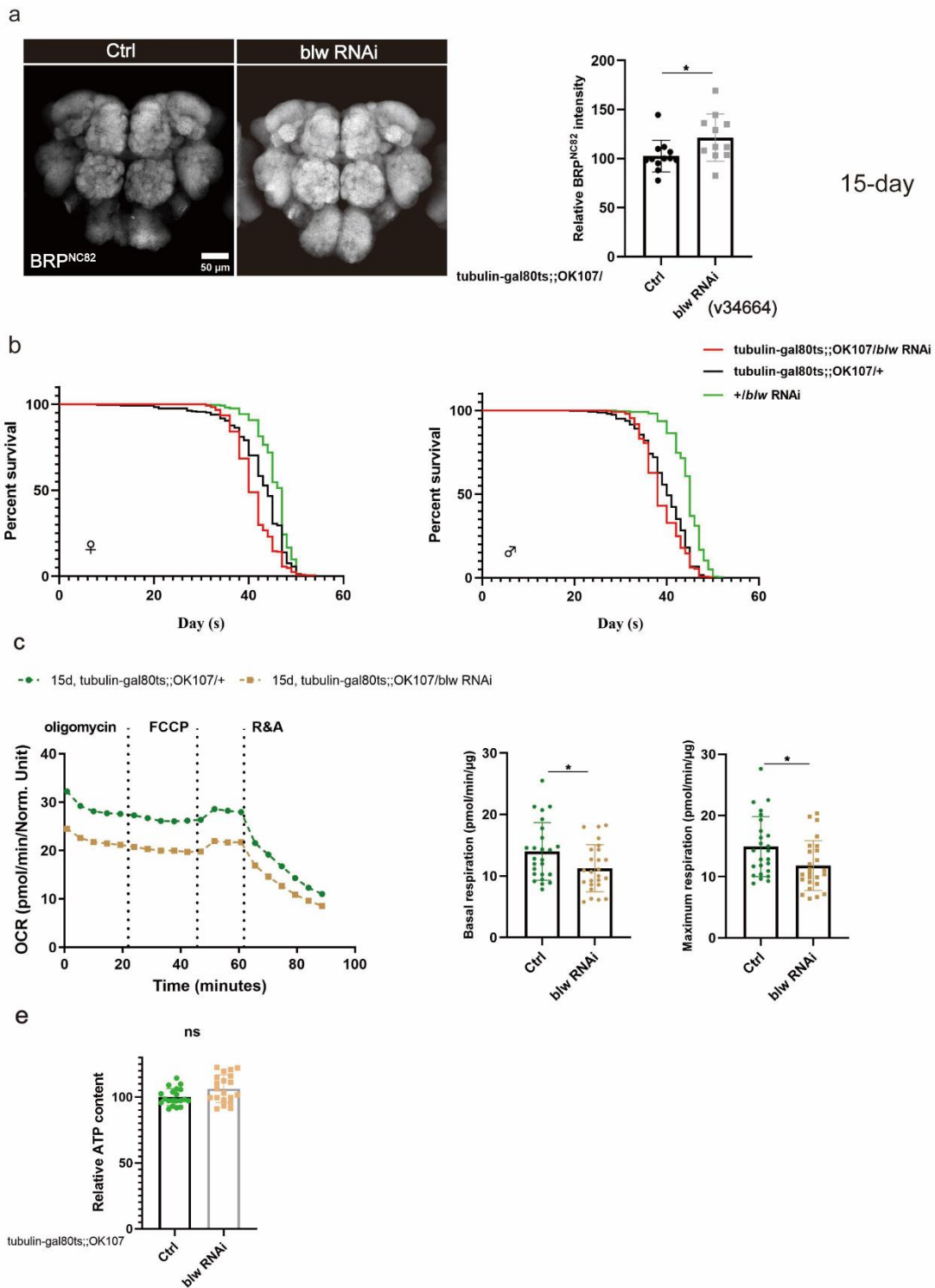


Fig.33. MB-specific attenuation of ATP subcomponent \bar{V} triggers premature PreScale. Adult brain, 15d. (a) Representative confocal images immunostained for BRP^{nc82} intensity in tubulin-

gal80ts;;OK107/+ and tubulin-gal80ts;;OK107/blw RNAi fly brain, quantification of BRP^{nc82} intensity within the central brain region normalized to control (n = 13-14 independent brains; ***p < 0.001; unpaired t test); (b). Representative confocal images immunostained for BRP^{nc82} intensity in OK107/+ and OK107/blw RNAi fly brain, quantification of BRP^{nc82} intensity within the central brain region normalized to control (n = 13-14 independent brains; ***p < 0.001; unpaired t test); (c). lifespan analysis for tubulin-gal80ts;;OK107/blw RNAi and corresponding control flies, females and males, n>200 for both genotypes, 3 replicates. ****p < 0.0001; Log-rank (Mantel-Cox) test; (d). Single-brain seahorse Mito Stress test. Basal and maximum OCR in fly brains of tubulin-gal80ts;;OK107/blw RNAi compared to corresponding control. Data are pooled from two independent experiments (n = 28-30 fly brains), ***p < 0.001, **p < 0.01, *p < 0.05, ns, no significance, unpaired, two-tailed t-test; (e). Relative ATP content in 15d tubulin-gal80ts;;OK107/blw RNAi and the corresponding control fly heads (n=30-45 independent heads; *p < 0.05; unpaired t test).

5.2.4 Changing mitochondrial functionality within sleep-controlling neurons, is insufficient to drive brain-wide PreScale-type plasticity

Based on the past observations, MB executes a high-level control over the other parts of the brain to integrate synaptic activity and memory formation. However, we did so far not analyze a potentially similar role of other neuron populations, such as sleep-promoting neuron populations. Possibly, MB neurons may not be the only group of neurons with the ability to prevail over the other regions of premature brain, propelling the alteration of age-related PreScale. We previously demonstrated (Huang *et al.*, 2022), genetically-installed PreScale reprograms the plastic activity of sleep-controlling dFB/R5 network (Donlea *et al.*, 2011; Pimentel *et al.*, 2016) and mediates the alterations of sleep behavior at advancing age. Hence, we hypothesized that, sleep-promoting neurons might also play a critical role in framing the age-related

phenotype of PreScale. Afterward, we planned to manipulate mitochondrial functionality within sleep-promoting neurons as conducted in the MB. UAS-dPGC1 and UAS-blw RNAi transgenes were combined with dFB neuron driver *R23E10*-Gal4 to bidirectionally manipulate mitochondrial metabolic status within dFB neurons (Donlea *et al.*, 2011; Pimentel *et al.*, 2016). According to the quantified results, we did not observe any significant change in BRP fluorescent intensity, neither an increase nor a reduction, after both mitochondrial enhancement and attenuation operations within the dFB neurons (Fig.34a and c). Collectively, genetic manipulation of mitochondrial functional status, including PGC1 overexpression and blw knockdown in the dFB neurons, were insufficient to regulate BRP levels across the entire brain. Another sleep-regulating neuron group—the ellipsoid body R5 (previously called R2) accepts an inhibitory signal released from the dFB neurons and forms a negatively interconnection with dFB neurons to control sleep (Donlea *et al.*, 2018). We continued to test R5 neurons along similar lines. *UAS-dPGC1* and *UAS-blw RNAi* transgenes were combined with R5 neuron driver *R58H05*-Gal4 to bidirectionally manipulate mitochondrial functionality within R5 neurons (Huang *et al.*, 2020; Liu *et al.*, 2016). Again, no significant changes in BRP levels could be detected after silencing ATP synthase subcomponent V in R5 neurons (*R58H05/blw* RNAi). At the same time, a slight but significant decline of BRP intensity across the brain was discerned in R5-overexpression of dPGC1 relative to the corresponding controls (Fig.34b and d). Taken together, the mitochondrial metabolic status within the dFB/R5 network does obviously not exert a high-level control of presynaptic plasticity across the drosophila brain.

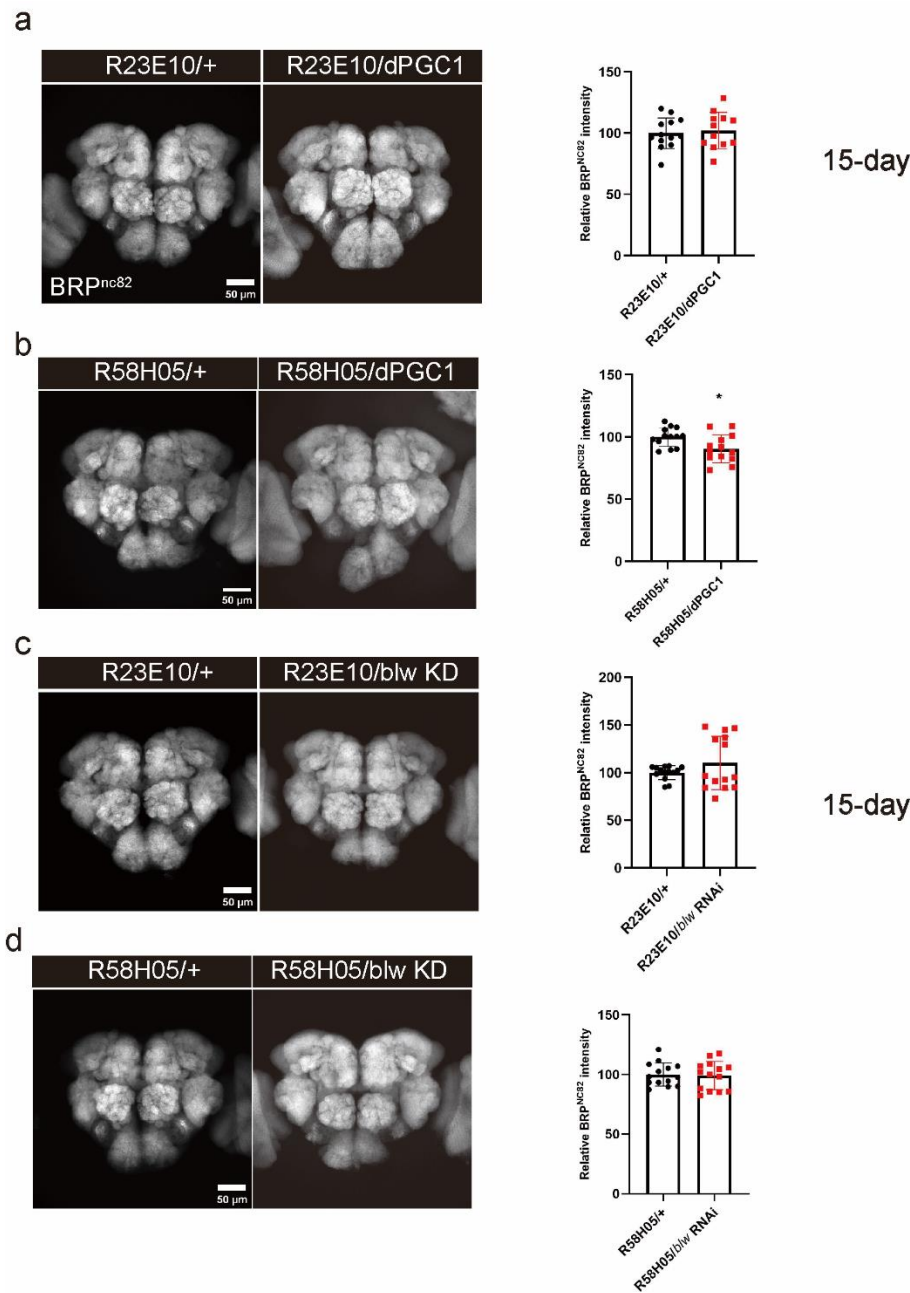


Fig.34. Sleep-controlling neurons—dorsal fan-shaped body(dFB)/R5 network, is insufficient to drive brain-wide PreScale-type plasticity. Adult brain,15d.(a) Representative confocal images stained for BRP^{nc82} intensity in *R23E10/+* and *R23E10/dPGC1* fly brain, quantification of BRP^{nc82} intensity within the central brain region normalized to control (n = 13-14 independent brains; ***p < 0.001; unpaired t test); (b) Representative confocal images stained for BRP^{nc82} intensity in *R58H05/+* and *R58H05/dPGC1* fly brain, quantification of BRP^{nc82} intensity within the

central brain region normalized to control (n = 13-14 independent brains; ***p < 0.001; unpaired t test); (c) Representative confocal images stained for BRP^{nc82} intensity in *R23E10/+* and *R23E10/blw* RNAi fly brain, quantification of BRP^{nc82} intensity in fly brain of *R23E10/blw* RNAi and *R23E10/+* within the central brain region normalized to control (n = 13-14 independent brains; ***p < 0.001; unpaired t test); (d) Representative confocal images stained for BRP^{nc82} intensity in *R58H05/+* and *R58H05/blw* RNAi fly brain; Quantification of BRP^{nc82} intensity in fly brain of *R58H05/+* and *R58H05/blw* RNAi within the central brain region normalized to control (n = 13-14 independent brains; ***p < 0.001; unpaired t test);

5.3 Short neuropeptide Y (sNPF) might link mitochondria status with PreScale

5.3.1 Robust sNPF signaling is needed for full mitochondrial activity in *Drosophila* brain

The neuropeptide F (NPF) family of neuropeptides, expressed by the MB Kenyon cells (KCs) (Johard *et al.*, 2008), exerts pleiotropic activities in drosophila nervous system and neuronal plasticity, modulating a series of behaviors like food intake, appetite controlling (Patel *et al.*, 2006) as well as sleep (Depetris-Chauvin *et al.*, 2014; Lee *et al.*, 2017). In our previous study (Bhukel *et al.*, 2019), short neuropeptide Y (sNPF) was found to signal an autophagy impairment from the MB intrinsic KCs, provoking an age-typical phenotype of PreScale throughout the entire fly brain. Moreover, MB-specific KD of the sNPF receptor induced a brain-wide metaplastic change of PreScale. The autocrine sNPF signaling in MB was competent in maintaining the presynaptic plasticity in a state conducive to memory formation (Bhukel *et al.*, 2019). In addition to its link with autophagy, NPY is closely intertwined with mitochondria in regulating energy balance in central nervous system (Sousa *et al.*, 2023). Thus, we assumed that signaling the mitochondrial status within the MB might rely on sNPF to tune the

PreScale across the brain. To test this hypothesis, we first determined whether indeed mitochondrial status within the MB might affect sNPF signaling. We here again took our advantages of genetic instruments to reduce mitochondrial functionality within the MB by combing RNA interference of *b/w* transgene with MB driver *OK107*. Subsequently, immune-histological fluorescence staining against sNPF precursor was performed in 15d fly brains with MB-specific *b/w* KD and their control counterparts. MB attenuation of *b/w* significantly decreased sNPF signals across the fly brains when compared to the controls (Fig. **35a**). This immunostaining results revealed that, deteriorating mitochondrial functionality within the MB by undermining ATP synthase functionality is effective in modulating NPY/sNPF signaling.

Mounting evidence indicates NPY contributes to counteracting aging and aging-related phenotypes. Specifically, NPY protects mitochondria from age-driven functional decay in central nervous system (Botelho & Cavadas, 2015). Therefore, we moved on to investigate the potential influence of defective sNPF activity on mitochondrial functionality. RNA interference against the sNPF receptor (sNPFr) was driven with the pan-neuronal driver *e/av-Gal4*. Then we carried out the single-brain seahorse assay to evaluate mitochondrial oxidative respiration in the context of compromised NPY activity. Indeed, mitochondrial basal respiration rate (basal OCR) significantly declined in the brains of neuronal sNPF-R KD flies relative to controls (Fig. **35b**). To confirm this impaired mitochondrial phenotype, we additionally employed the mitoTimer fluorescent probe to assess mitochondrial turnover. Likewise, a clear reduction in green to red ratio was witnessed in fly brains with neuronal sNPFr KD relative to the age-matched controls (Fig. **35c**). Accordingly, these results imply that robust NPY/sNPF signaling is required for sustaining normal mitochondrial capacity. To conclude, our experimental evidences demonstrated that, alterations of mitochondrial functionality, particularly after impairing the integrity of ATP synthase merely within the MB might well modulate NPY/sNPF signaling across the drosophila brain. On the other hand, deteriorating NPY/sNPF activity in neurons accelerated the

aging process of mitochondria and robust NPY signaling was indispensable for maintaining effective mitochondrial functionality in the fly brain.

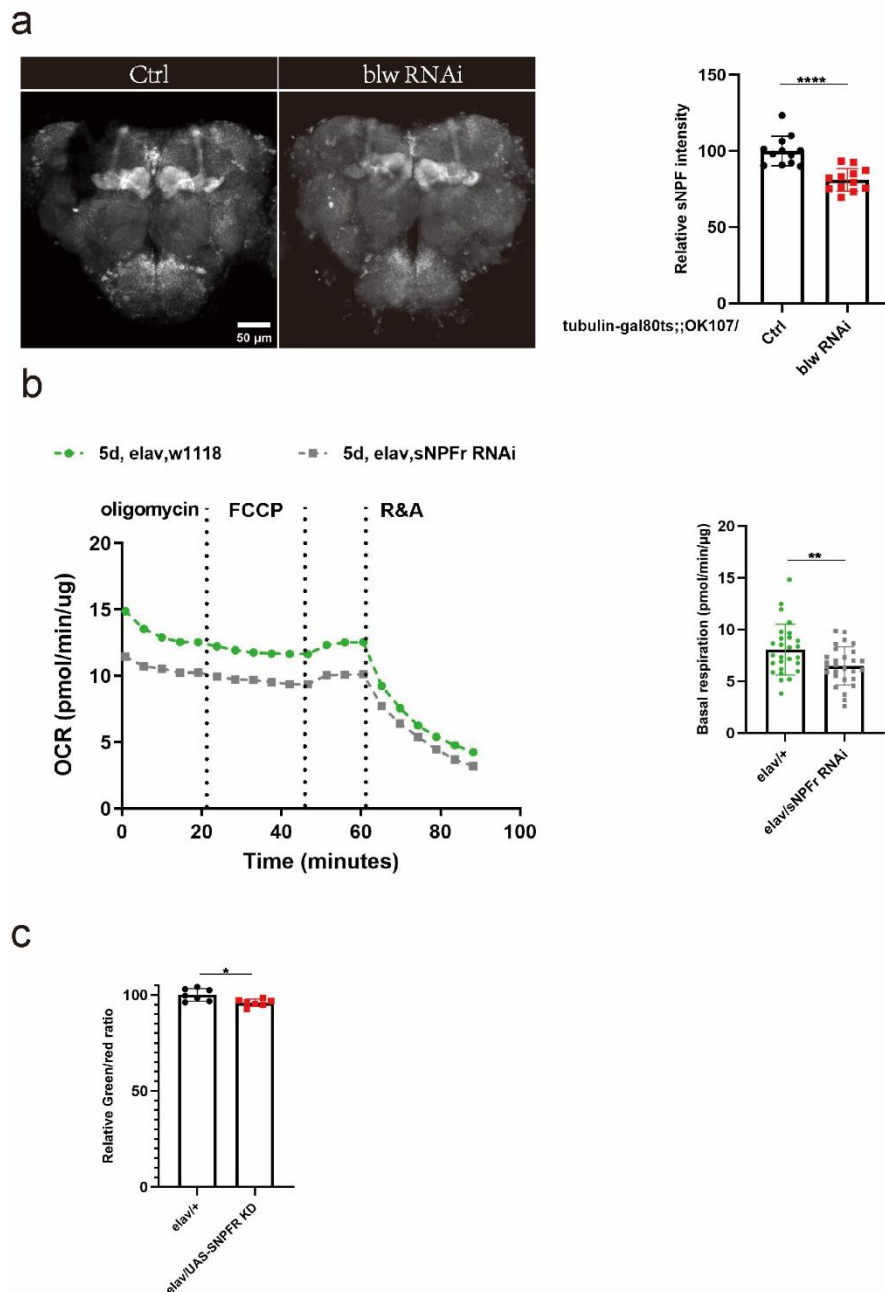


Fig.35. Robust sNPF signaling is needed for full mitochondrial activity in Drosophila brain.

Adult brain, 15d.(a). Representative confocal images immunostained for sNPF peptide precursor intensity in tubulin-gal80ts;*OK107*/*+* and tubulin-gal80ts;*OK107*/*blw* RNAi fly brain, quantification

of sNPF peptide precursor intensity within the central brain region normalized to control (n = 13-14 independent brains; ***p < 0.001; unpaired t test); Adult brain, 5d. (b). Single-brain seahorse Mito Stress test. Quantification of basal OCR in fly brains of *e/av/sNPF* RNAi compared to corresponding control. Data are pooled from two independent experiments (n = 16-18 fly brains), ***p < 0.001, **p < 0.01, *p < 0.05, ns, no significance, unpaired, two-tailed t-test; (c). Quantification of Green to red ratio for mitoTimer staining in 5d *e/av/sNPF* RNAi compared to corresponding control.

5.3.2 Neuronal attenuation of NPY activity impairs autophagy and propels age-dependent PreScale

The interplay between NPY and autophagic process has been explored extensively in other model systems. Hypothalamic autophagy induced by AMP-activated protein kinase (AMPK) potentially regulates NPY expression (Oh *et al.*, 2016). Besides, MB-specific impairment of autophagy in our previous works (Bhukel *et al.*, 2019) was found to suppress the transcriptional expression of sNPF and cause an approximately 40% reduction of sNPF transcript level in fly brain. Immuno-histological examinations (Bhukel *et al.*, 2019) revealed that the decline of sNPF ligand was visible in the entire brain with MB-specific Atg5 attenuation. The most prominent reduction occurred in the MB region, while other brain regions, such as the Sub-esophageal Ganglion (SOG), exhibited a relatively mild yet significant decrease. Conversely, the presence of NPY in rodent hypothalamus was documented to stimulate the autophagic status and delay the age-related changes in hypothalamic neurons (Aveleira *et al.*, 2015). With the aim of further dissecting the interactions between neuronal NPY/sNPF signaling and autophagy in early brain aging, we proceeded to explore the autophagic status related to damaged sNPF activity in drosophila brain. The efficacy of autophagy is indicated by the decomposition of the ubiquitin-binding scaffold protein p62/SQSTM1 (Bjørkøy

et al, 2009; Pankiv *et al*, 2007), so the accumulated p62/SQSTM1 aggregates signifies inefficient autophagic process. Soon after, we conducted brain immunostaining with p62/SQSTM117 (drosophila homolog Ref(2)p) antibody to detect autophagic process. Notably, after neuronal silencing of sNPF receptor, a drastic accumulation of p62 aggregates was visualized across the central brain compared to the age-matched control relatives (Fig.36a). Simultaneously, immunostaining against BRP protein witnessed a significant increase in BRP intensity in 10d fly brains after neuronal sNPF receptor attenuation when compared to age-matched controls (Fig.36b). The presynaptic phenotype observed in neuronal KD of the sNPF receptor is similar to that seen in sNPF hypomorph (sNPF^{c00448}) flies (Bhukel *et al.*, 2019). Considered collectively, neuronal attenuation of NPY/sNPF signaling impaired the autophagic process and same time provoked the upscaling phenotype of PreScale in early fly brain aging.

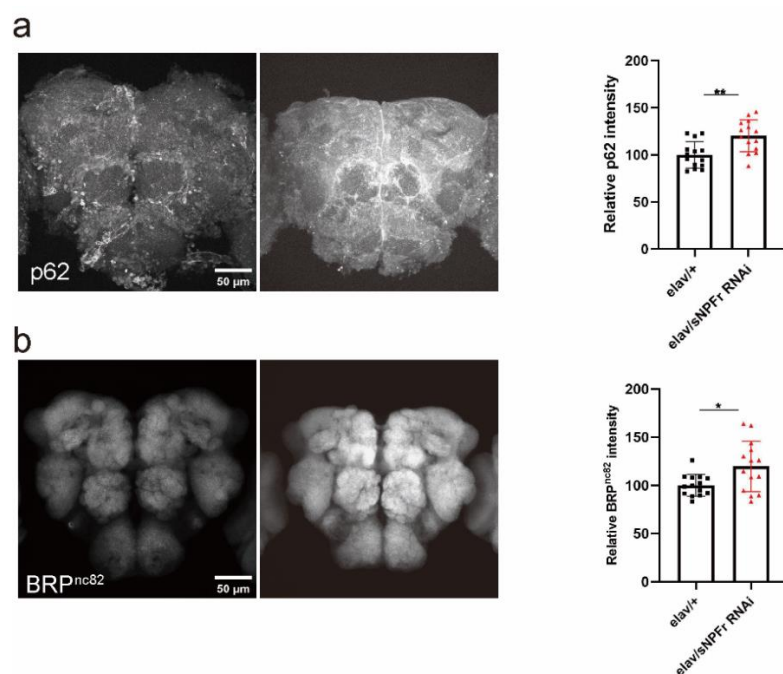


Fig.36. Neuronal attenuation of NPY activity impairs autophagy and propels age-dependent PreScale. Adult brain, 10d.(a) Representative confocal images immunostained for p62 intensity

in *e/av/+* and *e/av/UAS-SNPF* fly brain and quantification of average p62 intensity within the central brain region normalized to control (n = 13-14 independent brains; ***p < 0.001; unpaired t test); (b). Representative confocal images immunostained for BRP^{nc82} intensity in *e/av/+* and *e/av/UAS-sNPF* fly brain and quantification of average BRP^{nc82} intensity within the central brain region normalized to control (n = 13-14 independent brains; ***p < 0.001; unpaired t test);

5.3.3. Potential signaling pathways activated within the MB may link to brain-wide PreScale

5.3.3.1 Knock-down of Forkhead box O (FOXO) or minibrain (Mnb) within MB KCs disrupts autophagy status and provokes premature PreScale

We showed in the past, modulating autophagy in the MB affects the transcriptional expression of sNPF (Bhukel *et al.*, 2019). Also, according to our evidences, robust sNPF signaling is indispensable for effective MB autophagy. the regulatory mechanisms underlying the interaction between MB autophagy and NPY/sNPF signaling in Prescale remain to be explored.

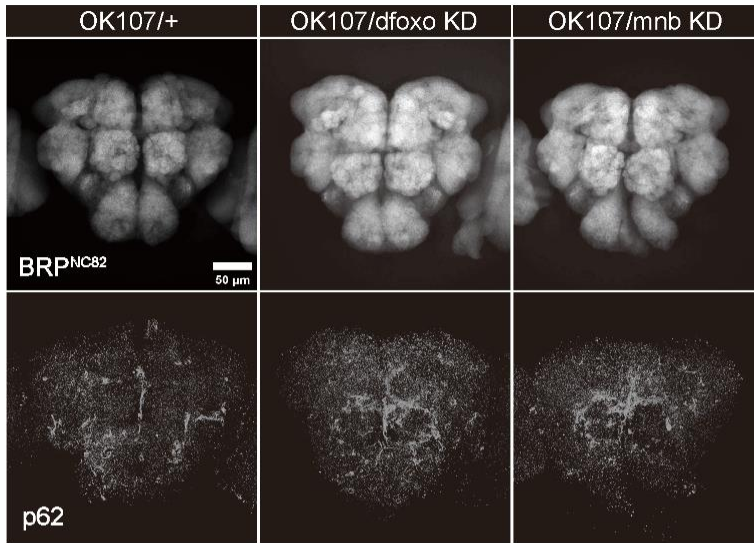
Previously, a signaling feedback loop was elucidated, demonstrating that an interaction between NPY/sNPF and FOXO regulates NPY/sNPF levels mediated via Dyrk1a/Mnb kinase. This regulatory Mnb-FOXO-sNPF signaling has been established in both *Drosophila* neurons and murine hypothalamic cells (Hong *et al.*, 2012). The family of transcription factors, known as FOXO, play a pivotal role in governing downstream gene expression. The regulatory function of FOXO encompasses cellular energy production, resistance to oxidative stress, as well as the modulation of cell viability and proliferation (Link, 2019). Particularly, activated FOXO elicits the upregulation of various crucial autophagy-related genes (Füllgrabe *et al.*, 2016). Accordingly, we assumed that the Mnb-FOXO-sNPF feedback loop might serve as the

key mediator linking autophagic status to sNPF signaling within the MB in regulating PreScale.

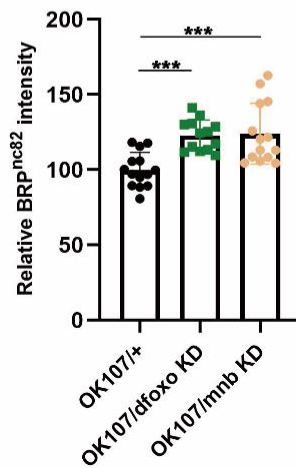
Therefore, in an effort to address whether FOXO and Mnb within the MB might be able to alter autophagic status, we set out with genetic tools to inhibit the Mnb-FOXO-sNPF signaling within the MB. Subsequently, we diminished the expression of dFOXO (drosophila FOXO) and Mnb in the MB by combining RNA interference transgenes versus FOXO and Mnb/Dyrk1a with MB driver *OK107*. Afterwards, we conducted the brain immunostaining against the ubiquitin-binding scaffold protein p62/SQSTM1. Strikingly, in the fly brain with MB KD of dFOXO, we visualized an extensive accumulation of p62 aggregates throughout the entire brain. To confirm whether this parallel autophagy impairment suffices to trigger PreScale (as observed after MB-specific *Atg5* attenuation), we performed the brain immunostaining with BRP^{NC82} antibody. Similarly, a dramatic and widespread increase of BRP intensity was witnessed throughout the entire brain relative to the control group (Fig. **37a-c**). Based on these results, FOXO and Mnb, integral components of the sNPF signaling pathway, seem to be mediators in connecting NPY/sNPF signaling and autophagic process with PreScale.

Taken as a whole, suppressing sNPF signaling by silencing FOXO or Mnb within the MB impaired autophagy and simultaneously triggered premature PreScale. A scheme visualizing the putative intersection between MB autophagy, sNPF signaling and mitochondrial functionality can be found in Fig. **38**.

a



b



c

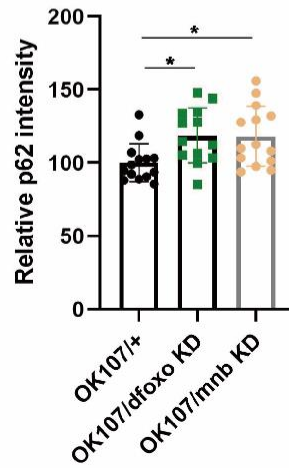


Fig.37. Knock-down of FOXO or Mnb within MB KCs disrupts autophagy status and provokes premature PreScale. Adult brain,10d.(a) Representative confocal images immunostained for BRP^{nc82} and p62 intensity in *OK107/+*, *OK107/dfoxo* RNAi and *OK107/mnb* RNAi fly brain;(b) Quantification of average BRP^{nc82} intensity within the central brain region normalized to control (n = 13-14 independent brains; ***p < 0.001; unpaired t test); (c) Quantification of average p62 intensity within the central brain region normalized to control (n = 13-14 independent brains; ***p < 0.001; unpaired t test).

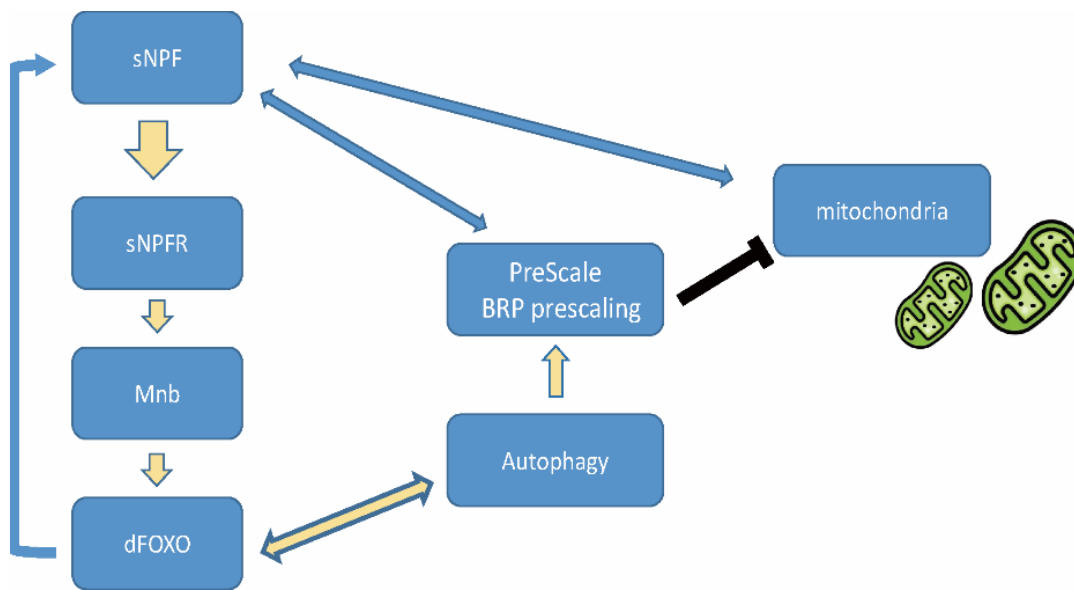


Fig.38. A scheme to illustrate a putative interplay between autophagy, sNPF signaling and mitochondria function in regulating PreScale.

5.4 PreScale might promote an energy-saving mode characterized by less mitochondrial activity and increased sNPF signaling

5.4.1 Genetically-implemented "PreScale" lowers mitochondrial abundance and respiratory function

We observed precedingly that alterations of mitochondrial functionality at the early aging stage led to the adaptations of age-associated PreScale. However, it is imperative to acknowledge that the interaction between mitochondria and presynaptic activity is definitely not unidirectional. Changes in synaptic activity can also influence mitochondrial behavior and efficiency (Thomas *et al*, 2019). Importantly, synaptic activity is highly dependent on the provision of energy and the maintenance of calcium homeostasis. Mitochondria are consistently mobilized and transported towards

presynaptic sites to fulfill the energy demands and facilitate the uptake of Ca^{2+} during the information processing at the presynaptic terminal (Devine & Kittler, 2018; Li *et al.*, 2020). To investigate the reciprocal relationship between mitochondrial functionality and age-driven PreScale, we employed a genetically-installed PreScale *3xBRP* scenario to delineate potential intersections. From our former study (Gupta *et al.*, 2016; Huang *et al.*, 2022), we technically implemented a *3xBRP/4xBRP* scenario by genetically augmenting BRP genomic copy numbers from wild type (2xBRP) to 4xBRP, resulting in a gradual elevation of BRP levels. The *3xBRP* configuration was found to be an optimal level of PreScale in early brain aging. For instance, young animals with *3xBRP* exhibited a comparatively moderate augmentation of BRP, aligning more closely with the increment observed in PreScale during normal aging. Furthermore, behavioral experiments (Huang *et al.*, 2022) illustrated *3xBRP* as another health-promoting mechanism, not only extending the lifespan of *Drosophila* but also conferring resilience to stress conditions such as sleep deprivation. Therefore, we employed young *3xBRP* animals as our priority to investigate the potential impact of PreScale on mitochondrial functionality. First of all, according to the immunostaining, a pronounced elevation of BRP was verified in the fly brains of 15d *3xBRP*, relative to isogenic wild-type relatives (Fig.39a). Subsequently, we proceeded to conduct the analysis of mitochondrial oxidative phosphorylation rates in young *3xBRP* and isogenic wild-type fly brains using the single-brain Seahorse assay. Noticeably, the quantitative OCR results unveiled a drastic reduction in mitochondrial basal respiration in *3xBRP* fly brains compared to age-matched wildtype siblings (Fig.39b). In accordance with the decline of respiration rate, the ATP amounts in the brains of *3xBRP* flies also showed a substantial decrease compared to the wild-type controls (Fig.39c). Furthermore, the fluorescent probe-mitoTimer coalesced with the pan-neuronal driver *elav* was expressed in *3xBRP* flies. As anticipated, a marginally but significantly lower green-to-red fluorescence ratio was observed in the brains of *3xBRP* flies relative to their isogenic wild-type counterparts (Fig.39d). While

decreased mitochondrial functionality was observed in the brains of *3xBRP* flies, we didn't see a similar reduction in mitochondrial mass measured via mitochondrial DNA (mtDNA) estimates (Fig. **39e**). Thus, we speculated that the decline in mitochondrial respiration in the brains of *3xBRP* flies might not be attributed to a reduced mitochondrial quantity but rather be explained via abundance changes of mitochondrial proteins. Mitochondrial Complex IV—cytochrome c oxidase IV (COXIV) and Complex V—ATP synthase are two crucial components involved in oxidative respiration and ATP production. To investigate whether the levels of COXIV and ATP5A are altered in the *3xBRP* scenario, we performed immunohistochemical analyses targeting COXIV and ATP5A proteins. From the analyzed results, a discernible reduction in ATP5A intensity was noted, while COXIV remained unchanged in the brains of *3xBRP* flies when compared to the isogenic control flies (Fig. **39f-g**). The reduction in ATP synthase 5A protein levels observed in *3xBRP* aligns with previously reported as age-related DNA damage to the α subunit of the mitochondrial F1 ATP synthase gene (Prins & Michalak, 2011). ATP synthase plays a pivotal role in connecting oxidative phosphorylation with ATP production. The compromised complex V component (ATP5A) in the brains of *3xBRP* flies disrupts proton transfer through the electron transport chain (ETC), slowing down oxidative respiration and ATP generation.

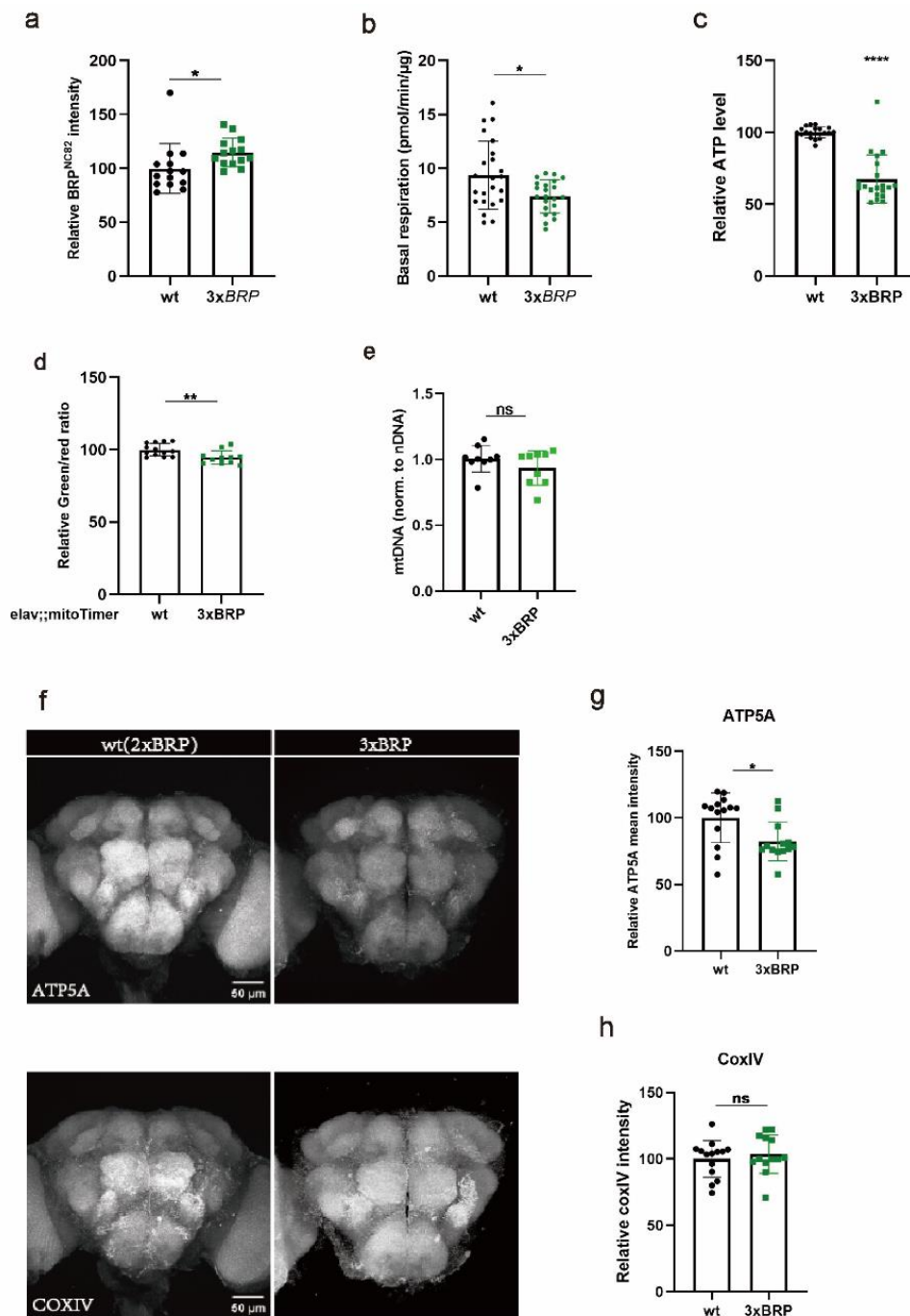


Fig.39. Genetically-implemented "PreScale" lowers mitochondrial abundance and respiratory function. Adult brain, 15d. (a) Quantification of confocal immunostaining for BRP^{nc82} intensity within the central brain region normalized to control in 3xBRP and isogenized w¹¹¹⁸ fly brains (n = 13-14 independent brains; ***p < 0.001; unpaired t test); Adult brain, 5d. (b) Relative

ATP content in the whole brain of 3xBRP flies normalized to isogenized *w*¹¹¹⁸. (c) Basal OCR in fly brains of 3xBRP and *wt* flies. Data are pooled from two independent experiments (n = 22-23 fly brains), ***p < 0.001, **p < 0.01, *p < 0.05, ns, no significance, unpaired, two-tailed t-test. (d) Quantification of mitoTimer Green/Red ratio in 3xBRP and *wt* fly brains, (n = 13-14 independent brains; **p < 0.01; unpaired t test); (e) qPCR of mitochondrial DNA copy number normalized to nuclear DNA in 3xBRP fly brains normalized to isogenized *wt* brains. (f) Representative confocal images immunostained for (f) ATP5A and CoxIV in *wt* and 3xBRP, scale bar:50um; (g-h) Quantification of average (g) ATP5A and (h) CoxIV intensity within the central brain region normalized to control (n = 13-14 independent brains; ***p < 0.001; unpaired t test).

Reactive oxygen species (ROS), generated as by-products of oxidative respiration, serve as an additional indicator of mitochondrial functionality. In the 3xBRP fly brain, proton transfer might be interrupted as a consequence of attenuated ATP synthase function, potentially leading to increased ROS production. Henceforth, we assessed ROS levels and ROS susceptibility in young 3xBRP and wild-type animals. Markedly, the amplex red assay disclosed an obvious increase in H₂O₂ level in the heads of 3xBRP flies (Fig.40a-b). Moreover, to our surprise, according to the survival rate with paraquat feeding, 3xBRP flies, despite exhibiting higher ROS levels in their brain, demonstrated an increased resilience to oxidative stress when compared to their wild-type counterparts (Fig.40c-d).

ROS embody a dual nature: a certain amount of ROS functions as signaling molecules, playing an indispensable role in organismal physiology and adaptive response (Shadel & Horvath, 2015). Nevertheless, an excess of ROS can lead to detrimental and damaging consequences. The concept of hormesis in biology, is defined as the phenomenon where low levels of physiological stress stemming from biological, chemical and physical pressures, upregulates adaptive responses that not only potentially repair existing damage, but also reduce or overcompensate for the injury (Calabrese, 2013, 2016). As a result, hormetic responses promote health span by

enhancing resilience and overall well-being in cells, organs and organisms (Calabrese *et al*, 2023). The survival analysis suggested, the heightened ROS levels observed in the heads of *3xBRP* flies might act as a form of hormetic signaling, eliciting beneficial and adaptive responses against external threats, such as higher oxidative stress. Furthermore, the boosted resilience against PQ feeding might be an adaptive hormetic response to promote the health and fitness of the whole organism.

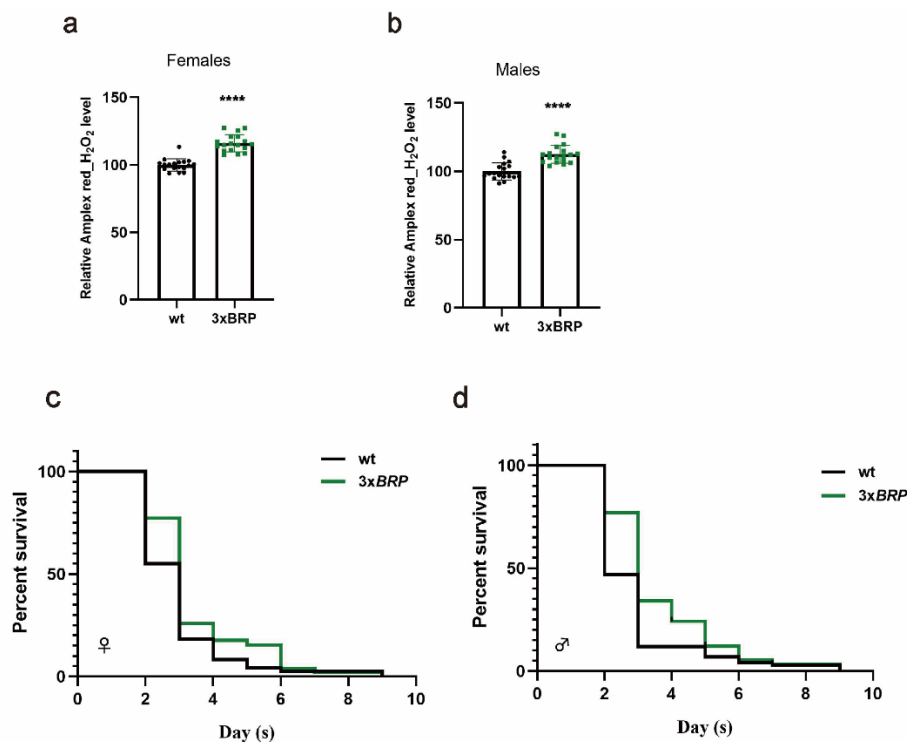


Fig.40. Relative ROS level in *3xBRP* fly brain and resilience against oxidative stress. (a-b) Quantification of Relative peroxide(H_2O_2) levels (Amplex red absorbance rate normalized to protein content) in wt and *3xBRP* (a) females and (b) males fly brains (n=19-20 independent animal brains, **p < 0.01, *P < 0.05, Unpaired, two-tailed t-test); (c-d) Survival rate against 5mM paraquat in wt and *3xBRP* (c) females and (d) males (n>200 animals per genotype, *p < 0.05, ns, no significance, Log-rank (Mantel-Cox) test)

In order to keep up with metabolic demands and facilitate clearance of impaired components, mitochondria undergo dynamic morphological changes, shaped by a balanced interplay of fusion and fission events (Wai & Langer, 2016). Acknowledging the impact of the *3xBRP* scenario on mitochondrial metabolic status, we chose to analyze mitochondrial change in *3xBRP* flies alternatively from the side of dynamic morphology by gSTED microscopy.

The MB serves as a central integration center crucial for memory acquisition and storage (de Belle & Heisenberg, 1994; Heisenberg, 1998). Within the olfactory system, the Mushroom Body Calyx is a key region where projection neurons (PN) synapse on the dendrites of Kenyon cells (Aso *et al.*, 2014). This structure provides an opportunity to concurrently examine the status of presynaptic mitochondria and mitochondria within the Kenyon cell body. Utilizing gSTED deconvolved images with ATP5A, we illustrated that the genetic installation of an additional copy of BRP resulted in less circular and less solid mitochondria in the pre-synapse (Fig. **41a-e**), whereas *3xBRP* induced an increase in the number of smaller mitochondria in the Kenyon cell body (Fig. **41f-i**). Collectively, according to gSTED analysis, we observed distinct differences in mitochondrial morphology within the MB calyx of *3xBRP* flies, which evidently occurred at both presynaptic terminal and KCs cell body region, when compared to wildtype animals.

The dynamic properties of mitochondria, consisting of fusion, fission and degradation, are crucial for sustaining the optimal status of mitochondrial energy generation (Chan, 2020). The observed alterations in mitochondrial dynamics within the MB calyx of *3xBRP* flies may be facilitated by changes in mitochondrial function, particularly a decrease in mitochondrial respiration. However, further in-depth investigations are required to provide mechanistic explanations for these observations.

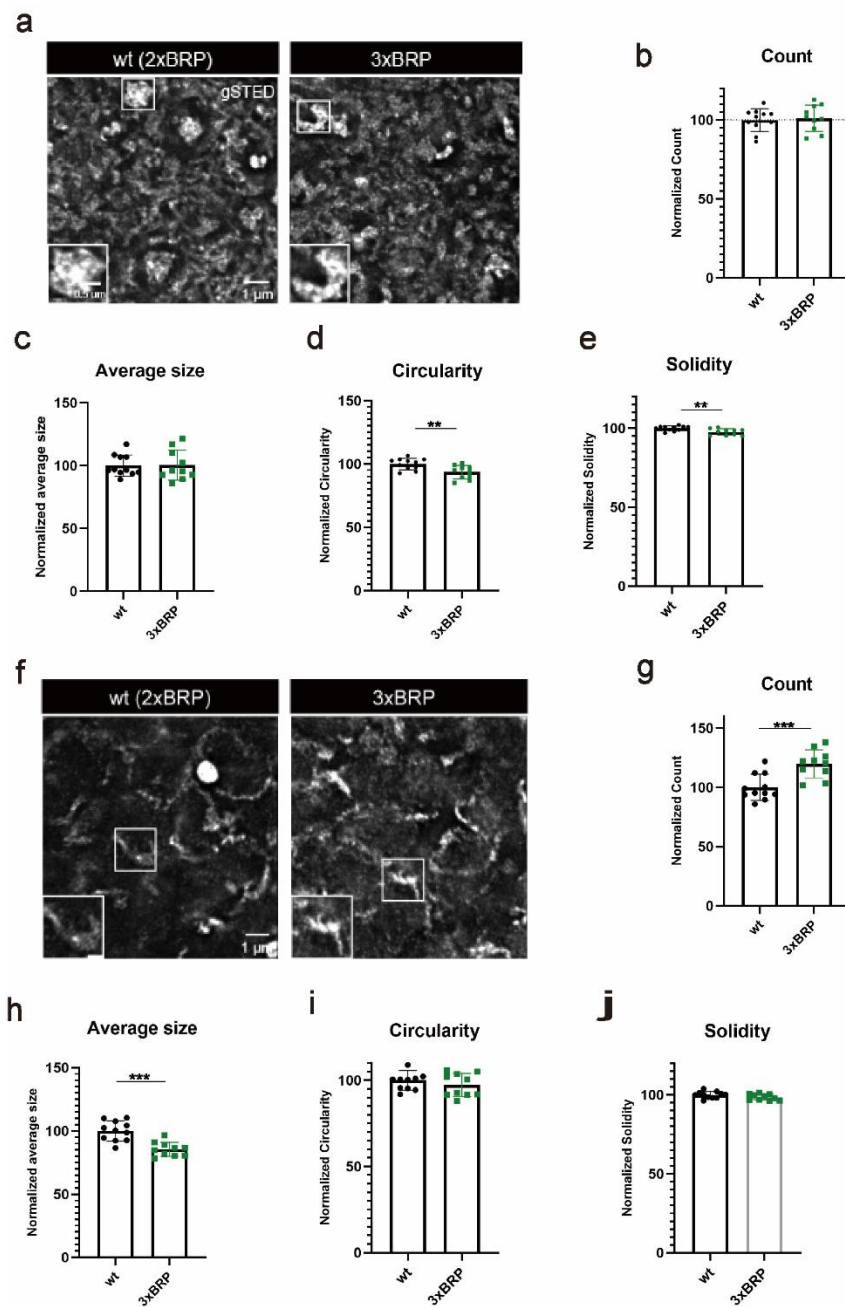


Fig.41. The dynamics of mitochondrial morphology are altered in the 3xBRP scenario. (a) Representative gSTED deconvolved (decon) images of mitochondrial morphology immunostained with ATP5A in calyx of drosophila brains in wt and 3xBRP, scale bar: 1 μ m; (b-e) Quantification of mitochondrial morphology:(b) count, (c) average size,(d) Solidity, (e) circularity normalized to corresponding driver control of ATP5A-stained mitochondria. Dot plots show all data points along with the mean (bar) \pm SD (n=9-11 independent animal brains) *P < 0.05. Unpaired, two-tailed t-test.

(f) Representative gSTED deconvolved (decon) images of mitochondrial morphology immunostained with ATP5A in kenyon cell body of drosophila brains in wt and 3xBRP, scale bar: 1µm;(g-i) Quantification of mitochondrial morphology:(g) count, (h) average size, (i) Solidity, (j) circularity normalized to corresponding driver control of ATP5A-stained mitochondria. Dot plots show all data points along with the mean (bar)±SD (n=9-11 independent animal brains) *P < 0.05. Unpaired, two-tailed t-test.

In summary, the genetically engineered PreScale provokes a mitochondrial phenotype normally associated with early aging, subsequently transitioning the brain's metabolic state into an energy-conserving mode. This PreScale-induced metabolic reprogramming, characterized by chronically elevated moderate ROS levels, potentially fosters prolonged vitality and heightens resilience against external stressors such as PQ feeding.

5.4.2 The genetically-engineered PreScale promotes the expression of neuropeptide Y signaling

Our previous data suggest that MB-specific KD of sNPF receptor was sufficient to induce a brain-wide metaplastic change in PreScale (Bhukel *et al.*, 2019). However, as a type of neurotransmitter, the release of NPY/sNPF from MB KCs, is also influenced by signal transmission at synapses. Thus, we assume that genetically encoded PreScale might be capable of emitting feedback signal to modulate the activity of sNPF-secreting MB neurons. Consequently, we sought to address whether genetically induced PreScale (3xBRP/4xBRP scenario) has the potential to alter sNPF ligand levels. Notably, relative to wildtype siblings, an obvious increase of sNPF peptide precursor intensity was detected in the brain of 5d 3xBRP flies. In contrast, we did not note a significant difference between 4xBRP flies and age-matched wt relatives (Fig.42a-b). Collectively, in 3xBRP scenario, the optimal dosage of age-related

PreScale promotes the expression of sNPF signaling. Given the significance of NPY/sNPF signaling in aging and lifespan determination (Botelho & Cavadas, 2015), the increased sNPF levels may potentially contribute to the prolonged lifetime observed in *3xBRP* flies.

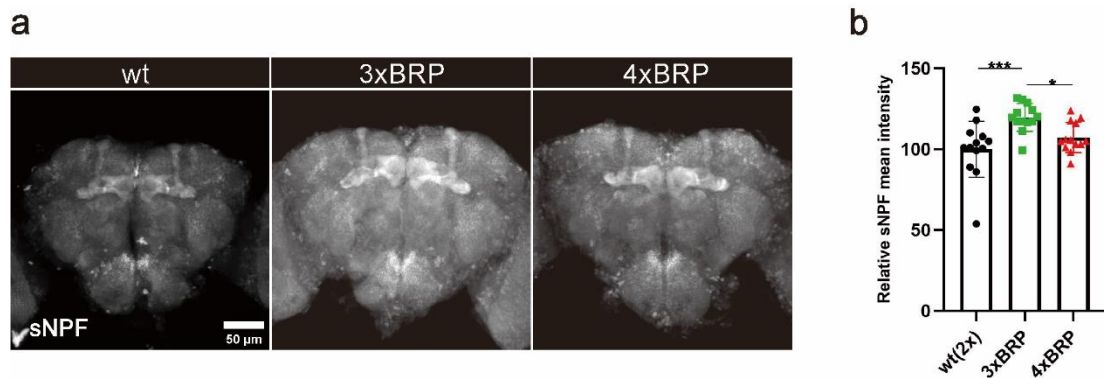


Fig.42. The genetically-engineered PreScale promotes the expression of neuropeptide Y signaling. Adult brain,5d.(a) Representative confocal images immunostained for sNPF precursor peptide in wt, *3xBRP* and *4xBRP*, scale bar:50um; (b) Quantification of average sNPF precursor peptide intensity within the central brain region normalized to control (n = 13-14 independent brains; ***p < 0.001; unpaired t test).

5.4.3 Mitochondrial calcium influx may contribute to the mitochondrial reprogramming induced by PreScale.

At the presynaptic terminal, mitochondrial functions are closely tied to calcium (Ca^{2+}) buffering. Mitochondrial Ca^{2+} within the matrix plays an essential role in regulating mitochondrial metabolism and ATP production (Boyman *et al*, 2020a). The accumulation of Ca^{2+} into the mitochondrial matrix, facilitated by the impermeable nature of the mitochondrial inner membrane to ions, necessitates the presence of an electrogenic channel known as the mitochondrial calcium uniporter (MCU). Importantly,

impaired mitochondrial calcium uptake by knocking out MCU leads to a reduction in mitochondrial ATP synthesis and compromises oxidative respiration in both *Drosophila* (Tufi *et al.*, 2019a) and mice skeletal muscles (Pan *et al.*, 2013). Nevertheless, the uptake of mitochondrial Ca^{2+} is significantly constrained by the concentration of cytosolic Ca^{2+} (Boyman *et al.*, 2020a; Fink *et al.*, 2017). The influx of Ca^{2+} into the mitochondrial matrix is heightened in response to an elevation in cytosolic Ca^{2+} . Accordingly, the Ca^{2+} elevations associated with continued action potential arrival and release might link to mitochondria functionality via presynaptic Ca^{2+} . Moreover, the influx of mitochondrial Ca^{2+} may trigger the mitochondrial remodeling we observed upon triggering PreScale (Fig.39). Hence, we investigated the potential impact of mitochondrial Ca^{2+} on PreScale. Apart from mitochondria, the endoplasmic reticulum (ER) is majorly involved in intracellular calcium storage (Prins & Michalak, 2011). The inositol 1,4,5-trisphosphate receptors (IP_3Rs) and Ryanodine receptors (RyRs) represent the distinct types of ER Ca^{2+} releasing channels responsible for mediating the release of Ca^{2+} from the ER into the cytoplasm. To determine the relevance of different Ca^{2+} sources to PreScale, we individually suppressed IP_3Rs , RyRs , and MCU in the brain using the UAS/Gal4 system and conducted BRP immunostaining. *UAS-IP₃R RNAi^{JF01957}* and *UAS-RyR RNAi^{JF03381}* were tested (Bi *et al.*, 2014) by RT-PCR to efficiently decrease mRNA levels of IP_3R and RyR . Besides, *UAS-MCU RNAi^{HMS01927}* was also proved to significantly decrease mito- Ca^{2+} signal by mito-GCaMP examination (Lee *et al.*, 2018).

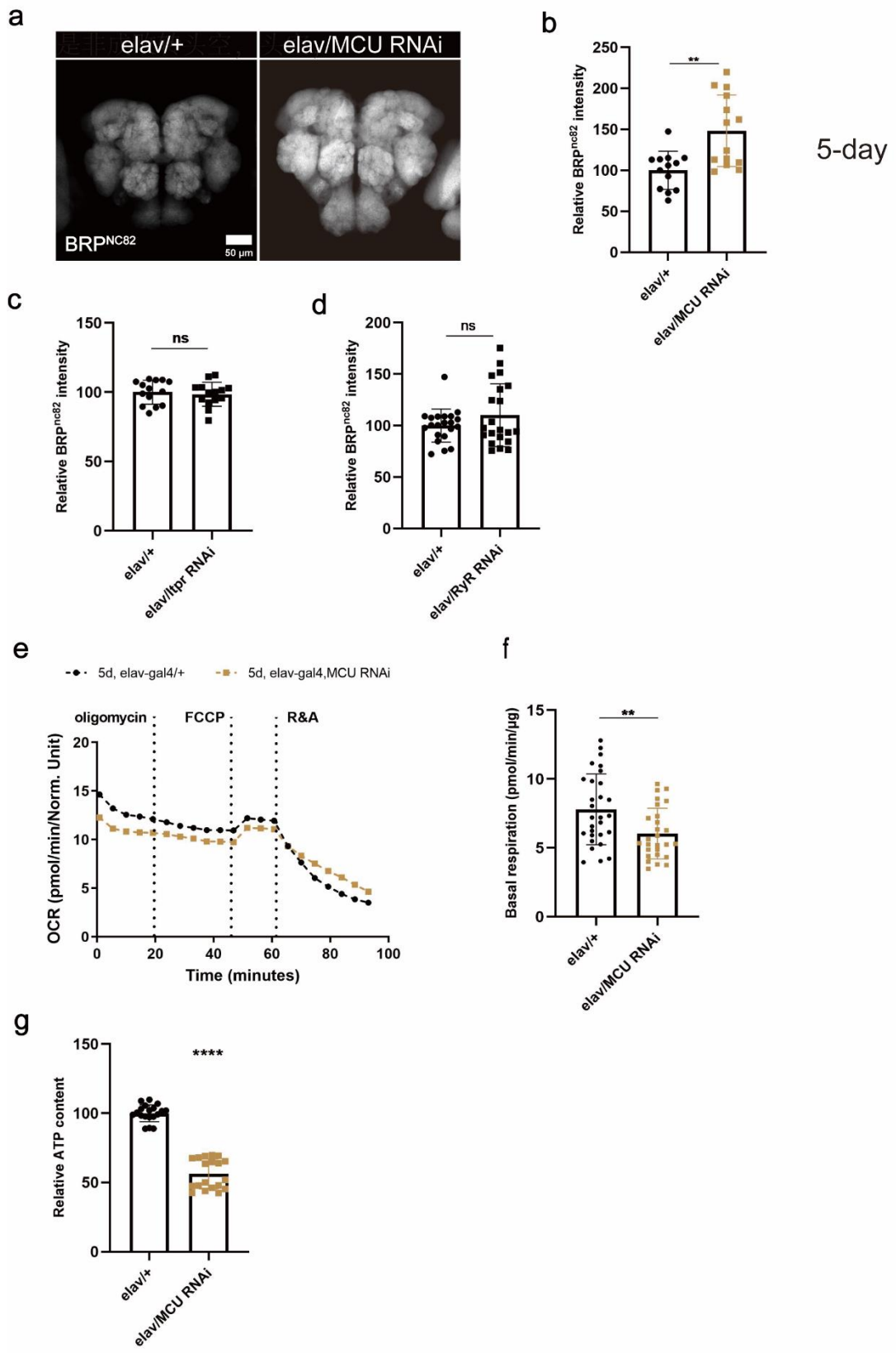
The immunostaining analysis revealed minimal changes in BRP levels when inhibiting either IP_3Rs or RyRs pan-neuronally, compared to the controls (Fig.43c-d). Notably, neuronally blocking MCU has evidently up-regulated BRP intensity when compared to *e/av/+* siblings (Fig.43a-b). To this end, we confirmed the impaired mitochondrial Ca^{2+} influx, rather than ER Ca^{2+} releasing, as the driving force of PreScale. Subsequently, with the effort to understand the ongoing change of mitochondrial functionality caused by neuronal MCU KD, we evaluated the basal respiration rate and ATP level in 5d fly

brains of neuronal attenuation of MCU compared to its control animals. Pan-neuronal ablation of MCU markedly decreased mitochondrial respiration and ATP levels relative to the corresponding controls (Fig. **43e-g**).

Our previous investigation (Huang *et al.*, 2022), by expressing calcium-dependent nuclear import of LexA (CaLexA) in *Drosophila* neurons, revealed insights into the mechanism by which genetically-installed PreScale reprograms early ageing-associated neuronal activity. The reduced Ca²⁺-associated activity in projection neurons (PNs), should be attributed to the genetic augmentation of BRP genomic copy numbers. Accordingly, we speculate that artificially induced PreScale may decrease mitochondrial Ca²⁺ uptake by attenuating neuronal activity and subsequently suppressing average Ca²⁺ elevation at the presynaptic terminal. Under these conditions, presynaptic mitochondria may reduce Ca²⁺ uptake through the MCU which simultaneously dampens metabolic processes within the mitochondrial matrix.

Comparably, the immunostaining targeting pre-synapses stained with BRP and postsynaptic structure stained with Drep2 revealed that, mitochondrial GFP signals expressed with the PN driver line *GH146* was tightly neighbored with synaptic scaffold in calyx (Fig. **43h**). Such spatial arrangement provides great opportunities for mitochondria to buffer Ca²⁺ at the synaptic terminal.

Taken together, Ca²⁺ influx into mitochondria serves as the bridge linking PreScale with mitochondrial functionality. Pan-neuronal ablation of MCU provoked PreScale and led to a decreased mitochondrial functional status similar to what we witnessed in the context of genetically-installed “PreScale”. Mechanistically, genetically engineered PreScale might influence mitochondrial functionality by reducing Ca²⁺ influx into mitochondria. As a consequence, downregulated mitochondrial Ca²⁺ uptake turns down metabolic process in mitochondria.



h

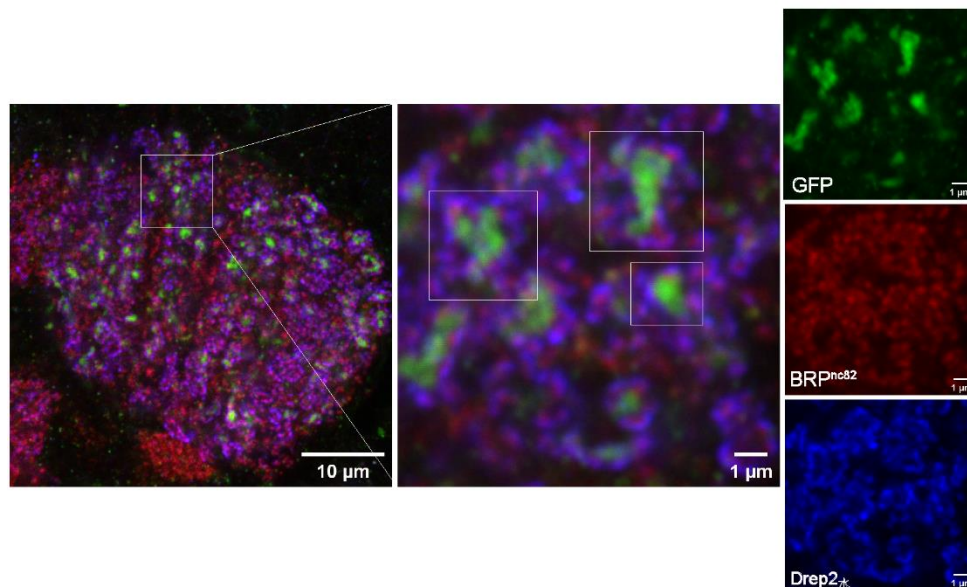


Fig.43. Mitochondrial calcium influx may contribute to the mitochondrial reprogramming induced by PreScale. Adult brain, 5d. (a). immunostained for BRP^{nc82} in fly brain of *elav/+* and *elav/MCU RNAi*, scale bar:50μm; (b) Quantification of BRP^{nc82} intensity within the central brain region normalized to control in *elav/+* and *elav/MCU RNAi* fly brains (n = 13-14 independent brains; *p < 0.05; unpaired t test); (c-d) Quantification of (c) BRP^{nc82} intensity within the central brain region normalized to control in *elav/+* and *elav/Itpr RNAi* fly brains; (n = 13-14 independent brains; *p < 0.05; unpaired t test); Quantification of (d) BRP^{nc82} intensity within the central brain region normalized to control in *elav/+* and *elav/RyR RNAi* fly brains;(e-f) Basal OCR was measured in single brain of *elav/MCU RNAi* and *elav/+* animals; (f) Quantification of Basal OCR in single brain of *elav/MCU RNAi* and *elav/+* animals. (n = 27-30 independent brains; *p < 0.05; unpaired t test) (g) Relative ATP content in the whole brain normalized to corresponding control in *elav/MCU RNAi* and *elav/+*; Data are pooled from two independent experiments (n = 27-29 fly brains, ***p < 0.001, **p < 0.01, *p < 0.05, ns, no significance, unpaired, two-tailed t-test.); (h) Representative confocal microscopy of 5d fly brains immunostained with GFP (Green) and synapses staining with BRP^{nc82} (red) and Drep2 (blue) of GH146/UAS-4mtGCamp3, Images represent single focal planes from calyx.

6. Discussion

6.1 Age-induced PreScale can be tuned by genetic manipulations of mitochondrial functionality in a bi-directional manner

Synapses face a significant challenge in preserving their optimal capacity for information processing and storage to ensure successful brain aging. Building on the past researches (Gupta *et al.*, 2016; Huang *et al.*, 2022), a brain-wide increase of presynaptic active zone proteins and related synaptic vesicle release factors until mid-age, referred to as “PreScale”, was demonstrated to modulate trade-offs among longevity, sleep architecture, and memory consolidation in aging drosophila brain. Mitochondrial functionality, as a crucial aging hallmark, deteriorates with aging. Dietary spermidine supplementation (Spd-S) prevents age-associated increase of presynaptic active zone proteins and protects from age-dependent mitochondrial functional decay (Liang *et al.*, 2021). On this occasion, we substantiated that mitochondrial functional status in premature drosophila brain intricately regulates age-associated alterations of PreScale. For instance, based on our experimental evidence, pan-neuronal activation of PGC1 rejuvenated age-related decay of oxidative respiration and ATP amount, and concomitantly, suppressed the onset of PreScale at an early stage of brain aging. Conversely, neuronal attenuation of ATP5A (*b/w*) even aggravated age-induced mitochondrial decline and provoked premature PreScale in early aging brain. The effect of pan-neuronal induction of PGC1 parallels that of another healthy aging paradigm, Spd-S. Besides, ATP synthase components are among the most abundant mitochondrial proteins enhanced by dietary rearing of spermidine (Liang *et al.*, 2021). Both findings together establish an implicit nexus between these two mitochondrial proteins (PGC1 and ATP5A) and brain aging.

The age-delaying effect of PGC-1 has been illustrated in both drosophila and mammalian models. Activation of PGC1alpha in mouse skeletal muscles was shown

to protect from sarcopenia in aged male animals (Yang *et al*, 2020). In addition, tissue-specific overexpression of PGC1 in the digestive tract delays age-related alterations in the intestine and prolongs the whole lifetime of drosophila (Rera *et al.*, 2011). Moreover, neuronal-specific stimulation of PGC1 in mice prevents from hypoxia-induced memory impairment and diminishes excess ROS in the hippocampus (Han *et al*, 2020). Similarly in our observations, pan-neuronal PGC1 stimulation delayed age-induced decline in mitochondrial respiration and boosted ATP contents in premature drosophila brain, extending the lifespan of male animals. Maintenance of mitochondrial functionality is believed to contribute effectively to the aging process and associated disorders (Wenz, 2011). The transcription coactivator PGC1 promotes mitochondrial biogenesis and consequently, rejuvenates age-related functional decline, opening up a promising anti-aging strategy for future work.

Mitochondria play a pivotal role in maintaining synaptic homeostasis by providing approximately 90% of cellular ATP, predominantly generated through oxidative respiration. The processes of Ca^{2+} clearance, synaptic vesicle recycling, and refilling at the presynaptic terminal are all highly energy-demanding. Moreover, due to the wide distribution and adaptive motility of mitochondria, neuronal mitochondria exhibit the functional advantages to satisfy energy need and actively buffer Ca^{2+} at synaptic terminal (Devine & Kittler, 2018). Hence, the plastic activity at synapses is significantly defined by mitochondrial dynamics and ATP provision. Our investigation also suggested, pan-neuronal attenuation of ATP5A (*b/w*) deteriorated mitochondrial functional decay and reset the starting point of age-driven PreScale in early aging fly brain. In alignment with our discoveries, mitochondrial aconitase 1(mAcon1)-converting citrate to isocitrate in the initial step of the Krebs cycle was previously acknowledged (Cho *et al*, 2021) for its capacity to bilaterally induce BRP plasticity (“PreScale”). ATP synthase, as a proton pump, utilizes the chemical potential energy from the proton gradient across the IMM to transfer ADP into ATP. Defective activity of ATP synthase and impaired F1F0 complex coupling within mitochondria, serve as

crucial factors in the process of brain aging (Ebanks *et al*, 2020; Gauba *et al*, 2017). In mechanistic explorations, we have identified ROS, byproducts of oxidative respiration, as the mediator, drives PreScale-type presynaptic plasticity in early aging brain. Forward electron transport (FET) and reverse electron transport (RET), induce ROS generation within mitochondria, linking with the pace of oxidative respiration and ATP production (Murphy, 2009; Scialò *et al*, 2017). In a physiological condition, FET ROS release (FETROS) occurs with high ATP consumption during which electrons from NADH flow along the transport chain and very few of them would react with oxygen to form superoxide (O_2^-). However, a reduction in energy demands signified by lowered ATP consumption will lead to an increase in ROS release (Chintaluri & Vogels, 2023; Murphy, 2009). This phenomenon arises when ATP is not utilized at expected rates, resulting in a shortage of mitochondrial ADP at complex V. The hindered ATP production facilitates electrons to escape from the ETC, subsequently captured by oxygen to generate what is referred to as reverse electron transport ROS release (RETROS). According to our analysis, ROS level in heads of neuronal PGC1 overexpression flies significantly decreased, while neuronal abrogation of ATP5A (*b/w*) notably elevated ROS content in fly heads when compared to their corresponding control siblings. Accordingly, we can assume that ROS production in neuronal PGC1 overexpression fly brains was associated with the FETROS process, while ROS release in ATP5A (*b/w*) attenuation was connected with RETROS. To clarify, PGC1 boosts mitochondrial respiration and facilitates ATP production during early brain aging, consequently, potentially inducing FET ROS release, while inhibiting ATP synthase subcomponent V disrupts ATP production and depresses oxidative respiration, probably triggering RET ROS release.

Following this, we undertook great efforts to unraveling the supposedly complex interplay between ROS levels and PreScale-type presynaptic plasticity in the fly brain. To begin with, pharmacological ROS agents were administered to flies following precise concentration gradients and temporal profile. As a result of our screening, we

found that 2% of fed H₂O₂ over 6-hour suffices to provoke PreScale throughout the entire brain. Genetically, we found that neuronal overexpression of Cat and SOD2 reduced PreScale. Experimental observations thus showed that effective antioxidant defense lowered the need of PreScale in early-aging brain. Collectively, ROS level has proved to control PreScale in early aging drosophila brain. This effect of short time (6h) ROS feeding parallels to widespread synaptic phenotype after sleep deprivation (SD) (Gilestro *et al.*, 2009). Besides, sleep loss was demonstrated to cause ROS accumulation in the drosophila brain (Kempf *et al*, 2019) and gut (Vaccaro *et al*, 2020). Specifically, ROS significantly promotes sleep behavior. The oxidation of potassium channel—“shaker” subunit “hyperkinetic” (Hk) caused by SD-induced ROS accumulation within dFB neurons was witnessed to in turn, facilitate sleep (Kempf *et al.*, 2019). Furthermore, different from traditional view of neurotoxic molecules, ROS at physiological concentration, acts as signaling molecules to trigger the functional and structural changes in synapses. For instance, neuronal ROS is an obligatory signal for activity-dependent increase of bouton number in larval neuromuscular junction (NMJ) (Oswald *et al.*, 2018). Additionally, ROS has dual role in the hippocampal long-term potentiation (LTP), serving as indispensable components of signal transduction cascades for the formation of normal LTP, while as the harmful molecule in age-driven decline of LTP (Knapp & Klann, 2000, 2002b; Serrano & Klann, 2004). Taken together, neuronal fine-tuning of mitochondrial functionality drives the adaptive alterations of PreScale in premature brain aging. As we described, ROS, byproducts of mitochondrial oxidative respiration, emerges as a signaling modality, sophisticatedly modulates the plastic change of age-dependent PreScale.

6.2 MB-secreted sNPF signaling is necessary for sustained mitochondrial capacity.

We previously witnessed that MB seemingly executes a high-level control of PreScale over the entire brain via sNPF secretion (Bhukel *et al.*, 2019). Autophagic attenuation within the MB triggers brain-wide change of PreScale and presynaptic ultrastructure by reducing the expression of a NPF family peptide—drosophila homologue sNPF (Bhukel *et al.*, 2019). Our study provided further evidence that mitochondrial functionality in the MB succeeded to drive similar brain-wide metaplastic changes of PreScale in premature brain aging. MB-exclusive PGC1 overexpression suppressed the increase of PreScale across the whole brain, while ATP5A (*b/w*) inhibition in the MB provoked PreScale-type plasticity. Age-associated PreScale steers trade-off between survival, memory formation and sleep behaviors (Huang *et al.*, 2022). Whereas, mitochondrial functional status within sleep-controlling neurons—dFB/R5 network cannot regulate PreScale in other brain regions, which further illustrated, MB exerts a high-level control of energy metabolism over the other regions of brain during the process of synaptic aging. The fruit fly monitors the energy status and modulates satiety-driven food-seeking behavior at the KC-mushroom body output neuron (MBON) synapses (Tsao *et al.*, 2018). Additionally, changes of energy metabolism solely in the MB suffices to induce the formation of long-term memory (LTM) mediated by afferent dopaminergic signaling (Plaçais *et al.*, 2017).

In our mechanistic investigation into the underlying regulatory factors, we noted that neither the rate of mitochondrial respiration nor ATP level changes can account for the widespread signals required to transmit the information within the MB into the other brain regions. sNPF, mainly secreted by MB Kenyon cells, was previously recognized as the signaling molecule to provoke the brain-wide alteration of PreScale (Bhukel *et al.*, 2019). Obviously, silencing ATP5A in the MB substantially reduced the level of sNPF in premature fly brain. Collectively, we assume that mitochondrial metabolic

status in the MB potentially drives the metaplastic change of PreScale in early aging brain via sNPF signaling.

Accumulating evidences (Botelho & Cavadas, 2015; Sousa *et al.*, 2023) support an essential role of NPY in aging and lifespan determination. Notably, NPY signaling protects from age-related mitochondrial dysfunction (Botelho & Cavadas, 2015). The NPY₁₇₋₃₆ peptide, encoded by an initial translation sequence of NPY mRNA, targets and binds to the mitochondrial outer membrane, impacting the energy balance of the mitochondrial membrane in human neuronal cells (Kaipio & Pesonen, 2009; Kallio *et al.*, 2001). The presence of NPY is necessary for maintaining efficient mitochondrial respiration and reducing excessive oxidative stress (Kir *et al.*, 2013; Zhang *et al.*, 2010). Apart from that, the NPY signaling has also correlated with mitochondrial biogenesis. The transcript level and protein abundance of PGC1 showed a significantly dosage-dependent increase induced by the administration of NPY in rat cardiomyocytes (Luo *et al.*, 2015), while the absence of muscle NPY Y1 receptor was reported to increase the protein level of PGC1 in a mice model (Zhang *et al.*, 2010). Correspondingly, we also observed a drastic decline in mitochondrial oxidative respiration in young fly brains after attenuating sNPF activity in neurons based on the Seahorse analysis. Accordingly, it is tempting to speculate that sNPF release is essential for the robustness of mitochondrial functional capacity in the central fly brain.

On the contrary, mitochondria, as the cellular powerhouse and essential signaling hub of metabolism, fuels various cellular processes involved in neurotransmission and brain activity. The activity of NPY/proopiomelanocortin (POMC) neurons in the hypothalamus are conditioned by mitochondrial functional status and ROS release (Andrews *et al.*, 2008; Gyengesi *et al.*, 2012). Moreover, from our brain immunostaining with sNPF precursor antibody, MB-specific attenuation of ATP synthase 5A reduced the level of sNPF ligand in fly brain. This observation suggests that the secretion of sNPF is potentially conditioned by energy supply from mitochondria. Taken together, the interactions between sNPF and mitochondrial functionality underscore the

underlying connections between energy metabolism and neurochemical signaling in maintaining physiological balance.

6.3 Functional and morphological plasticity of mitochondria is orchestrated with PreScale

The close physical neighborhood between synaptic release sites and mitochondria makes close communication and cooperation between two locales highly likely.

Spatial configuration between synaptic proteins and mitochondria (Fig.43h) offers a high propensity for their communication and cooperation. According to what we observed before, mitochondrial functional status in neurons finely tuned in age-driven PreScale in a bi-directional manner. Besides, we further acknowledged that their connection is not in one-way, but that both locales are reciprocally intersected. Generally, in reaction to a changing neuronal energy state, mitochondria undergo adaptations to facilitate energy homeostasis and support the proper functioning of the synaptic system, which is referred to as “mitochondrial plasticity” at synaptic sites (Rossi & Pekkurnaz, 2019). In our investigations, artificially installed “PreScale” was used to mimic age-driven presynaptic upscaling in early age of drosophila brain. A moderately engineered augmentation of BRP copy number (the 3xBRP constellation), designed to form premature PreScale at young age, induced a transition in the brain metabolic state into an energy-conserving mode. The mitochondrial respiration and ATP content in young 3xBRP flies were noted to significantly decrease across the entire brain when compared to their wildtype counterparts. Concurrently, this decline of energy demand triggered reverse electron transport (RET), resulting in elevated ROS generation due to the disrupted ATP production.

The energy metabolism of the brain is intrinsically linked to its neuronal activity. Obviously, synaptic vesicle recycling especially endocytosis, requires large amounts of energy consumption, therefore, several metabolic adaptations can occur at nerve

terminals to satisfy these needs. In the initial phase, the glucose transporter GLUT4 was observed to insert into the axonal plasma membrane to satisfy the activity-driven elevation in energy demands (Ashrafi *et al.*, 2017); Moreover, co-compartmentalization of glycolytic machinery alongside mitochondria potentially enables metabolic flexibility and efficiency at active synapses (Jang *et al.*, 2016). As another form of metabolic adaptations, genetically-installed “PreScale” triggered a metabolic reprogramming in fly brains, on the basis of Seahorse and ATP analysis under the 3xBRP scenario.

After a rigorous mechanistic scrutiny, we have pinpointed Ca^{2+} imported into mitochondrial matrix via MCU as a potential link to couple PreScale with mitochondrial metabolism. Notably, Ca^{2+} influx into mitochondria is elevated in response to an elevation of cytosolic Ca^{2+} levels (Williams *et al.*, 2013). From our past experiment using Calcein staining (Huang *et al.*, 2022), we found that genetically triggered PreScale is associated with reduced neuronal activity and also inhibits average Ca^{2+} levels within presynaptic terminals. This decline in cytosolic Ca^{2+} might then also provoke a drop in mitochondrial Ca^{2+} uptake via MCU. Ca^{2+} signaling within mitochondrial matrix regulates mitochondrial metabolism and ATP production (Boyman *et al.*, 2020b). Genetic abrogation of MCU was reported to impair the rate of oxidative respiration and ATP production (Tufi *et al.*, 2019b); Suppression of MCU in *Drosophila* MB lobes resulted in reduced synaptic vesicles and impaired memory (Drago & Davis, 2016). Such memory decline is also similar to what we observed in PreScale-driven behavior alterations (Huang *et al.*, 2022). To conclude, we drew a scheme to elucidate the reciprocal interaction between mitochondrial functionality and PreScale (Fig.44).

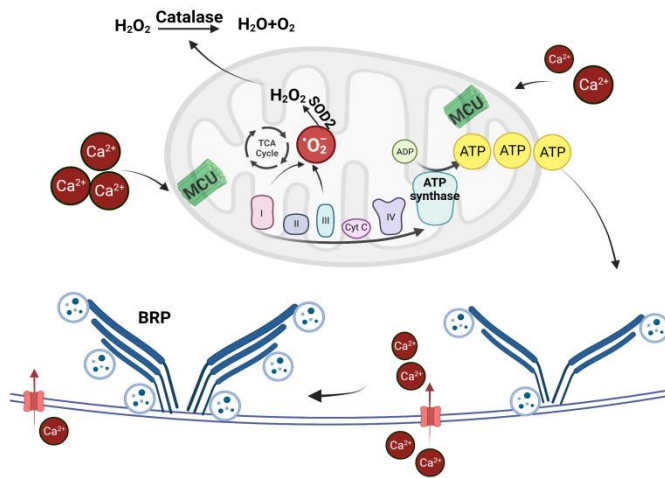


Fig.44. The Scheme to elucidate the reciprocal interaction between mitochondrial functionality and PreScale

In accordance with the survival curve with PQ feeding (Fig.40), a chronic and moderate increase in ROS may potentially enhance resilience against external stressors, such as additional oxidative stress. This concept of “mitohormesis” (Ristow, 2014) suggests that an initial exposure to ROS typically activates signaling events that can be health-promoting and life-extending. Hence, “Mitohormesis”, denoted as a novel anti-aging paradigm, is defined as a biological process wherein mild mitochondrial stress induces a mitochondrial hormetic response driving the cell into a state of greater capacity against transient threat, in the long run contributing to overall cellular health and viability (Yun & Finkel, 2014). ROS, as one of mitochondrial stressors, can activate mitochondrial unfolded protein response (UPR_{mt}) during the process of mitohormesis (Melber & Haynes, 2018). Such favorable effects of ROS-induced mitohormesis have been acknowledged across various organisms. Moderate mitochondrial insults targeting complex I component in drosophila muscle (Owusu-Ansah *et al.*, 2013) promotes the longevity of drosophila and protects against age-dependent locomotion impairment. In contrast overexpression of antioxidant-Catalase

and glutathione peroxidase I (GTPx-1) dampens the salutary effect of lifespan extension. Apart from genetic models, low-dose Arsenite stimulated the growth of cultured cells and prolonged longevity of worms through a mechanism involving ROS-induced mitochondrial hormesis in worms (Schmeisser *et al*, 2013). Based on our findings, we assume, the heightened mitochondrial ROS production might provide a protective feedback mechanism, enhancing the resistance of *Drosophila* under mildly stressed situations. We used to discover that PreScale-type plasticity is conducive to survival rather than memory establishment (Huang *et al.*, 2022). Accumulating evidences have also underscored the indispensable role of mitochondrial functionality and ROS in behavior adaptations. Mitochondrial functionality and ROS concentration are engaged in regulating longevity (Schmeisser *et al.*, 2013) (Owusu-Ansah *et al.*, 2013) and a series of other behaviors, such as control of sleep/wake cycle (Abdel-Rahman *et al*, 2021; Song *et al*, 2022), and cognitive impairment (Tönnies & Trushina, 2017; Zhao *et al*, 2021). It is tempting to speculate that PreScale-driven behavior alterations may be associated with this metabolic remodeling. However, more solid and supportable demonstration should be provided to validate this assumption. For the in-depth investigation, genetic attenuation of oxidative stress or administration of ROS scavenger chemicals to mitigate ROS levels under the 3xBRP scenario could be a worthwhile endeavor to substantiate the essential role of ROS in the observed prolonged longevity in 3xBRP flies.

Taking the results of this thesis together, mitochondrial metabolic status seems to reciprocally intersects with age-driven PreScale. Notably, as a result of our mechanistic exploration, ROS might be the critical species linking mitochondria to PreScale. Conversely, the changes in overall Ca²⁺ levels resulting from PreScale might tune mitochondrial plasticity via Ca²⁺ shuttling through MCU. This 3xBRP constellation, templated in terms of age-related PreScale offered us an opportunity to further explore the underlying connection between the metabolic homeostasis and presynaptic status in early *Drosophila* aging brain.

7. Reference

- Abdel-Rahman EA, Hosseiny S, Aaliya A, Adel M, Yasseen B, Al-Okda A, Radwan Y, Saber SH, Elkholy N, Elhanafy E *et al* (2021) Sleep/wake calcium dynamics, respiratory function, and ROS production in cardiac mitochondria. *J Adv Res* 31: 35-47
- Agostini M, Romeo F, Inoue S, Niklison-Chirou MV, Elia AJ, Dinsdale D, Morone N, Knight RA, Mak TW, Melino G (2016) Metabolic reprogramming during neuronal differentiation. *Cell Death Differ* 23: 1502-1514
- Albrecht SC, Barata AG, Grosshans J, Teleman AA, Dick TP (2011) In vivo mapping of hydrogen peroxide and oxidized glutathione reveals chemical and regional specificity of redox homeostasis. *Cell Metab* 14: 819-829
- Amorim JA, Coppotelli G, Rolo AP, Palmeira CM, Ross JM, Sinclair DA (2022) Mitochondrial and metabolic dysfunction in ageing and age-related diseases. *Nat Rev Endocrinol* 18: 243-258
- Anderson S, Bankier AT, Barrell BG, de Bruijn MH, Coulson AR, Drouin J, Eperon IC, Nierlich DP, Roe BA, Sanger F *et al* (1981) Sequence and organization of the human mitochondrial genome. *Nature* 290: 457-465
- Andrews ZB, Liu ZW, Wallingford N, Erion DM, Borok E, Friedman JM, Tschöp MH, Shanabrough M, Cline G, Shulman GI *et al* (2008) UCP2 mediates ghrelin's action on NPY/AgRP neurons by lowering free radicals. *Nature* 454: 846-851
- Ascenzi F, Barberi L, Dobrowolny G, Villa Nova Bacurau A, Nicoletti C, Rizzuto E, Rosenthal N, Scicchitano BM, Musarò A (2019) Effects of IGF-1 isoforms on muscle growth and sarcopenia. *Aging Cell* 18: e12954
- Ashrafi G, Wu Z, Farrell RJ, Ryan TA (2017) GLUT4 Mobilization Supports Energetic Demands of Active Synapses. *Neuron* 93: 606-615.e603
- Aso Y, Hattori D, Yu Y, Johnston RM, Iyer NA, Ngo TT, Dionne H, Abbott LF, Axel R, Tanimoto H *et al* (2014) The neuronal architecture of the mushroom body provides a logic for associative learning. *eLife* 3: e04577
- Aveleira CA, Botelho M, Cavadas C (2015) NPY/neuropeptide Y enhances autophagy in the hypothalamus: a mechanism to delay aging? *Autophagy* 11: 1431-1433
- Barata AG, Dick TP (2013) In vivo imaging of H₂O₂ production in Drosophila. *Methods Enzymol* 526: 61-82
- Baur JA, Pearson KJ, Price NL, Jamieson HA, Lerin C, Kalra A, Prabhu VV, Allard JS, Lopez-Lluch G, Lewis K *et al* (2006) Resveratrol improves health and survival of mice on a high-calorie diet. *Nature* 444: 337-342
- Baxter PS, Hardingham GE (2016) Adaptive regulation of the brain's antioxidant defences by neurons and astrocytes. *Free Radic Biol Med* 100: 147-152
- Benador IY, Veliova M, Liesa M, Shirihai OS (2019) Mitochondria Bound to Lipid Droplets: Where Mitochondrial Dynamics Regulate Lipid Storage and Utilization. *Cell Metab* 29: 827-835
- Berthet A, Margolis EB, Zhang J, Hsieh I, Zhang J, Hnasko TS, Ahmad J, Edwards RH, Sesaki H, Huang EJ *et al* (2014) Loss of mitochondrial fission depletes axonal mitochondria in midbrain dopamine neurons. *J Neurosci* 34: 14304-14317
- Bhukel A, Beuschel CB, Maglione M, Lehmann M, Juhász G, Madeo F, Sigrist SJ (2019) Autophagy within the mushroom body protects from synapse aging in a non-cell autonomous manner. *Nat Commun* 10: 1318
- Bi J, Wang W, Liu Z, Huang X, Jiang Q, Liu G, Wang Y, Huang X (2014) Seipin promotes adipose tissue fat storage through the ER Ca²⁺-ATPase SERCA. *Cell Metab* 19: 861-871
- Bick AG, Calvo SE, Mootha VK (2012) Evolutionary diversity of the mitochondrial calcium uniporter. *Science* 336: 886
- Bindokas VP, Jordán J, Lee CC, Miller RJ (1996) Superoxide production in rat hippocampal neurons: selective imaging with hydroethidine. *J Neurosci* 16: 1324-1336

Bjørkøy G, Lamark T, Pankiv S, Øvervatn A, Brech A, Johansen T (2009) Monitoring autophagic degradation of p62/SQSTM1. *Methods Enzymol* 452: 181-197

Böhme MA, Beis C, Reddy-Alla S, Reynolds E, Mampell MM, Grasskamp AT, Lützkendorf J, Bergeron DD, Driller JH, Babikir H *et al* (2016) Active zone scaffolds differentially accumulate Unc13 isoforms to tune Ca²⁺ channel-vesicle coupling. *Nat Neurosci* 19: 1311-1320

Botelho M, Cavadas C (2015) Neuropeptide Y: An Anti-Aging Player? *Trends Neurosci* 38: 701-711

Boyman L, Karbowski M, Lederer WJ (2020a) Regulation of Mitochondrial ATP Production: Ca²⁺ Signaling and Quality Control. *Trends Mol Med* 26: 21-39

Boyman L, Karbowski M, Lederer WJ (2020b) Regulation of Mitochondrial ATP Production: Ca²⁺ Signaling and Quality Control. *Trends Mol Med* 26: 21-39

Brand MD, Affourtit C, Esteves TC, Green K, Lambert AJ, Miwa S, Pakay JL, Parker N (2004) Mitochondrial superoxide: production, biological effects, and activation of uncoupling proteins. *Free Radic Biol Med* 37: 755-767

Brand MD, Orr AL, Perevoshchikova IV, Quinlan CL (2013) The role of mitochondrial function and cellular bioenergetics in ageing and disease. *Br J Dermatol* 169 Suppl 2: 1-8

Calabrese EJ (2013) Hormetic mechanisms. *Crit Rev Toxicol* 43: 580-606

Calabrese EJ (2016) Preconditioning is hormesis part II: How the conditioning dose mediates protection: Dose optimization within temporal and mechanistic frameworks. *Pharmacol Res* 110: 265-275

Calabrese EJ, Osakabe N, Di Paola R, Siracusa R, Fusco R, D'Amico R, Impellizzeri D, Cuzzocrea S, Fritsch T, Abdelhameed AS *et al* (2023) Hormesis defines the limits of lifespan. *Ageing Res Rev* 91: 102074

Caldeira da Silva CC, Cerqueira FM, Barbosa LF, Medeiros MH, Kowaltowski AJ (2008) Mild mitochondrial uncoupling in mice affects energy metabolism, redox balance and longevity. *Aging Cell* 7: 552-560

Cantó C, Houtkooper RH, Pirinen E, Youn DY, Oosterveer MH, Cen Y, Fernandez-Marcos PJ, Yamamoto H, Andreux PA, Cettour-Rose P *et al* (2012) The NAD⁽⁺⁾ precursor nicotinamide riboside enhances oxidative metabolism and protects against high-fat diet-induced obesity. *Cell Metab* 15: 838-847

Chan DC (2020) Mitochondrial Dynamics and Its Involvement in Disease. *Annu Rev Pathol* 15: 235-259

Chintaluri C, Vogels TP (2023) Metabolically regulated spiking could serve neuronal energy homeostasis and protect from reactive oxygen species. *Proc Natl Acad Sci U S A* 120: e2306525120

Cho Y-H, Kim G-H, Park J-J (2021) Mitochondrial aconitase 1 regulates age-related memory impairment via autophagy/mitophagy-mediated neural plasticity in middle-aged flies. *Aging Cell* 20: e13520

Cobley JN (2018) Synapse Pruning: Mitochondrial ROS with Their Hands on the Shears. *Bioessays* 40: e1800031

Cortopassi GA, Arnheim N (1990) Detection of a specific mitochondrial DNA deletion in tissues of older humans. *Nucleic Acids Res* 18: 6927-6933

Courchet J, Lewis TL, Jr., Lee S, Courchet V, Liou DY, Aizawa S, Polleux F (2013) Terminal axon branching is regulated by the LKB1-NUAK1 kinase pathway via presynaptic mitochondrial capture. *Cell* 153: 1510-1525

Cserép C, Pósfai B, Schwarcz AD, Dénes Á (2018) Mitochondrial Ultrastructure Is Coupled to Synaptic Performance at Axonal Release Sites. *eNeuro* 5

Davinelli S, De Stefani D, De Vivo I, Scapagnini G (2020) Polyphenols as Caloric Restriction Mimetics Regulating Mitochondrial Biogenesis and Mitophagy. *Trends Endocrinol Metab* 31: 536-550

de Belle JS, Heisenberg M (1994) Associative odor learning in *Drosophila* abolished by chemical ablation of mushroom bodies. *Science* 263: 692-695

De Stefani D, Bononi A, Romagnoli A, Messina A, De Pinto V, Pinton P, Rizzuto R (2012) VDAC1 selectively transfers

apoptotic Ca²⁺ signals to mitochondria. *Cell Death Differ* 19: 267-273

Deepa SS, Walsh ME, Hamilton RT, Pulliam D, Shi Y, Hill S, Li Y, Van Remmen H (2013) Rapamycin Modulates Markers of Mitochondrial Biogenesis and Fatty Acid Oxidation in the Adipose Tissue of db/db Mice. *J Biochem Pharmacol Res* 1: 114-123

Deluca HF, Engstrom GW (1961) Calcium uptake by rat kidney mitochondria. *Proc Natl Acad Sci U S A* 47: 1744-1750

Denton RM, Randle PJ, Martin BR (1972) Stimulation by calcium ions of pyruvate dehydrogenase phosphate phosphatase. *Biochem J* 128: 161-163

Denton RM, Richards DA, Chin JG (1978) Calcium ions and the regulation of NAD⁺-linked isocitrate dehydrogenase from the mitochondria of rat heart and other tissues. *Biochem J* 176: 899-906

Depetris-Chauvin A, Fernández-Gamba A, Gorostiza EA, Herrero A, Castaño EM, Ceriani MF (2014) Mmp1 processing of the PDF neuropeptide regulates circadian structural plasticity of pacemaker neurons. *PLoS Genet* 10: e1004700

Devine MJ, Kittler JT (2018) Mitochondria at the neuronal presynapse in health and disease. *Nat Rev Neurosci* 19: 63-80

Di Benedetto G, Scalzotto E, Mongillo M, Pozzan T (2013) Mitochondrial Ca²⁺ uptake induces cyclic AMP generation in the matrix and modulates organelle ATP levels. *Cell Metab* 17: 965-975

Di Cara F, Duca E, Dunbar DR, Cagney G, Heck MM (2013) Invadolysin, a conserved lipid-droplet-associated metalloproteinase, is required for mitochondrial function in *Drosophila*. *J Cell Sci* 126: 4769-4781

Dietz LJ, Venkatasubramani AV, Müller-Eigner A, Hrabe de Angelis M, Imhof A, Becker L, Peleg S (2019) Measuring and Interpreting Oxygen Consumption Rates in Whole Fly Head Segments. *J Vis Exp*

Donlea JM, Pimentel D, Talbot CB, Kempf A, Omoto JJ, Hartenstein V, Miesenböck G (2018) Recurrent Circuitry for Balancing Sleep Need and Sleep. *Neuron* 97: 378-389.e374

Donlea JM, Thimman MS, Suzuki Y, Gottschalk L, Shaw PJ (2011) Inducing sleep by remote control facilitates memory consolidation in *Drosophila*. *Science* 332: 1571-1576

Drago I, Davis RL (2016) Inhibiting the Mitochondrial Calcium Uniporter during Development Impairs Memory in Adult *Drosophila*. *Cell Reports* 16: 2763-2776

Duarte CB, Carvalho CA, Ferreira IL, Carvalho AP (1991) Synaptosomal [Ca²⁺]_i as influenced by Na⁺/Ca²⁺ exchange and K⁺ depolarization. *Cell Calcium* 12: 623-633

Dugan LL, Sensi SL, Canzoniero LM, Handran SD, Rothman SM, Lin TS, Goldberg MP, Choi DW (1995) Mitochondrial production of reactive oxygen species in cortical neurons following exposure to N-methyl-D-aspartate. *J Neurosci* 15: 6377-6388

Ebanks B, Ingram TL, Chakrabarti L (2020) ATP synthase and Alzheimer's disease: putting a spin on the mitochondrial hypothesis. *Aging (Albany NY)* 12: 16647-16662

Fink BD, Bai F, Yu L, Sivitz WI (2017) Regulation of ATP production: dependence on calcium concentration and respiratory state. *Am J Physiol Cell Physiol* 313: C146-c153

Finkel T (2012) Signal transduction by mitochondrial oxidants. *J Biol Chem* 287: 4434-4440

Fontana GA, Gahlon HL (2020) Mechanisms of replication and repair in mitochondrial DNA deletion formation. *Nucleic Acids Res* 48: 11244-11258

Fontana L, Partridge L, Longo VD (2010) Extending healthy life span--from yeast to humans. *Science* 328: 321-326

Formentini L, Sánchez-Aragó M, Sánchez-Cenizo L, Cuezva JM (2012) The mitochondrial ATPase inhibitory factor

1 triggers a ROS-mediated retrograde prosurvival and proliferative response. *Mol Cell* 45: 731-742

Fortmann SP, Burda BU, Senger CA, Lin JS, Whitlock EP (2013) Vitamin and mineral supplements in the primary prevention of cardiovascular disease and cancer: An updated systematic evidence review for the U.S. Preventive Services Task Force. *Ann Intern Med* 159: 824-834

Füllgrabe J, Ghislat G, Cho DH, Rubinsztein DC (2016) Transcriptional regulation of mammalian autophagy at a glance. *J Cell Sci* 129: 3059-3066

Gahtan E, Auerbach JM, Groner Y, Segal M (1998) Reversible impairment of long-term potentiation in transgenic Cu/Zn-SOD mice. *Eur J Neurosci* 10: 538-544

Garay RP (2021) Investigational drugs and nutrients for human longevity. Recent clinical trials registered in ClinicalTrials.gov and clinicaltrialsregister.eu. *Expert Opin Investig Drugs* 30: 749-758

Garcia JF, Carbone MA, Mackay TFC, Anholt RRH (2017) Regulation of Drosophila Lifespan by bellwether Promoter Alleles. *Sci Rep* 7: 4109

Gauba E, Guo L, Du H (2017) Cyclophilin D Promotes Brain Mitochondrial F1FO ATP Synthase Dysfunction in Aging Mice. *J Alzheimers Dis* 55: 1351-1362

Gilestro GF, Tononi G, Cirelli C (2009) Widespread changes in synaptic markers as a function of sleep and wakefulness in Drosophila. *Science* 324: 109-112

Giniatullin AR, Darios F, Shakirzyanova A, Davletov B, Giniatullin R (2006) SNAP25 is a pre-synaptic target for the depressant action of reactive oxygen species on transmitter release. *J Neurochem* 98: 1789-1797

Giniatullin AR, Giniatullin RA (2003) Dual action of hydrogen peroxide on synaptic transmission at the frog neuromuscular junction. *J Physiol* 552: 283-293

Go YM, Chandler JD, Jones DP (2015) The cysteine proteome. *Free Radic Biol Med* 84: 227-245

Gómez-Isla T, Price JL, McKeel DW, Jr., Morris JC, Growdon JH, Hyman BT (1996) Profound loss of layer II entorhinal cortex neurons occurs in very mild Alzheimer's disease. *J Neurosci* 16: 4491-4500

Gonzalez-Freire M, Diaz-Ruiz A, Hauser D, Martinez-Romero J, Ferrucci L, Bernier M, de Cabo R (2020) The road ahead for health and lifespan interventions. *Ageing Res Rev* 59: 101037

Gottlieb RA, Stotland A (2015) MitoTimer: a novel protein for monitoring mitochondrial turnover in the heart. *J Mol Med (Berl)* 93: 271-278

Grodstein F, O'Brien J, Kang JH, Dushkes R, Cook NR, Okereke O, Manson JE, Glynn RJ, Buring JE, Gaziano M *et al* (2013) Long-term multivitamin supplementation and cognitive function in men: a randomized trial. *Ann Intern Med* 159: 806-814

Guo J, Huang X, Dou L, Yan M, Shen T, Tang W, Li J (2022) Aging and aging-related diseases: from molecular mechanisms to interventions and treatments. *Signal Transduct Target Ther* 7: 391

Gupta VK, Pech U, Bhukel A, Fulterer A, Ender A, Mauermann SF, Andlauer TF, Antwi-Adjei E, Beuschel C, Thriene K *et al* (2016) Spermidine Suppresses Age-Associated Memory Impairment by Preventing Adverse Increase of Presynaptic Active Zone Size and Release. *PLoS Biol* 14: e1002563

Gyengesi E, Paxinos G, Andrews ZB (2012) Oxidative Stress in the Hypothalamus: the Importance of Calcium Signaling and Mitochondrial ROS in Body Weight Regulation. *Curr Neuropharmacol* 10: 344-353

Hacker K, Medler KF (2008) Mitochondrial calcium buffering contributes to the maintenance of Basal calcium levels in mouse taste cells. *J Neurophysiol* 100: 2177-2191

Hamanaka RB, Chandel NS (2010) Mitochondrial reactive oxygen species regulate cellular signaling and dictate biological outcomes. *Trends Biochem Sci* 35: 505-513

Han B, Jiang W, Liu H, Wang J, Zheng K, Cui P, Feng Y, Dang C, Bu Y, Wang QM *et al* (2020) Upregulation of neuronal

PGC-1 α ameliorates cognitive impairment induced by chronic cerebral hypoperfusion. *Theranostics* 10: 2832-2848

Heisenberg M (1998) What do the mushroom bodies do for the insect brain? an introduction. *Learn Mem* 5: 1-10

Holford N (2017) Pharmacodynamic principles and the time course of immediate drug effects. *Transl Clin Pharmacol* 25: 157-161

Homem CCF, Steinmann V, Burkard TR, Jais A, Esterbauer H, Knoblich JA (2014) Ecdysone and mediator change energy metabolism to terminate proliferation in *Drosophila* neural stem cells. *Cell* 158: 874-888

Hong SH, Lee KS, Kwak SJ, Kim AK, Bai H, Jung MS, Kwon OY, Song WJ, Tatar M, Yu K (2012) Minibrain/Dyrk1a regulates food intake through the Sir2-FOXO-sNPF/NPY pathway in *Drosophila* and mammals. *PLoS Genet* 8: e1002857

Huang S, Piao C, Beuschel CB, Götz T, Sigrist SJ (2020) Presynaptic Active Zone Plasticity Encodes Sleep Need in *Drosophila*. *Curr Biol* 30: 1077-1091.e1075

Huang S, Piao C, Beuschel CB, Zhao Z, Sigrist SJ (2022) A brain-wide form of presynaptic active zone plasticity orchestrates resilience to brain aging in *Drosophila*. *PLoS Biol* 20: e3001730

Ishihara N, Fujita Y, Oka T, Mihara K (2006) Regulation of mitochondrial morphology through proteolytic cleavage of OPA1. *EMBO J* 25: 2966-2977

James AM, Sharpley MS, Manas AR, Frerman FE, Hirst J, Smith RA, Murphy MP (2007) Interaction of the mitochondria-targeted antioxidant MitoQ with phospholipid bilayers and ubiquinone oxidoreductases. *J Biol Chem* 282: 14708-14718

Jang S, Nelson JC, Bend EG, Rodríguez-Laureano L, Tueros FG, Cartagena L, Underwood K, Jorgensen EM, Colón-Ramos DA (2016) Glycolytic Enzymes Localize to Synapses under Energy Stress to Support Synaptic Function. *Neuron* 90: 278-291

Jeong J, Pandey S, Li Y, Badger JD, 2nd, Lu W, Roche KW (2019) PSD-95 binding dynamically regulates NLGN1 trafficking and function. *Proc Natl Acad Sci U S A* 116: 12035-12044

Jheng HF, Tsai PJ, Guo SM, Kuo LH, Chang CS, Su IJ, Chang CR, Tsai YS (2012) Mitochondrial fission contributes to mitochondrial dysfunction and insulin resistance in skeletal muscle. *Mol Cell Biol* 32: 309-319

Johard HA, Enell LE, Gustafsson E, Trifilieff P, Veenstra JA, Nässel DR (2008) Intrinsic neurons of *Drosophila* mushroom bodies express short neuropeptide F: relations to extrinsic neurons expressing different neurotransmitters. *J Comp Neurol* 507: 1479-1496

Ju TC, Lin YS, Chern Y (2012) Energy dysfunction in Huntington's disease: insights from PGC-1 α , AMPK, and CKB. *Cell Mol Life Sci* 69: 4107-4120

Kaipio K, Pesonen U (2009) The intracellular mobility of NPY and a putative mitochondrial form of NPY in neuronal cells. *Neurosci Lett* 450: 181-185

Kallio J, Pesonen U, Kaipio K, Karvonen MK, Jaakkola U, Heinonen OJ, Uusitupa MI, Koulu M (2001) Altered intracellular processing and release of neuropeptide Y due to leucine 7 to proline 7 polymorphism in the signal peptide of preproneuropeptide Y in humans. *FASEB J* 15: 1242-1244

Kamer KJ, Mootha VK (2015) The molecular era of the mitochondrial calcium uniporter. *Nat Rev Mol Cell Biol* 16: 545-553

Kandel ER, Dudai Y, Mayford MR (2014) The molecular and systems biology of memory. *Cell* 157: 163-186

Kempf A, Song SM, Talbot CB, Miesenböck G (2019) A potassium channel β -subunit couples mitochondrial electron transport to sleep. *Nature* 568: 230-234

Kir HM, Sahin D, Oztaş B, Musul M, Kuskay S (2013) Effects of single-dose neuropeptide Y on levels of hippocampal BDNF, MDA, GSH, and NO in a rat model of pentylentetrazole-induced epileptic seizure. *Bosn J Basic Med Sci* 13: 242-247

Kirichok Y, Krapivinsky G, Clapham DE (2004) The mitochondrial calcium uniporter is a highly selective ion channel. *Nature* 427: 360-364

Kittel RJ, Wichmann C, Rasse TM, Fouquet W, Schmidt M, Schmid A, Wagh DA, Pawlu C, Kellner RR, Willig KI *et al* (2006) Bruchpilot promotes active zone assembly, Ca²⁺ channel clustering, and vesicle release. *Science* 312: 1051-1054

Klann E, Roberson ED, Knapp LT, Sweatt JD (1998) A role for superoxide in protein kinase C activation and induction of long-term potentiation. *J Biol Chem* 273: 4516-4522

Knapp LT, Klann E (2000) Superoxide-induced stimulation of protein kinase C via thiol modification and modulation of zinc content. *J Biol Chem* 275: 24136-24145

Knapp LT, Klann E (2002a) Potentiation of hippocampal synaptic transmission by superoxide requires the oxidative activation of protein kinase C. *J Neurosci* 22: 674-683

Knapp LT, Klann E (2002b) Role of reactive oxygen species in hippocampal long-term potentiation: contributory or inhibitory? *J Neurosci Res* 70: 1-7

Lee DA, Andreev A, Truong TV, Chen A, Hill AJ, Oikonomou G, Pham U, Hong YK, Tran S, Glass L *et al* (2017) Genetic and neuronal regulation of sleep by neuropeptide VF. *eLife* 6

Lee K-S, Huh S, Lee S, Wu Z, Kim A-K, Kang H-Y, Lu B (2018) Altered ER-mitochondria contact impacts mitochondria calcium homeostasis and contributes to neurodegeneration in vivo in disease models. *Proc Natl Acad Sci U S A* 115: E8844-E8853

Lees RM, Johnson JD, Ashby MC (2019) Presynaptic Boutons That Contain Mitochondria Are More Stable. *Front Synaptic Neurosci* 11: 37

Lehninger AL, Rossi CS, Greenawalt JW (1963) Respiration-dependent accumulation of inorganic phosphate and Ca ions by rat liver mitochondria. *Biochem Biophys Res Commun* 10: 444-448

Lewis TL, Jr., Kwon SK, Lee A, Shaw R, Polleux F (2018) MFF-dependent mitochondrial fission regulates presynaptic release and axon branching by limiting axonal mitochondria size. *Nat Commun* 9: 5008

Li S, Xiong G-J, Huang N, Sheng Z-H (2020) The cross-talk of energy sensing and mitochondrial anchoring sustains synaptic efficacy by maintaining presynaptic metabolism. *Nat Metab* 2: 1077-1095

Liang Y, Piao C, Beuschel CB, Toppe D, Kollipara L, Bogdanow B, Maglione M, Lützkendorf J, See JCK, Huang S *et al* (2021) eIF5A hypusination, boosted by dietary spermidine, protects from premature brain aging and mitochondrial dysfunction. *Cell Reports* 35: 108941

Liguori I, Russo G, Curcio F, Bulli G, Aran L, Della-Morte D, Gargiulo G, Testa G, Cacciatore F, Bonaduce D *et al* (2018) Oxidative stress, aging, and diseases. *Clin Interv Aging* 13: 757-772

Lin JS, O'Connor E, Rossom RC, Perdue LA, Eckstrom E (2013) Screening for cognitive impairment in older adults: A systematic review for the U.S. Preventive Services Task Force. *Ann Intern Med* 159: 601-612

Lin SJ, Kaeberlein M, Andalis AA, Sturtz LA, Defossez PA, Culotta VC, Fink GR, Guarente L (2002) Calorie restriction extends *Saccharomyces cerevisiae* lifespan by increasing respiration. *Nature* 418: 344-348

Link W (2019) Introduction to FOXO Biology. *Methods Mol Biol* 1890: 1-9

Liu S, Liu Q, Tabuchi M, Wu MN (2016) Sleep Drive Is Encoded by Neural Plastic Changes in a Dedicated Circuit. *Cell* 165: 1347-1360

Longo VD, Antebi A, Bartke A, Barzilay N, Brown-Borg HM, Caruso C, Curiel TJ, de Cabo R, Franceschi C, Gems D

et al (2015) Interventions to Slow Aging in Humans: Are We Ready? *Aging Cell* 14: 497-510

López-Otín C, Blasco MA, Partridge L, Serrano M, Kroemer G (2013) The hallmarks of aging. *Cell* 153: 1194-1217

López-Otín C, Blasco MA, Partridge L, Serrano M, Kroemer G (2023) Hallmarks of aging: An expanding universe. *Cell* 186: 243-278

Luo G, Xu X, Guo W, Luo C, Wang H, Meng X, Zhu S, Wei Y (2015) Neuropeptide Y damages the integrity of mitochondrial structure and disrupts energy metabolism in cultured neonatal rat cardiomyocytes. *Peptides* 71: 162-169

Ly CV, Verstreken P (2006) Mitochondria at the synapse. *Neuroscientist* 12: 291-299

Mackert O, Wirth EK, Sun R, Winkler J, Liu A, Renko K, Kunz S, Spranger J, Brachs S (2022) Impact of metabolic stress induced by diets, aging and fasting on tissue oxygen consumption. *Mol Metab* 64: 101563

Matkovic T, Siebert M, Knoche E, Depner H, Mertel S, Oswald D, Schmidt M, Thomas U, Sickmann A, Kamin D *et al* (2013) The Bruchpilot cytomatrix determines the size of the readily releasable pool of synaptic vesicles. *J Cell Biol* 202: 667-683

McCormack JG, Denton RM (1979) The effects of calcium ions and adenine nucleotides on the activity of pig heart 2-oxoglutarate dehydrogenase complex. *Biochem J* 180: 533-544

McGuire SE, Le PT, Osborn AJ, Matsumoto K, Davis RL (2003) Spatiotemporal rescue of memory dysfunction in *Drosophila*. *Science* 302: 1765-1768

Mears JA, Lackner LL, Fang S, Ingerman E, Nunnari J, Hinshaw JE (2011) Conformational changes in Dnm1 support a contractile mechanism for mitochondrial fission. *Nat Struct Mol Biol* 18: 20-26

Melber A, Haynes CM (2018) UPR(mt) regulation and output: a stress response mediated by mitochondrial-nuclear communication. *Cell Res* 28: 281-295

Milton VJ, Jarrett HE, Gowers K, Chalak S, Briggs L, Robinson IM, Sweeney ST (2011) Oxidative stress induces overgrowth of the *Drosophila* neuromuscular junction. *Proc Natl Acad Sci U S A* 108: 17521-17526

Mishra P, Chan DC (2014) Mitochondrial dynamics and inheritance during cell division, development and disease. *Nat Rev Mol Cell Biol* 15: 634-646

Misko AL, Sasaki Y, Tuck E, Milbrandt J, Baloh RH (2012) Mitofusin2 mutations disrupt axonal mitochondrial positioning and promote axon degeneration. *J Neurosci* 32: 4145-4155

Missirlis F, Hu J, Kirby K, Hilliker AJ, Rouault TA, Phillips JP (2003) Compartment-specific protection of iron-sulfur proteins by superoxide dismutase. *J Biol Chem* 278: 47365-47369

Missirlis F, Phillips JP, Jäckle H (2001) Cooperative action of antioxidant defense systems in *Drosophila*. *Curr Biol* 11: 1272-1277

Mitchell P (1961) Coupling of phosphorylation to electron and hydrogen transfer by a chemi-osmotic type of mechanism. *Nature* 191: 144-148

Miyawaki A, Griesbeck O, Heim R, Tsien RY (1999) Dynamic and quantitative Ca²⁺ measurements using improved cameleons. *Proc Natl Acad Sci U S A* 96: 2135-2140

Morrison JH, Baxter MG (2012) The ageing cortical synapse: hallmarks and implications for cognitive decline. *Nat Rev Neurosci* 13: 240-250

Murphy MP (2009) How mitochondria produce reactive oxygen species. *Biochem J* 417: 1-13

Nagai T, Sawano A, Park ES, Miyawaki A (2001) Circularly permuted green fluorescent proteins engineered to sense Ca²⁺. *Proc Natl Acad Sci U S A* 98: 3197-3202

Namgaladze D, Hofer HW, Ullrich V (2002) Redox control of calcineurin by targeting the binuclear Fe(2+)-Zn(2+) center at the enzyme active site. *J Biol Chem* 277: 5962-5969

Neniskyte U, Gross CT (2017) Errant gardeners: glial-cell-dependent synaptic pruning and neurodevelopmental disorders. *Nat Rev Neurosci* 18: 658-670

Neville KE, Bosse TL, Klekos M, Mills JF, Tipping M (2018a) Metabolic Analysis of *Drosophila melanogaster* Larval and Adult Brains. *J Vis Exp*

Neville KE, Bosse TL, Klekos M, Mills JF, Weickel SE, Waters JS, Tipping M (2018b) A novel ex vivo method for measuring whole brain metabolism in model systems. *J Neurosci Methods* 296: 32-43

Niu X, Trifunovic A, Larsson NG, Canlon B (2007) Somatic mtDNA mutations cause progressive hearing loss in the mouse. *Exp Cell Res* 313: 3924-3934

Nunnari J, Suomalainen A (2012) Mitochondria: in sickness and in health. *Cell* 148: 1145-1159

Oh TS, Cho H, Cho JH, Yu SW, Kim EK (2016) Hypothalamic AMPK-induced autophagy increases food intake by regulating NPY and POMC expression. *Autophagy* 12: 2009-2025

Oswald MC, Brooks PS, Zwart MF, Mukherjee A, West RJ, Giachello CN, Morarach K, Baines RA, Sweeney ST, Landgraf M (2018) Reactive oxygen species regulate activity-dependent neuronal plasticity in *Drosophila*. *eLife* 7

Owusu-Ansah E, Song W, Perrimon N (2013) Muscle mitohormesis promotes longevity via systemic repression of insulin signaling. *Cell* 155: 699-712

Pan X, Liu J, Nguyen T, Liu C, Sun J, Teng Y, Fergusson MM, Rovira II, Allen M, Springer DA (2013) The physiological role of mitochondrial calcium revealed by mice lacking the mitochondrial calcium uniporter. *Nature cell biology* 15: 1464-1472

Pankiv S, Clausen TH, Lamark T, Brech A, Bruun JA, Outzen H, Øvervatn A, Bjørkøy G, Johansen T (2007) p62/SQSTM1 binds directly to Atg8/LC3 to facilitate degradation of ubiquitinated protein aggregates by autophagy. *J Biol Chem* 282: 24131-24145

Patel HR, Qi Y, Hawkins EJ, Hileman SM, Elmquist JK, Imai Y, Ahima RS (2006) Neuropeptide Y deficiency attenuates responses to fasting and high-fat diet in obesity-prone mice. *Diabetes* 55: 3091-3098

Pekkurnaz G, Wang X (2022) Mitochondrial heterogeneity and homeostasis through the lens of a neuron. *Nat Metab* 4: 802-812

Pimentel D, Donlea JM, Talbot CB, Song SM, Thurston AJF, Miesenböck G (2016) Operation of a homeostatic sleep switch. *Nature* 536: 333-337

Plaçais PY, de Tredern É, Scheunemann L, Trannoy S, Goguel V, Han KA, Isabel G, Preat T (2017) Upregulated energy metabolism in the *Drosophila* mushroom body is the trigger for long-term memory. *Nat Commun* 8: 15510

Pogson JH, Ivatt RM, Sanchez-Martinez A, Tufi R, Wilson E, Mortiboys H, Whitworth AJ (2014) The complex I subunit NDUFA10 selectively rescues *Drosophila* pink1 mutants through a mechanism independent of mitophagy. *PLoS Genet* 10: e1004815

Pooryasin A, Maglione M, Schubert M, Matkovic-Rachid T, Hasheminasab SM, Pech U, Fiala A, Mielke T, Sigrist SJ (2021) Unc13A and Unc13B contribute to the decoding of distinct sensory information in *Drosophila*. *Nat Commun* 12: 1932

Price NL, Gomes AP, Ling AJ, Duarte FV, Martin-Montalvo A, North BJ, Agarwal B, Ye L, Ramadori G, Teodoro JS *et al* (2012) SIRT1 is required for AMPK activation and the beneficial effects of resveratrol on mitochondrial function. *Cell Metab* 15: 675-690

Prins D, Michalak M (2011) Organellar calcium buffers. *Cold Spring Harb Perspect Biol* 3

Rajman L, Chwalek K, Sinclair DA (2018) Therapeutic Potential of NAD-Boosting Molecules: The In Vivo Evidence. *Cell Metab* 27: 529-547

Rangaraju V, Calloway N, Ryan TA (2014) Activity-driven local ATP synthesis is required for synaptic function. *Cell* 156: 825-835

Rangaraju V, Lewis TL, Jr., Hirabayashi Y, Bergami M, Motori E, Cartoni R, Kwon SK, Courchet J (2019) Pleiotropic Mitochondria: The Influence of Mitochondria on Neuronal Development and Disease. *J Neurosci* 39: 8200-8208

Rera M, Bahadorani S, Cho J, Koehler CL, Ulgherait M, Hur JH, Ansari WS, Lo T, Jones DL, Walker DW (2011) Modulation of longevity and tissue homeostasis by the Drosophila PGC-1 homolog. *Cell Metab* 14: 623-634

Riccomagno MM, Kolodkin AL (2015) Sculpting neural circuits by axon and dendrite pruning. *Annu Rev Cell Dev Biol* 31: 779-805

Ring J, Tadic J, Ristic S, Poglitsch M, Bergmann M, Radic N, Mossmann D, Liang Y, Maglione M, Jerkovic A *et al* (2022) The HSP40 chaperone Ydj1 drives amyloid beta 42 toxicity. *EMBO Molecular Medicine* 14: e13952

Ristow M (2014) Unraveling the truth about antioxidants: mitohormesis explains ROS-induced health benefits. *Nat Med* 20: 709-711

Ristow M, Zarse K (2010) How increased oxidative stress promotes longevity and metabolic health: The concept of mitochondrial hormesis (mitohormesis). *Exp Gerontol* 45: 410-418

Rizzuto R, Pinton P, Carrington W, Fay FS, Fogarty KE, Lifshitz LM, Tuft RA, Pozzan T (1998) Close contacts with the endoplasmic reticulum as determinants of mitochondrial Ca²⁺ responses. *Science* 280: 1763-1766

Rizzuto R, Simpson AW, Brini M, Pozzan T (1992) Rapid changes of mitochondrial Ca²⁺ revealed by specifically targeted recombinant aequorin. *Nature* 358: 325-327

Rossi MJ, Pekkurnaz G (2019) Powerhouse of the mind: mitochondrial plasticity at the synapse. *Curr Opin Neurobiol* 57: 149-155

Rusinek H, De Santi S, Frid D, Tsui WH, Tarshish CY, Convit A, de Leon MJ (2003) Regional brain atrophy rate predicts future cognitive decline: 6-year longitudinal MR imaging study of normal aging. *Radiology* 229: 691-696

Sanchez-Contreras M, Kennedy SR (2022) The Complicated Nature of Somatic mtDNA Mutations in Aging. *Front Aging* 2

Sanyal S, Sandstrom DJ, Hoeffler CA, Ramaswami M (2002) AP-1 functions upstream of CREB to control synaptic plasticity in Drosophila. *Nature* 416: 870-874

Schmeisser S, Schmeisser K, Weimer S, Groth M, Priebe S, Fazius E, Kuhlow D, Pick D, Einax JW, Guthke R *et al* (2013) Mitochondrial hormesis links low-dose arsenite exposure to lifespan extension. *Aging Cell* 12: 508-517

Schneeberger M, Dietrich MO, Sebastián D, Imbernón M, Castaño C, Garcia A, Esteban Y, Gonzalez-Franquesa A, Rodríguez IC, Bortolozzi A *et al* (2013) Mitofusin 2 in POMC neurons connects ER stress with leptin resistance and energy imbalance. *Cell* 155: 172-187

Schulz TJ, Zarse K, Voigt A, Urban N, Birringer M, Ristow M (2007) Glucose restriction extends *Caenorhabditis elegans* life span by inducing mitochondrial respiration and increasing oxidative stress. *Cell Metab* 6: 280-293

Scialò F, Fernández-Ayala DJ, Sanz A (2017) Role of Mitochondrial Reverse Electron Transport in ROS Signaling: Potential Roles in Health and Disease. *Front Physiol* 8: 428

Sena LA, Chandel NS (2012) Physiological roles of mitochondrial reactive oxygen species. *Mol Cell* 48: 158-167

Serrano F, Klann E (2004) Reactive oxygen species and synaptic plasticity in the aging hippocampus. *Ageing Res Rev* 3: 431-443

Sgammeaglia N, Sprecher SG (2022) Interplay between metabolic energy regulation and memory pathways in Drosophila. *Trends Neurosci* 45: 539-549

Shadel GS, Horvath TL (2015) Mitochondrial ROS signaling in organismal homeostasis. *Cell* 163: 560-569

Sidlauskaite E, Gibson JW, Megson IL, Whitfield PD, Tovmasyan A, Batinic-Haberle I, Murphy MP, Moulton PR, Copley

JN (2018) Mitochondrial ROS cause motor deficits induced by synaptic inactivity: Implications for synapse pruning. *Redox Biol* 16: 344-351

Smit-Rigter L, Rajendran R, Silva CA, Spierenburg L, Groeneweg F, Ruimschotel EM, van Versendaal D, van der Togt C, Eysel UT, Heimel JA *et al* (2016) Mitochondrial Dynamics in Visual Cortex Are Limited In Vivo and Not Affected by Axonal Structural Plasticity. *Curr Biol* 26: 2609-2616

Smith HL, Bourne JN, Cao G, Chirillo MA, Ostroff LE, Watson DJ, Harris KM (2016) Mitochondrial support of persistent presynaptic vesicle mobilization with age-dependent synaptic growth after LTP. *eLife* 5

Sobieski C, Fitzpatrick MJ, Mennerick SJ (2017) Differential Presynaptic ATP Supply for Basal and High-Demand Transmission. *J Neurosci* 37: 1888-1899

Somlyo AP (1984) Cell physiology: cellular site of calcium regulation. *Nature* 309: 516-517

Song F, Lin J, Zhang H, Guo Y, Mao Y, Liu Z, Li G, Wang Y (2022) Long-Term Sleep Deprivation-Induced Myocardial Remodeling and Mitochondrial Dysfunction in Mice Were Attenuated by Lipoic Acid and N-Acetylcysteine. *Pharmaceuticals (Basel)* 16

Sousa D, Lopes E, Rosendo-Silva D, Matafome P (2023) The Bidirectional Relationship of NPY and Mitochondria in Energy Balance Regulation. *Biomedicines* 11

Symposia BS, Kay J, Weitzman PDJ (1987) *Krebs' Citric Acid Cycle: Half a Century and Still Turning : Biochemical Society Symposium No. 54 Held at University of Leicester, April 1987*. Biochemical Society

Szabadkai G, Simoni AM, Rizzuto R (2003) Mitochondrial Ca²⁺ uptake requires sustained Ca²⁺ release from the endoplasmic reticulum. *J Biol Chem* 278: 15153-15161

Szalai G, Csordás G, Hantash BM, Thomas AP, Hajnóczky G (2000) Calcium signal transmission between ryanodine receptors and mitochondria. *J Biol Chem* 275: 15305-15313

TAINTER ML, STOCKTON AB, CUTTING WC (1933) USE OF DINITROPHENOL IN OBESITY AND RELATED CONDITIONS: A PROGRESS REPORT. *Journal of the American Medical Association* 101: 1472-1475

Tang Y, Zucker RS (1997) Mitochondrial involvement in post-tetanic potentiation of synaptic transmission. *Neuron* 18: 483-491

Territo PR, Mootha VK, French SA, Balaban RS (2000) Ca²⁺ activation of heart mitochondrial oxidative phosphorylation: role of the F₀/F₁-ATPase. *Am J Physiol Cell Physiol* 278: C423-435

Tessema B, Haag J, Sack U, König B (2023) The Determination of Mitochondrial Mass Is a Prerequisite for Accurate Assessment of Peripheral Blood Mononuclear Cells' Oxidative Metabolism. *Int J Mol Sci* 24

Thomas CI, Keine C, Okayama S, Satterfield R, Musgrove M, Guerrero-Given D, Kamasawa N, Young SM (2019) Presynaptic Mitochondria Volume and Abundance Increase during Development of a High-Fidelity Synapse. *J Neurosci* 39: 7994-8012

Tiefenbock SK, Baltzer C, Egli NA, Frei C (2010) The Drosophila PGC-1 homologue Spargel coordinates mitochondrial activity to insulin signalling. *Embo J* 29: 171-183

Tönnies E, Trushina E (2017) Oxidative Stress, Synaptic Dysfunction, and Alzheimer's Disease. *J Alzheimers Dis* 57: 1105-1121

Tsao CH, Chen CC, Lin CH, Yang HY, Lin S (2018) Drosophila mushroom bodies integrate hunger and satiety signals to control innate food-seeking behavior. *eLife* 7

Tufi R, Gleeson TP, von Stockum S, Hewitt VL, Lee JJ, Terriente-Felix A, Sanchez-Martinez A, Ziviani E, Whitworth AJ (2019a) Comprehensive Genetic Characterization of Mitochondrial Ca²⁺ Uniporter Components Reveals Their Different Physiological Requirements In Vivo. *Cell Reports* 27

Tufi R, Gleeson TP, von Stockum S, Hewitt VL, Lee JJ, Terriente-Felix A, Sanchez-Martinez A, Ziviani E, Whitworth

AJ (2019b) Comprehensive Genetic Characterization of Mitochondrial Ca²⁺ Uniporter Components Reveals Their Different Physiological Requirements In Vivo. *Cell Rep* 27: 1541-1550.e1545

Ugbode C, Garnham N, Fort-Aznar L, Evans GJO, Chawla S, Sweeney ST (2020) JNK signalling regulates antioxidant responses in neurons. *Redox Biol* 37: 101712

Unies N (2015) *World Population Ageing, 2015: Highlights*. UN

Vaccaro A, Kaplan Dor Y, Nambara K, Pollina EA, Lin C, Greenberg ME, Rogulja D (2020) Sleep Loss Can Cause Death through Accumulation of Reactive Oxygen Species in the Gut. *Cell* 181: 1307-1328.e1315

Van Raamsdonk JM, Hekimi S (2012) Superoxide dismutase is dispensable for normal animal lifespan. *Proc Natl Acad Sci U S A* 109: 5785-5790

Vasington FD, Murphy JV (1962) Ca ion uptake by rat kidney mitochondria and its dependence on respiration and phosphorylation. *J Biol Chem* 237: 2670-2677

Wagh DA, Rasse TM, Asan E, Hofbauer A, Schwenkert I, Dürrbeck H, Buchner S, Dabauvalle M-C, Schmidt M, Qin G *et al* (2006) Bruchpilot, a protein with homology to ELKS/CAST, is required for structural integrity and function of synaptic active zones in *Drosophila*. *Neuron* 49: 833-844

Wai T, Langer T (2016) Mitochondrial Dynamics and Metabolic Regulation. *Trends Endocrinol Metab* 27: 105-117

Wallace DC, Chalkia D (2013) Mitochondrial DNA genetics and the heteroplasmy conundrum in evolution and disease. *Cold Spring Harb Perspect Biol* 5: a021220

Wang XJ, Davis RL (2021) Early Mitochondrial Fragmentation and Dysfunction in a *Drosophila* Model for Alzheimer's Disease. *Mol Neurobiol* 58: 143-155

Warburton DE, Nicol CW, Bredin SS (2006) Health benefits of physical activity: the evidence. *Cmaj* 174: 801-809

Wenz T (2011) Mitochondria and PGC-1 α in Aging and Age-Associated Diseases. *J Aging Res* 2011: 810619

Williams GSB, Boyman L, Chikando AC, Khairallah RJ, Lederer WJ (2013) Mitochondrial calcium uptake. *Proc Natl Acad Sci U S A* 110: 10479-10486

Wong HC, Zhang Q, Beirl AJ, Petralia RS, Wang YX, Kindt K (2019) Synaptic mitochondria regulate hair-cell synapse size and function. *eLife* 8

Wu KL, Wu CA, Wu CW, Chan SH, Chang AY, Chan JY (2013) Redox-sensitive oxidation and phosphorylation of PTEN contribute to enhanced activation of PI3K/Akt signaling in rostral ventrolateral medulla and neurogenic hypertension in spontaneously hypertensive rats. *Antioxid Redox Signal* 18: 36-50

Yang CH, Lee KH, Ho WK, Lee SH (2021) Inter-spike mitochondrial Ca²⁺ release enhances high frequency synaptic transmission. *J Physiol* 599: 1567-1594

Yang S, Loro E, Wada S, Kim B, Tseng WJ, Li K, Khurana TS, Arany Z (2020) Functional effects of muscle PGC-1 α in aged animals. *Skelet Muscle* 10: 14

Yang W, Hekimi S (2010) A mitochondrial superoxide signal triggers increased longevity in *Caenorhabditis elegans*. *PLoS Biol* 8: e1000556

Youle RJ, van der Bliek AM (2012) Mitochondrial fission, fusion, and stress. *Science* 337: 1062-1065

Yun J, Finkel T (2014) Mitohormesis. *Cell Metab* 19: 757-766

Zhang L, Macia L, Turner N, Enriquez RF, Riepler SJ, Nguyen AD, Lin S, Lee NJ, Shi YC, Yulyaningsih E *et al* (2010) Peripheral neuropeptide Y Y1 receptors regulate lipid oxidation and fat accretion. *Int J Obes (Lond)* 34: 357-373

Zhao Y, Zhang J, Zheng Y, Zhang Y, Zhang XJ, Wang H, Du Y, Guan J, Wang X, Fu J (2021) NAD⁺ improves cognitive function and reduces neuroinflammation by ameliorating mitochondrial damage and decreasing ROS production in chronic cerebral hypoperfusion models through Sirt1/PGC-1 α pathway. *J Neuroinflammation* 18: 207

Zhou J, Wang H, Shen R, Fang J, Yang Y, Dai W, Zhu Y, Zhou M (2018) Mitochondrial-targeted antioxidant MitoQ

provides neuroprotection and reduces neuronal apoptosis in experimental traumatic brain injury possibly via the Nrf2-ARE pathway. *Am J Transl Res* 10: 1887-1899

8. List of publications

1. Neuron-specific modulation of Mitochondrial metabolism tunes in age-driven PreScale (**First author**, in preparation)

Appendix

PGC1	Peroxisome proliferator-activated receptor gamma coactivator 1
blw (ATP5A)	the alpha subunit of the mitochondrial F1F0 ATP synthase complex
ROS	Reactive oxygen species
sNPF	short Neuropeptide F
sNPFr	short Neuropeptide F receptor
MB	Mushroom body
Cat	catalase
SOD2	superoxide dismutase 2
NPY	Neuropeptide Y
Drosophila	<i>Drosophila melanogaster</i>
BRP	Bruchpilot
Spd-S	Spermidine supplementation
CalexA	Calcium-dependent nuclear import of LexA
PN	projection neuron
dFB	dorsal fan-shaped body
Dlg	the homolog of the mammalian scaffold protein PSD95, Discs large
PQ	paraquat
O ₂ ⁻	superoxide
H ₂ O ₂	Hydrogen superoxide
ETC	Electron transport chain
MCU	Mitochondrial calcium uniporter
STED	Stimulated Emission depletion microscopy
KCs	Kenyon cells
p62/SQSTM117	drosophila homolog Ref(2)p
FOXO	Forkhead box O
Mnb	minibrain
COXIV	Mitochondrial Complex IV—cytochrome c oxidase IV
IP ₃ Rs	inositol 1,4,5-trisphosphate receptors
RyRs	Ryanodine receptors
Drep2	DNA fragmentation factor-related protein 2